SYNTHESIS, STRUCTURE, AND REACTIVITY OF DIAMIDE-SUPPORTED MOLYBDENUM COMPLEXES.

By

CARLOS GILBERTO ORTIZ VAZQUEZ

A DISSERTATION PRESENTED TO THE GRADUATE SCHOOL
OF THE UNIVERSITY OF FLORIDA IN PARTIAL FULFILLMENT
OF THE REQUIREMENTS FOR THE DEGREE OF
DOCTOR OF PHILOSOPHY

UNIVERSITY OF FLORIDA

1999

Dedicated to my Parents and Brother

Empezar porque si
y acabar cocechando
el azul que lleva el cielo.
Y seguir buscando
los astros que estan mas lejos
y ahora van dentro de mi.

ACKNOWLEDGMENTS

The reasons why I started this doctoral work have been forgotten in its process. However, there have been a number of people who in some way or another have reminded me of how important it was to complete it.

First and foremost, I want to thank my parents, Carlos and Rosa, for all their efforts in helping me through, not only my college career, but also my life. Their help, in every way, has been of indispensable importance. Also, my brother Javier has not only been there for me as a friend but as a constant source of laughter and fun. It is for this reason that I dedicate this dissertation to them.

If it were not for the tutelage of Dr. James M. Boncella, I would have not reached this point in my life. Jim's quest for finding new and different ways of doing chemical reactions, even if the results have been observed before, has helped me to attempt to understand how the often abstract science of organometallic chemistry works. In addition, on many occasions he has also showed me how important it is to keep a level head and that all the hours that we spend in the lab do pay off in the long run.

I also wish to thank Dr. Khalil A. Abboud. Khalil has not only been a co-worker and teacher, but also a friend. He performed all of the X-ray crystallography experiments contained in this dissertation, sometimes allowing me to sit close by trying to learn as much as I could about his craft. His patience and efforts while teaching me all I wanted

to learn about crystallography will never be forgotten and are responsible for all I know about the subject.

The first time that I met Dr. Richard A. Walton, he implanted in my head the idea of obtaining a doctoral degree. I still have not forgotten his teachings and the message he sent me off to graduate school with: HAVE FUN! I would like to thank him for that and all the time he spent teaching me how a metal works.

All the hours spent in the laboratory in the course of these five years would have been unbearable if it were not for the brotherly relationship among the members of the Boncella research group. Like brothers and sisters we sometimes had our arguments yet, only good memories remain. After all a large portion of what I have learned about chemistry and life in the past few years comes from our discussions by the solvents fume hood. I wish to thank all the past members of the Boncella group, but specially, Dr. Faisal Shafiq, Dr. David Knoeppel, Dr. Percefoni Doufou, Dr. Daniel Vanderlende, Dr. William Vaughan, Dr. Shu-Yu Steve Wang, Dr. Jonathan Penney, Justine P. Roth, and Rebecca Leigh Huff. Special thanks go to Dave Knoeppel for getting me back on the bicycle and being a great cycling partner.

I hope that in some way I have been helpful to the present members of the Boncella group. They certainly have been of great help and incomparable co-workers. Thanks to Dr. James Fisher, Ryan Mills, Ken Weakly, Tim Foley, Tom Cameron, and Patricia Gore.

I also would like to thank all the friends that I have made in my time at UF. Being so far away from home has been easier due to all the fun that I have had with all of them. Every single one of them is special in their own way and will not be forgotten. Honorable

mentions go to Dr. Harvey Ramirez, Dr. Alexis Garcia, Carlos and Maricel Rodriguez, Luis Suau, Gabriel and Ivellise Alcaraz, Gabo Alcaraz, Clinton and Jeannie Kaiser, Ivan Guzman, Marcus Garcia, Joaquin and Laura Alonzo, Andres Alonzo, Luis and Johana Zorrilla, Richard Pietri, Franco Ortiz, Fernando Gomez, Carlos Medina, Felisa Mora, Dr. Wendy Kozak, Brian and Dr. Amy Huff, Tabitha Hannacka, Abdul Azizi, and Tania White. I also wish to thank my friend Priscilla Magno who has always been there for me, although from a distance.

Finally, I wish to thank a very special person, Andrea Douat. She has not only given me strength and inspiration, but she has also given me back my soul.

TABLE OF CONTENTS

page

ACKNOWLEDGMENTS iii

ABSTRACT ix

1 INTRODUCTION AND BACKGROUND 1

Early-Transition Metal Complexes in High-Oxidation States. 1
Ancillary Ligands in Early-Transition Metal High Oxidation State Complexes. 4
Non-Cp Ancillary Ligands in Early Transition Metal Complexes. 5
Alkoxide Ancillary Ligands. 5
Organo-Imido Ancillary Ligands 7
Amido Ancillary Ligands 8
Transition Metal Alkyls 9
Transition-Metal Olefin Complexes 12
Transition-Metal Arene Complexes 16
Homogeneous Catalytic Hydrogenation of Olefins 19
Scope of the Dissertation 21

2 SYNTHESIS OF CHELATE-SUPPORTED DIALKYL AND ALKYLIDENE COMPLEXES OF MOLYBDENUM(VI) 23

Synthesis of Imido-Bridged Dimer 25
Synthesis of Chelate-Supported Dichloride Species 28
Synthesis of Dialkyl Complexes 35
Reactivity of **2** With Alkylating Agents 38
Synthesis of Chelate-Supported Alkylidenes 42
Polymerization Reactions 44
Conclusions 44

3 SYNTHESIS AND REACTIVITY OF MOLYBDENUM(IV) OLEFIN COMPLEXES SUPPORTED BY A CHELATING ANCILLARY LIGAND 46

Formation of Mo(VI) Metallacyclopentane 47
Formation of Mo(IV) Ethylene Complex 52
Synthesis of η^2-Olefin Complexes 53
Reactions of Olefin Complexes With σ-Donor Ligands 60
Crystal Structure of Mo(NPh)(CN(*t*-Bu))$_3$(*o*-(Me$_3$SiN)$_2$C$_6$H$_4$) (**23**) 63

Crystal Structure of Mo(NPh)(PMe_3)$_3$(*o*-(Me_3SiN)$_2C_6H_4$) (**24**) 65
Other Reactions of Mo(NPh)(η^2-olefin)(*o*-(Me_3SiN)$_2C_6H_4$) Complexes 66
Conclusions 68

4 LOW-PRESSURE HYDROGENOLYSIS OF MOLYBDENUM(IV) AND MOLYBDENUM(VI) COMPLEXES 69

Hydrogenolysis of Mo(IV) Olefin Complexes 70
Synthesis of Other Arene Complexes 72
Crystal Structure of Mo(NPh)(η^6-*m*-xylene)(*o*-(Me_3SiN)$_2C_6H_4$) (**30**) 75
Crystal Structure of Mo(NPh)(η^6-*p*-xylene)(*o*-(Me_3SiN)$_2C_6H_4$) (**31**) 77
Substitution of the Coordinated Arene Ligands 78
Catalytic Hydrogenation and Isomerization of Olefins 81
Hydrogenolysis of Mo(IV) Olefin Complexes in the Absence of Arene Ligands 84
Hydrogenolysis of Mo(VI) Dialkyl Complexes 86
Hydrogenolysis of Mo(VI) Dialkyl Complexes in the Presence of PMe_3 87
Crystal Structure of Mo(NPh)(PMe_3)$_3$(*o*-(Me_3SiN)(HN)C_6H_4) (**36**) 90
Conclusions 91

5 EXPERIMENTAL 93
General Methods 93
Synthesis of [Mo(NPh)(μ-NPh)(*o*-(Me_3SiN)$_2C_6H_4$)]$_2$ **1** 94
Synthesis of Mo(NPh)Cl_2(*o*-(Me_3SiN)$_2C_6H_4$)(NH_2Ph) **2** 95
Using Two Equivalents of Diamine 95
Using One Equivalent of Diamine 95
Synthesis of Mo(NPh)Cl_2(*o*-(Me_3SiN)$_2C_6H_4$)(PMe_3) **3** 96
Synthesis of Mo(NPh)Cl_2(*o*-(Me_3SiN)$_2C_6H_4$)(THF) **4** 96
Synthesis of Mo(NPh)Me_2(*o*-(Me_3SiN)$_2C_6H_4$) **5** 97
Synthesis of Mo(NPh)Ph_2(*o*-(Me_3SiN)$_2C_6H_4$) **6** 98
Synthesis of Mo(NPh)(CH_2CMe_3)$_2$(*o*-(Me_3SiN)$_2C_6H_4$) **7** 98
Synthesis of Mo(NPh)(CH_2Ph)$_2$(*o*-(Me_3SiN)$_2C_6H_4$) **8** 99
Synthesis of Mo(NPh)(CH_2SiMe_3)$_2$(*o*-(Me_3SiN)$_2C_6H_4$) **9** 100
Reactivity of **2** With Alkylating Agents 101
Synthesis of Mo(NPh)$_2$(CH_2CMe_3)$_2$ **10** 101
Synthesis of Mo(NPh)$_2$(CH_2SiMe_3)$_2$ **11** 102
Synthesis of Mo(NPh)(C(H)CMe_3)(*o*-(Me_3SiN)$_2C_6H_4$)(PMe_3) **13** 102
Synthesis of Mo(NPh)(C(H)$SiMe_3$)(*o*-(Me_3SiN)$_2C_6H_4$)(PMe_3) **14** 103
Synthesis of Mo(NPh)($CH_2CH_2CH_2CH_2$)(*o*-(Me_3SiN)$_2C_6H_4$) **16** 103
Method 1 103
Method 2 104
Method 3 104
Synthesis of η^2-Olefin Complexes (**19-22**) 105
R = $CH_2CH_2C_6H_5$ (**19**) 105
R = $CH_2CH_2CH_3$ (**20**) 106

R = $CH_2CH(CH_3)_2$ (**21**) 107
R = $CH_2CH_2CH_2CH_3$, $CH(CH_3)CH_2CH_3$, or $Mg(CH_2CH_2CH_2CH_3)_2$ (**22**) 107
Synthesis of Mo(NPh)(CN(*t*-Bu))$_3$(*o*-$(Me_3SiN)_2C_6H_4$) (**23**) 107
Synthesis of Mo(NPh)$(PMe_3)_3$(*o*-$(Me_3SiN)_2C_6H_4$) (**24**) 108
Reaction of **19** With Ethylene 109
Reaction of Mo(NPh)(η^2-styrene)(*o*-$(Me_3SiN)_2C_6H_4$) (**19**) with H_2 109
Synthesis of Mo(NPh)(η^6-arene)(*o*-$(Me_3SiN)_2C_6H_4$) (**26-33**) 110
Arene = Ethylbenzene (**26**) 110
Arene = Benzene (**27**) 111
Arene = Toluene (**28**) 111
Arene = *o*-Xylene (**29**) 112
Arene = *m*-Xylene (**30**) 112
Arene = *p*-Xylene (**31**) 113
Arene = Diphenylmethane (**32**) 113
Arene = Bibenzyl (**33**) 114
Reaction of **26** With Excess $CNC(CH_3)_3$ to Make **23** 114
Reaction of **26** With Excess PMe_3 to Make **24** 115
Reaction of **26** With Ethylene 115
Reaction of **26** With Styrene 115
Reaction of **7** With H_2 116
Reaction of Mo(NPh)(η^2-propene)(*o*-$(Me_3SiN)_2C_6H_4$) (**20**) With Hydrogen to Make **17** 116
Reaction of **7** With H_2 in the Presence of Excess PMe_3 to Make Mo(NPh)$(PMe_3)_3$(*o*-$(Me_3SiN)(HN)C_6H_4$) (**36**) 117
Synthesis of **36** From the Reaction of **24** and H_2 117
X-ray Experimental for Mo(NPh)Cl_2(*o*-$(Me_3SiN)_2C_6H_4$)(PMe_3) **3** 118
X-ray Experimental for Mo(NPh)(η^2-styrene)(*o*-$(Me_3SiN)_2C_6H_4$) **19** 119
X-ray Experimental for Mo(NPh)(CN(*t*-Bu))$_3$(*o*-$(Me_3SiN)_2C_6H_4$) (**23**) 119
X-ray Experimental for Mo(NPh)$(PMe_3)_3$(*o*-$(Me_3SiN)_2C_6H_4$) (**24**) 120
X-ray Experimental for Mo(NPh)(η^6-*m*-xylene)(*o*-$(Me_3SiN)_2C_6H_4$) (**30**) 121
X-ray Experimental for Mo(NPh)(η^6-*p*-xylene)(*o*-$(Me_3SiN)_2C_6H_4$) (**31**) 122
X-ray Experimental for Mo(NPh)$(PMe_3)_3$(*o*-$(Me_3SiN)(HN)C_6H_4$) (**36**) 123

APPENDICES

A NUCLEAR MAGNETIC RESONANCE SPECTRA 124

B TABLES OF CRYSTALLOGRAPHIC DATA 177

LIST OF REFERENCES 245

BIOGRAPHICAL SKETCH 262

Abstract of Dissertation Presented to the Graduate School
of the University of Florida in Partial Fulfillment of the
Requirements for the Degree of Doctor of Philosophy

SYNTHESIS, STRUCTURE, AND REACTIVITY OF DIAMIDE-SUPPORTED MOLYBDENUM COMPLEXES

By

Carlos Gilberto Ortiz Vazquez

August, 1999

Chairman: James M. Boncella
Major Department: Chemistry

The use of chelating diamide $[o\text{-}(Me_3SiN)_2C_6H_4]^{2-}$ as a co-ligand for high-oxidation early transition metal complexes has been investigated. Reaction of $Mo(NPh)_2Cl_2DME$ with $Li_2[o\text{-}(Me_3SiN)_2C_6H_4]$ afforded $[Mo(NPh)(\mu\text{-}NPh)(o\text{-}(Me_3SiN)_2C_6H_4)]_2$, while reaction of $Mo(NPh)_2Cl_2DME$ with $H_2[o\text{-}(Me_3SiN)_2C_6H_4]$ gave $Mo(NPh)Cl_2(o\text{-}(Me_3SiN)_2C_6H_4)(NH_2Ph)$. Two derivatives of $Mo(NPh)Cl_2(o\text{-}(Me_3SiN)_2C_6H_4)(NH_2Ph)$ are reported, $Mo(NPh)Cl_2(o\text{-}(Me_3SiN)_2C_6H_4)(PMe_3)$ and $Mo(NPh)Cl_2(o\text{-}(Me_3SiN)_2C_6H_4)(THF)$. Reaction of $Mo(NPh)Cl_2(o\text{-}(Me_3SiN)_2C_6H_4)(PMe_3)$ or $Mo(NPh)Cl_2(o\text{-}(Me_3SiN)_2C_6H_4)(THF)$ with RMgX (X = Cl or Br) gave $Mo(NPh)R_2(o\text{-}(Me_3SiN)_2C_6H_4)$ (R = Me, Ph, CH_2CMe_3, CH_2Ph, CH_2SiMe_3). Reaction of $Mo(NPh)Cl_2(o\text{-}(Me_3SiN)_2C_6H_4)(NH_2Ph)$ with RMgCl (R = CH_2CMe_3, CH_2SiMe_3) gave mixtures of $Mo(NPh)R_2(o\text{-}(Me_3SiN)_2C_6H_4)$ and

$Mo(NPh)_2R_2$. Both $Mo(NPh)_2(CH_2CMe_3)_2$ and $Mo(NPh)_2(CH_2SiMe_3)_2$ were isolated from the reaction of $Mo(NPh)_2Cl_2DME$ and RMgCl (R = CH_2CMe_3, CH_2SiMe_3). The alkylidene, $Mo(NPh)(C(H)CMe_3)(o\text{-}(Me_3SiN)_2C_6H_4)(PMe_3)$, was isolated from the reaction of $Mo(NPh)(CH_2CMe_3)_2(o\text{-}(Me_3SiN)_2C_6H_4)$ and an excess of PMe_3 at 80°C.

The reactivity of $Mo(NPh)Cl_2(o\text{-}(Me_3SiN)_2C_6H_4)(THF)$ toward alkyl Grignard reagents with β-hydrogens was examined. $Mo(NPh)Cl_2(o\text{-}(Me_3SiN)_2C_6H_4(THF)$ reacted with two equivalents of ethylmagnesium chloride to give a mixture of metallacyclopentane $Mo(NPh)(CH_2CH_2CH_2CH_2)(o\text{-}(Me_3SiN)_2C_6H_4)$ and Mo(IV) species $[Mo(\mu\text{-}NPh)(o\text{-}(Me_3SiN)_2C_6H_4)]_n$ (n = 1 or 2). Pure $Mo(NPh)(CH_2CH_2CH_2CH_2)(o\text{-}(Me_3SiN)_2C_6H_4)$ was obtained by reaction of $Mo(NPh)Cl_2(o\text{-}(Me_3SiN)_2C_6H_4)(THF)$ with two equivalents of EtMgCl under an atmosphere of ethylene. $Mo(NPh)Cl_2(o\text{-}(Me_3SiN)_2C_6H_4)(THF)$ reacted with RMgCl (R = CH_2CH_2Ph, $CH_2CH_2CH_3$, $CH_2CH(CH_3)_2$, $CH_2CH_2CH_2CH_3$, and $CH(CH_3)CH_2CH_3$) to give Mo(IV) olefin complexes of the type $Mo(NPh)(\eta^2\text{-olefin})(o\text{-}(Me_3SiN)_2C_6H_4)$ (olefin = styrene, propene, isobutene, 1-butene, and 2-butene). Excess trimethylphosphine and *tert*-butyl isocyanide reacted with $Mo(NPh)(\eta^2\text{-olefin})(o\text{-}(Me_3SiN)_2C_6H_4)$ to give six-coordinate compounds of the type $Mo(NPh)(o\text{-}(Me_3SiN)_2C_6H_4)L_3$.

The hydrogenolysis of $Mo(NPh)R_2(o\text{-}(Me_3SiN)_2C_6H_4)$ and $Mo(NPh)(olefin)(o\text{-}(Me_3SiN)_2C_6H_4)$ was studied. The Mo(IV) olefin complexes reacted with hydrogen and resulted in the hydrogenation of the olefin. In the presence of excess arene, $Mo(NPh)(arene)(o\text{-}(Me_3SiN)_2C_6H_4)$ complexes were isolated (arene = ethylbenzene, benzene, toluene, *o*-xylene, *m*-xylene, *p*-xylene, diphenylmethane, bibenzyl. In the

absence of a coordinating molecule, $[Mo(NPh)(o\text{-}(Me_3SiN)_2C_6H_4)]_n$ was isolated. Reaction of $Mo(NPh)(CH_2CMe_3)_2(o\text{-}(Me_3SiN)_2C_6H_4)$ with hydrogen also gave $[Mo(NPh)(o\text{-}(Me_3SiN)_2C_6H_4)]_n$. In the presence of excess PMe_3, $Mo(NPh)(o\text{-}(Me_3SiN)(HN)C_6H_4)(PMe_3)_3$ was isolated. Through the reaction of $Mo(NPh)(o\text{-}(Me_3SiN)_2C_6H_4)(PMe_3)_3$ with H_2, $Mo(NPh)(o\text{-}(Me_3SiN)(HN)C_6H_4)(PMe_3)_3$ was also isolated. The $Mo(NPh)(arene)(o\text{-}(Me_3SiN)_2C_6H_4)$ complexes were found to catalytically hydrogenate and isomerize olefins at ambient temperatures.

CHAPTER 1
INTRODUCTION AND BACKGROUND

While Organometallic Chemistry is a relatively young science, when compared to other fields of chemistry, it has continuously been a source of innovative and exciting breakthroughs. Transition metal organometallic chemistry lies at the crossroads between organic chemistry and inorganic chemistry since it is concerned with the interactions between inorganic metal atoms or ions and organic fragments or molecules.[1] By unifying these two "classical" fields of chemistry, organometallic chemistry has opened new frontiers in the search for discoveries and inventions to be used for the good of mankind.

Since organometallic chemistry can be viewed as a bridge between organic and inorganic chemistry, an organometallic compound can generally be defined as one that possesses a metal-carbon bond.[2] The nature of this bond often varies among single, double, triple bonds, or other types of interactions (e.g. π-complexes and σ-bond complexes). However, the common theme of an interaction between an organic fragment and a metal ion or atom is always maintained. Even though this definition might seem restrictive, the combinations and possibilities are virtually endless.

Early Transition Metal Complexes in High Oxidation States

Due to the wide range of uses in, for example, organic synthesis, catalysis, and polymerization, the study of early transition metal complexes can be considered as one of

the most important topics of study in organometallic chemistry.[3-6] The study of the properties and reactivities of these compounds is essential to develop an understanding of their role in these transformations and for the design of novel catalysts for further applications.

Complex organic molecules can easily be constructed with reactions involving high-oxidation state metal complexes. For example, as shown in Figure 1.1, many researchers have shown that the Cp_2MCl_2/n-BuLi system is ideal to build complex organic molecules by constructing metallacyclic species from common organic precursors.[7-15] Alkylidenes have also been conveniently used to construct complex organic ring systems through the metathesis of olefins, acetylenes, dienes, and similar species.[16-20] In addition, mono- and bis-imido species have been used to catalytically metathesize imines.[21-24]

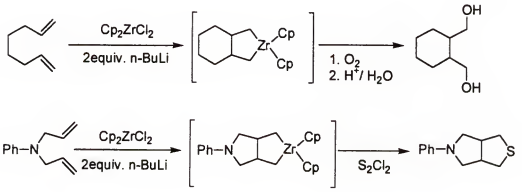

Figure 1.1. Metallacyclopentane-mediated organic synthesis with the Negishi "Cp_2Zr" system.

There is an immense amount of study into the use of early transition metal complexes in high oxidation states to catalytically polymerize strained cyclic-olefins, and

acetylenes through the olefin and acetylene metathesis reaction.[25-32] Ring-opening metathesis polymerization (ROMP)[25-27] and acyclic-diene metathesis (ADMET)[33] are two examples of alkylidene-catalyzed polymerizations.

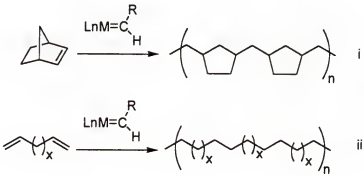

Figure 1.2. i) Ring-opening metathesis polymerization. ii) Acyclic-diene metathesis polymerization.

The study of the homogeneous polymerization of olefins by Ziegler-Natta type organometallic systems has been at the forefront of early-transition metal organometallic chemistry.[34-38] It has been shown that Group 3, 4, and 5 complexes in their highest oxidation states (d^0) can polymerize olefins into high molecular weight polymer chains with controllable structures when an alkyl aluminum compound is used as a co-catalyst.[36] More recently, it has been discovered that also late-transition[39-45] and f-block[46-48] metal catalysts can polymerize olefins with similar activities to the early-transition metal catalysts.

Ancillary Ligands in Early Transition Metal High Oxidation State Complexes

The structure and properties given to metal complexes by ancillary ligands are some of the most important factors influencing the reactivity of these complexes. Both electronic and steric factors influence the outcome of reactions while also providing stability and structural integrity. Thus the use of new, and sometimes exotic, co-ligands has been a major part of new developments seen in organometallic chemistry.[49]

By far, the most widely used ligands in early transition metal chemistry are cyclopentadienyl (Cp)-type ring systems. Commonly, Cp systems are purposely used to influence yields of reactions, chirality of products, and activity of catalysts. For example, C_5Me_5 (Cp*) provides more steric hindrance and electron density than C_5H_5 (Cp) and protects metal complexes from bimolecular decomposition pathways, although it has been observed to participate in intramolecular decomposition reactions.[50] As shown in Figure 1.3, metallocenes can be made which produce polypropylene of varying tacticity depending on the structure of the catalytic species.[51]

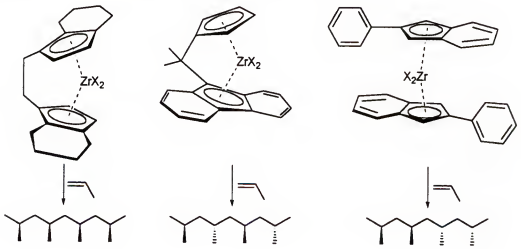

Figure 1.3. Catalysts for stereospecific propylene polymerization.

Non-Cp Ancillary Ligands in Early Transition Metal Complexes

A direction recently taken by researchers has been to use ligands that donate six electrons to the metal as cyclopentadienyls would. For example, the coordination of tris-pyrazolyl borates (Tp) ligands has been considered by some to be analogous to Cp coordination.[52] Another direction has been to explore 6π-electron donor heterocyclic ligands that bind to the metal in a fashion similar to cyclopentadienyl ligands. For example, Group IV metal π-complexes with boron-carbon and phosphorus-carbon heterocyclic ligands have been examined for catalyst activity.[53] Brown *et al.* have developed a phosopholyl-amido ligand, $(C_4PMe_4)SiMe_2(N\text{-}t\text{-}Bu)^{-2}$, that is analogous to $C_5H_4(SiMe_2)N(t\text{-}Bu)^{-2}$ and that when bound to Ti(IV) shows comparable activity towards the polymerization of ethylene.[54]

Alkoxide Ancillary Ligands

Many research programs have been carried out emphasizing the development of alkoxide ligands as alternatives to cyclopentadienyl. Wolczanski has used bulky alkoxides $(t\text{-}Bu)_3CO^-$ (tritox) and siloxide $(t\text{-}Bu)_3SiO^-$ (silox) ligands to prepare d^0 and d^2 metal-complexes of groups 4, 5, and 6.[55] Many of the results observed have been significantly aided by the bulkiness provided by these ligands. For example, low coordination number d^2 complexes like $(silox)_3Ta$ and $(silox)_2W{=}(N\text{-}t\text{-}Bu)$ have shown remarkable stability and very rich reactivity.[55] Wigley has suggested that aryloxide-supported tantalum(III) centers can serve as models for dehydronitrogenation (HDN) of pyridines and quinolines (Figure 1.4).[56] On the other hand, Rothwell has demonstrated

how aryloxide coordination can enhance reactivity to the point of promoting the hydrogenation of arene rings and the intramolecular activation of C-H bonds.[57,58]

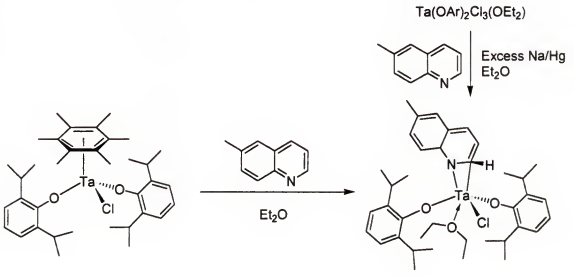

Figure 1.4. Models for dehydronitrogenation (HDN) using alkoxide ligands.

Extensive studies by Basset[59] have shown how aryloxide ligated W(VI) complexes can be used as highly active ROMP catalysts of functionalized olefins. Likewise, Schrock[32] and others[60] have developed the use of alkoxy supported metathesis catalysts for the polymerization of olefins and acetylenes, and the ring-closing metathesis (RCM) of olefins. Furthermore, chiral bis-alkoxy ligands have recently been used to catalytically and asymmetrically synthesize ring systems through RCM (Figure 1.5).[61,62]

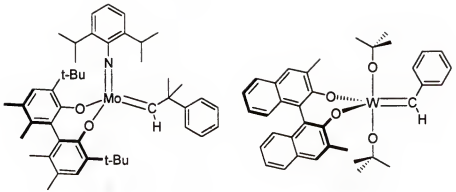

Figure 1.5. Structures of two forms of group 6 catalysts used in chiral metathesis chemistry.

Organoimido Ancillary Ligands

Isolobal relationships like that between the metal-ligand fragments Cp_2Zr and $(RN)_2Mo$, established by quantum-mechanical calculations and by experimental studies, have prompted the study of imido ligands (NR^{-2}) as potential alternatives to Cp ligation in early transition metal complexes.[63-66] Gibson,[67,68] and others,[69-85] have for many years concentrated their efforts into using organoimido ligands to support group 5 and 6 complexes in high oxidation states. Imido complexes of d^0-metals have been synthesized with a wide range of subtituents varying in bulkiness and electronic demands. This has been a direct result of the central role imide ligands play in the stabilization of metathesis catalyst of Mo, W, and Re.[27,32] In particular, four-coordinate molybdenum complexes of the type $Mo(NAr)(C(H)CMe_2Ph)(OR)$ have found widespread application in the controlled synthesis of polymers via ROMP.[75]

Amido Ancillary Ligands

For many years, there has been an extensive and important chemistry surrounding transition metal to nitrogen single bonds. The chemistry of transition metal to nitrogen σ-bonds in complexes of the type ML_n, where $L = NR_2^-$, has revealed the stabilization of unusual coordination numbers and valence states of metal ions by extremely bulky ligands such as N-*i*-Pr_2 and $N(SiMe_3)_2$.[86] For early transition metals, work by many researchers has provided the synthesis of d^0 metal-polyamides of group 4, 5 and 6.[86-90]

The use of amide ligands for organometallic complexes has recently re-emerged as a very active area for early transition metal complexes in the hope that these may provide the next generation of reagents and catalysts.[91] The focus has been mainly on group 4 metal complexes. For example, Roesky *et al.* have recently reported the syntheses of group 4 $Cp^*(NR_2)MX_2$ and $(NR_2)_2MX_2$ complexes which were shown to be effective ethylene polymerization catalysts in the presence of methylaluminoxane (MAO).[92,93]

Work from our group has focused on the use of bidentate amide ligands to support early transition metal complexes in high oxidation states.[94,95] While amide ligands have been successfully used in the past to stabilize early transition metal complexes in high oxidation states, bidentate ligands have been shown to provide additional stabilization because of the chelate effect.

Previous work from our group has focused on the chemistry of tungsten-imido dichloride, dialkyl, alkylidene, and olefin compounds supported by ligands derived from N,N'-bis-trimethylsilyl-o-phenylenediamine (H_2-*o*-$(Me_3SiN)_2C_6H_4$).[94-100] During the conversion of pre-catalyst species to active catalysts, it has sometimes been observed that

the metal center can become inactive due to decomposition reactions related to the instability of the active species. Thus, we have been interested in using N,N'-disubstituted-*o*-phenylenediamides (*o*-pda) as ancillary ligands that, due to the chelate effect, can provide better stability for high-oxidation state early transition metal systems that could serve as active catalysts in transformations promoted by organometallic species. This could in turn, allow for longer-lived catalysts and higher productivity.

While disubstituted-pda compounds have already been reported for Zr(IV), Ti(IV)[101] and recently Ta(V)[102] our efforts with other members of Group 6 had until now been unsuccessful. Other researchers have shown that bidentate diamide ligands can effectively support groups 4 and 5 d^0-metal compounds.[101-105] Tilley has used [*o*-(i-$Pr_3SiN)_2C_6H_4]^{2-}$ to support Ti(IV), Zr(IV), and Ta(V) complexes.[101,102] Jeon *et al.*[106] and Lee *et al.*[107] have shown how some d^0-diamide metal complexes can effectively serve as catalysts in the polymerization of olefins. Likewise, Ti(IV) complexes supported by $[(2,6\text{-i-}Pr_2C_6H_3)NCH_2CH_2CH_2N(2,6\text{-i-}Pr_2C_6H_3)]^{2-}$ have been shown to polymerize olefins in a living manner.[108] Tridentate and tetradentate amides have also played a relevant role in early transition metal chemistry.[109-121]

Transition Metal Alkyls

The chemistry of main-group metal-carbon bonds dates back to the 19th century. Transition-metal compounds containing metal-carbon single, double, and triple bonds have only come to be understood much more recently.[2] Edward Frankland's discovery of Zn alkyls in 1849 promoted numerous attempts to prepare transition metal analogues.[3,5]

Although evidence for unstable species was made at low temperatures, no compounds could be isolated. In 1907 Pope and Peachy isolated $[(CH_3)_3PtI]_4$ and $[AuBrEt_2]_2$ was synthesized, but more typically only organic decomposition products, transition metals, or reduced metal species were obtained.[6] Other stable complexes were not isolated until the 1950's, which led to the assumption that metal-carbon bonds were thermodynamically unstable.[2,3]

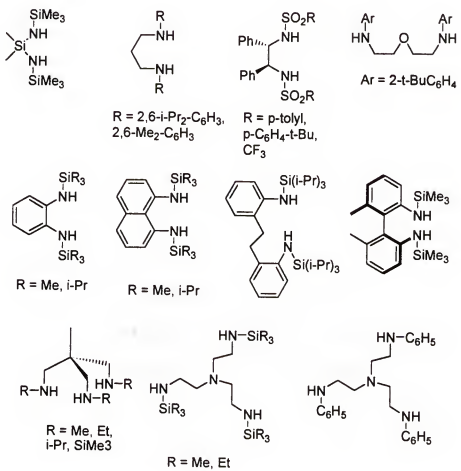

Figure 1.6. Some amines used as precursors to polydentate amido ligands.

The availability of low-energy decomposition pathways has been the main reason why isolating transition-metal alkyl complexes has proven to be difficult.[6] Many compounds containing M-C σ-bonds are known, however, these commonly contain other ancillary ligands to improve the stability.[6] The stability of metal alkyl complexes having Cp, CO, or PR_3 groups present is the result of the blocking of vacant coordination sites needed for H-atom transfers by these firmly bound ligands.[3]

Even in the absence of stabilizing ligands, transition metal alkyl compounds that are stable to H-atom transfer decomposition processes have been isolated. The use of groups without β-hydrogens allows isolation of stable alkyls. Common alkyl ligands that do not show β-H transfers are methyl, neopentyl, trimethylsilylmethyl, benzyl, and metallacycles.[4,6,122,123] Yet, in some instances, alkyl ligands that do contain β-hydrogens have been isolated. The stability of compounds like Cr(*t*-butyl)$_4$ and Os(cyclohexyl)$_4$ has been attributed to ligand conformations inhibiting β-H transfers.[124] Also, because of the instability of the olefins that would be formed by β-H transfer, 1-adamantyl and 1-norbornyl groups form stable metal complexes.[122,125,126]

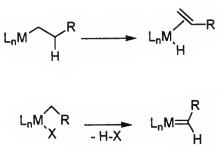

Figure 1.7. Beta-hydride elimination and α-abstraction

Transition-metal alkyl complexes commonly decompose by well-known pathways like β-H elimination, α-abstraction, and reductive elimination. The availability of these decomposition pathways depends both on structural and electronic factors. Hence, dialkyl compounds that cannot attain conformations necessary for decomposition or where no molecular orbital is low enough in energy to participate in decomposition are usually stable.[127]

For this reason, we started the task of isolating alkyl complexes of group 6 metals in which the diamide ligand (*o*-pda) became the stabilizing factor while providing opportunities for the derivatization of these into species active in the polymerization of olefins, hydrogenation of unsaturated species, and other organic synthesis transformations.

Transition-Metal Olefin Complexes

The involvement of transition metal olefin complexes in many industrially important reactions has prompted their study by many researchers.[4] Since the early stages of organometallic chemistry, they have also sparked the interest of the scientific community because of their special bonding and structural characteristics.

Olefin complexes are more common for the late transition metals than for the early transition metals (obviously due to increased π-backbonding capabilities). Early transition metal olefin complexes are proposed intermediates in many important synthetic reactions.[1,4,5,15] However, the isolation of these has sometimes proven difficult when the metal is in a high oxidation state (0-2 d-electrons).

Metal complexes with two d-electrons are more commonly seen to bind olefins than their d^0 counterparts. The choice of an appropriate ancillary ligand seems to play a major role in the isolation of an olefin complex. There are a few examples of Cp-ligated olefin complexes. Bercaw *et al.* successfully isolated and characterized $Cp^*_2Ti(\eta^2$-ethylene) from either the reduction of $Cp^*_2TiCl_2$ under an atmosphere of ethylene or by the reaction of $[Cp^*_2Ti]_2(\mu\text{–}N_2)$ with ethylene.[128] This complex also showed reactivity with free ethylene as the coordinated ethylene was oxidatively coupled to free ethylene molecules. However, no coupling was observed when propene or butene were used. More recently, Bergman reported the reactivity of $Cp^*_2Ti(\eta^2$-ethylene) with diazoalkane to yield stable η^2-diazoalkane complexes.[129,130]

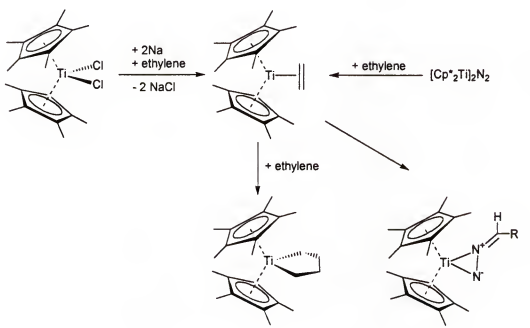

Figure 1.8. Synthesis and reactivity of $Cp^*_2Ti(\eta^2$-ethylene).

Other examples of Cp-ligated d^2-metal olefin complexes include $Cp_2Zr(\eta^2$-ethylene$)(PMe_3)$,[131] $Cp_2Ta(\eta^2$-ethylene$)(CH_3)$,[132,133] and $Cp_2Nb(\eta^2\text{-}CH_2{=}CHC_6H_4\text{-}p\text{-}X)(H)$[123,134] (X = H, CF_3, OMe, NMe_2). Buchwald *et al.*[135] have also been able to isolate a rare example of an isobutene complex, $Cp_2Hf(\eta^2\text{-}CH_2{=}CMe_2)(PMe_3)$, which is analogous to $Cp_2Zr(\eta^2$-butene$)(PMe_3)$ and $Cp_2Hf(\eta^2$-butene$)(PMe_3)$ made by Negishi.[136-139] Schrock has isolated and characterized the alkylidene-olefin complex $Cp^*Ta(=C(H)(t\text{-}Bu))(\eta^2$-ethylene$)(PMe_3)$ from the reaction of alkylidyne $Cp^*Ta(C\text{-}t\text{-}Bu)(PMe_3)Cl$ and 0.5 equivalents of $MgEt_2$(dioxane).[140] Likewise, Green *et al.* has reported making $CpMoCl(N\text{-}t\text{-}Bu)(\eta^2\text{-}CH_2{=}CHR)$ (R = H, Ph) although they reported very low yields.[141,142]

Few reports can be found in the literature where olefin complexes are ligated by alkoxide ligands. LaPointe *et al.*[143] has reported that $(silox)_3Ta$ reacts with ethylene or propene to give η^2-olefin complexes in good yield. Robbins *et al.*[144] reported $Mo(NAr)(OR)_2(\eta^2\text{-}CH_2{=}CHSiMe_3)$ although it quickly decomposes out of solution. However they did isolate $Mo(NAr)(OR)_2(\eta^2$-ethylene$)(PMe_3)$ from the reaction of metallacyclopentane, $Mo(NAr)(OR)_2(C_4H_8)$, with PMe_3.

Some olefin complexes of d^2-imido complexes have been prepared by Dyer *et al.*[145,146] Both $Mo(N\text{-}t\text{-}Bu)_2(\eta^2$-ethylene$)(PMe_3)$ and $Mo(N\text{-}t\text{-}Bu)_2(\eta^2$-ethylene$)(PMe_3)_2$ were isolated from the reaction of $Mo(N\text{-}t\text{-}Bu)_2Cl_2$(DME) with EtMgCl in the presence of one or two equivalents of PMe_3, respectively. The use of *n*-PrMgCl gave the analogous propene complexes. Similar results were obtained for aryl and adamantyl imido analogs.[147,148] Schrock reported that $Ta(NPh)(PMe_3)_4Cl$ reacts with ethylene or styrene to

give $Ta(NPh)(\eta^2\text{-olefin})(PMe_3)_3Cl$ while $W(NPh)_2(PMe_2Ph)_2$ reacts with norbornene to give an η^2-norbornene complex.[149,150] Likewise, $W(NAr)Cl_2(PMe_3)_2(\eta^2\text{-olefin})$ (olefin = ethylene, propene, cis-2butene, isobutene) have been prepared by Clark *et al.* from the reduction of W(V) complex $W(NPh)Cl_3(PMe_3)_2$.[151,152] A related complex is $W(O)Cl_2(\eta^2\text{-ethylene})(PMePh_2)_2$ which was reported by Su *et al.* to be made from $W(O)Cl_2(PMePh_2)_3$.[153]

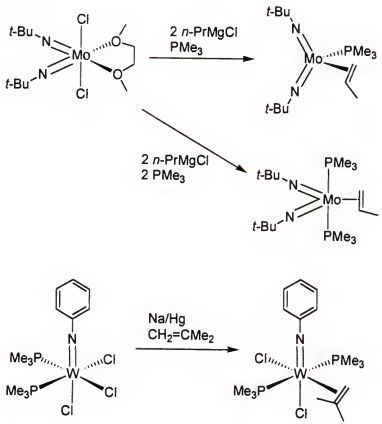

Figure 1.9. Synthesis of some d^2-imido alkene complexes.

Transition-Metal Arene Complexes

Metal complexes of six-membered aromatic carbocycle ligands have attracted the interest of inorganic chemists since Fischer and Hafner characterized $Cr(\eta^6\text{-benzene})_2$, obtained from the reduction of $CrCl_3$ with $Al/AlCl_3$ in benzene as solvent.[154-156] Since then the chemistry of π-arene complexes has been considerably developed.[157] While this chemistry was initially believed to be confined to low-oxidation-state transition metals, it has now been shown that stable and isolable π-arene metal complexes can also exist for transition elements in higher oxidation states.[157]

Arene complexes of the early transition metals have been known for some time. Many of the results obtained have been of low-oxidation-state complexes,[158-167] although examples of d^0-metal-arenes[168-174] have become more common in the literature. Strangely, arene complexes of d^2-metal centers have not been as common.

Troyanov has studied group 4 arene complexes in the +2 oxidation-state.[175] It was reported that the reduction of metal-tetrahalides MX_4 (M = Ti, Zr) by another metal in the presence of AlX_3 and arene ligand affords $M(\eta^6\text{-arene})$ complexes, as shown in Figure 1.10.[176]

Cotton has also reported that the reduction of HfI_4 with two equivalents of sodium amalgam in benzene or toluene, followed by the addition of two equivalents of PMe_2Ph afforded the isolation of $(\mu\text{-}\eta^{12}\text{-arene})Hf_2I_4(PMe_2Ph)_4$.[177] A different product was isolated from the reduction of $ZrCl_4$ with two equivalents of Na/Hg in toluene and two equivalents of PMe_2Ph. This reaction gave the dimeric compound shown in Figure 1.11ii.[178,179] This is different than what Green *et al.* observed upon treatment of $ZrCl_4$

with Na/K and PMe_3 in toluene.[180] This reaction gave $Zr(\eta^6\text{-toluene})Cl_2(PMe_3)_2$. Green has also reported the synthesis of $M(\eta^6\text{-arene})(\eta^3\text{-allyl})_2$ (M = Hf, Zr; arene = benzene, toluene) although no obvious mechanism is available (Figure 1.11iv).[181]

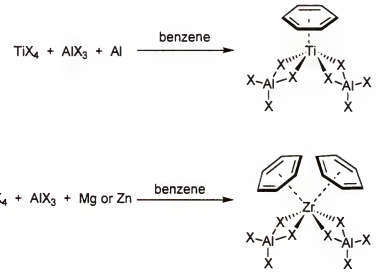

Figure 1.10. Arenes prepared by reduction in the presence of AlX_3 and benzene.

Alkyne trimerization has been a major way of obtaining arene complexes of the transition metals.[157] Bruck *et al.* have used this method to obtain d^2-tantalum arene complexes. By reducing $Ta(OAr)_2Cl_3$ with two equivalents of Na/Hg in the presence of excess RC≡CR (R = Me, Et), $(C_6R_6)Ta(OAr)_2Cl$ were obtained.[182] Evidence that these arene ligands were assembled at the metal center was provided by the fact that no $(C_6Me_6)Ta(OAr)_2Cl$ was obtained by reducing $Ta(OAr)_2Cl_3$ in the presence of hexamethylbenzene. Later publications from Wigley's lab have shown the coordinatively rigid nature of the arene ligand in these tantalum metal centers and the generality of cyclotrimerization reactions by Ta(III) centers.[182-187]

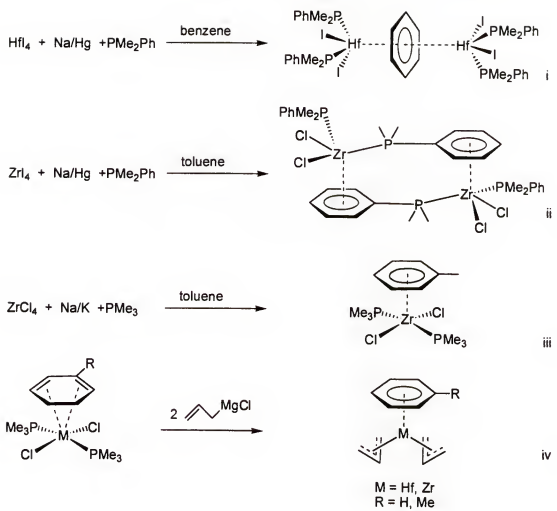

Figure 1.11. Group 4 arene complexes with oxidation-state +2. Cotton (i and ii), Green (iii and iv).

Tantalum(III) complexes where the arene coordinates in an η^2-fashion have also been reported. This is the case for $[(silox)_3Ta]_2(\mu\text{-}\eta^2(1,2)\text{-}\eta^2(4,5)\text{-benzene})$ which is a product of the dissolution of $(silox)_3Ta$ in benzene for 10-14 days.[188]

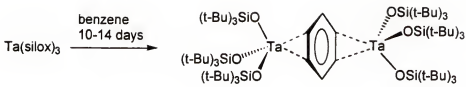

Figure 1.12. Arene dimer of tantalum(III) reported by Wolczanski.

Homogeneous Catalytic Hydrogenation of Olefins

Homogeneously catalyzed hydrogenation of unsaturated organic substrates is an important class of organometallic reactions.[4,189] Olefins have been the most thoroughly studied substrates although other functional groups, such as acetylenes and carbonyls, can be hydrogenated in the presence of soluble catalysts.[189,190]

Two accepted mechanisms for homogeneously catalyzed olefin hydrogenation are shown in Figure 1.13. Intermediate metal dihydrides transfer hydrogen to olefins by insertion and reductive elimination steps. However, both monohydride and dihydride species are known to hydrogenate substrates and can be generated in different ways. Monohydride intermediates hydrogenate olefins by inserting the substrate into the M-H bond and undergoing σ-bond metathesis of the M-H bond with H_2.

The most famous hydrogenation catalyst is commonly known as Wilkinson's catalyst, $RhCl(PPh_3)_3$.[189-192] It is widely used in organic chemistry because of its reliability and selectivity. Like Wilkinson's catalyst, most of the hydrogenation catalysts that are commonly used are of the late transition metals.[189] Some remarkable advances have been made in this field, specially marked by the development of catalysts for asymmetric hydrogenation.[193] Yet, since the 1960s the development of early-transition-

metal hydrogenation catalysts has gained importance because of the interest in learning whether Ziegler-Natta type catalyst would activate hydrogen for the hydrogenation of organic molecules.[194]

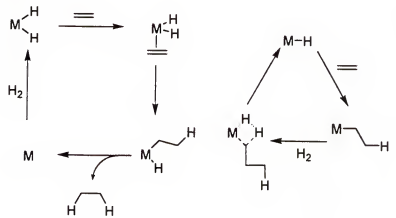

Figure 1.13. Two general mechanisms for the hydrogenation of olefins by hydride species.

Sloan *et al.* found that $Cp_2TiCl_2/AlEt_3$ gave 70% yield of *n*-octane from 1-octene on standing overnight at room temperature under 4.4 atm of H_2.[194] Catalysts systems like $Ti(i\text{-}Pr)_4/Al(i\text{-}Bu)_3$ also gave reduction of olefins to alkanes. More recently, Halterman *et al.* designed Ziegler-Natta type systems that enantioselectively hydrogenated alkenes.[195,196] Figure 1.14 shows the systems used by Vollhardt which upon addition of *n*-BuLi and exposure to H_2 hydrogenated 2-phenyl-1-butene to 2-phenylbutene with optical purity in excess of 95%. Other researchers have also shown the asymmetric hydrogenation of olefins[197-200] and imines[201] by Ziegler-Natta type systems.

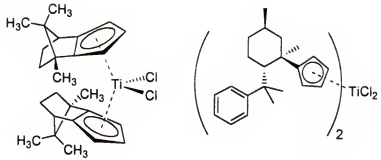

Figure 1.14. Pre-catalyst systems used by Vollhardt *et. al.* for the asymmetric hydrogenation of olefins.

Scope of the Dissertation

In this dissertation, my research on the synthesis, structure and reactivity of chelate-stabilized molybdenum dialkyl, alkylidene, olefin, and arene complexes is presented. With this work, we have tried to accomplish the synthesis of stable organometallic species that can serve as pre-catalysts for polymerization, hydrogenation, isomerization, and coupling reactions. The added stability provided by the chelating ligand is expected to enhance reactivity and productivity in catalytic reactions by increasing the lifetime of the active species.

The introduction to each chapter cites our group's previous related studies. Chapter 2 presents the results obtained from the synthesis of chelate-stabilized dichloride and dialkyl complexes. The conversion of some of the dialkyl complexes into alkylidene complexes is also presented along with the preliminary results related to the catalytic polymerization activity of these complexes. In chapter 3 the discussion focuses on the spontaneous decomposition of dialkyl complexes when the alkyl chains contain hydrogen atoms on the β-carbon. A series of olefin complexes and a metallacycle were easily

isolated. Also, comments about their synthesis, structure, and reactivity are presented. Chapter 4 then talks about the reactivity of both the Mo(VI) and Mo(IV) complexes presented in chapter 2 and chapter 3 with molecular hydrogen. A series of arene complexes were isolated and characterized. In chapter 4, possible mechanisms by which the isolated products can be made from the starting materials studied are presented along with the discussion of their ability to catalytically hydrogenate and isomerize olefins.

CHAPTER 2
SYNTHESIS OF CHELATE-SUPPORTED DIALKYL AND ALKYLIDENE COMPLEXES OF MOLYDENUM(VI)

Previous research from our group has focused on the chemistry of W(VI) imido dichloride, dialkyl, and alkylidene compounds supported by ligands derived from N,N'-bis-trimethylsilyl-o-phenylenediamine (H_2-*o*-$(Me_3SiN)_2C_6H_4$).[94,95] By using this chelating ligand, the synthesis of a large number of thermally stable, coordinatively unsaturated dialkyl species of W(VI) was achieved.[96] These complexes displayed insertion chemistry with alkyl isocyanides,[97] and undergo β-hydride-abstraction in the presence of Lewis bases.[98,99] In addition, the neopentylidene complex W(NPh)(C(H)CMe_3)(*o*-$(Me_3SiN)_2C_6H_4$)(PMe_3) was shown to catalyze the ROMP of norbornene and cyclooctene, and catalyze the ADMET oligomerization of 1,9-decadiene.[100]

For some time, we have been interested in using N,N'-disubstituted-*o*-phenylenediamides (*o*-pda) as ancillary ligands for other high-oxidation state early transition metal systems. While disubstituted-pda compounds have already been reported for Zr(IV), Ti(IV),[101] and recently Ta(V),[102-202] our efforts with other elements of Group 6 were initially unsuccessful.

It seems to be that the metallic starting materials and diamide ligand precursors used to attach diamide groups to early transition metal complexes can not be used arbitrarily. While [*o*-$(Me_3SiN)_2C_6H_4]^{-2}$ was attached fairly easily to W(VI), by reacting

$Li_2[o\text{-}(Me_3SiN)_2C_6H_4]$ with $W(NPh)Cl_4(OEt_2)$, the same reaction was not effective for the analogous Mo(VI) compounds and similar Mo species. For example, $Mo(NPh)Cl_4(THF)$ was allowed to react with $Li_2[o\text{-}(Me_3SiN)_2C_6H_4]$ to give an intractable mixture. Similar results were obtained if other metals were used. Mixtures of unidentifiable products were obtained if $ZrCl_4$ or $TaCl_5$ were allowed to react with $Li_2[o\text{-}(Me_3SiN)_2C_6H_4]$. Yet, Aoyagi *et al.* reported that $Li_2[o\text{-}(i\text{-}Pr_3SiN)_2C_6H_4]$ reacted with $ZrCl_4$ and $TiCl_4$ to give compounds of the type $MCl_2(o\text{-}(i\text{-}Pr_3SiN)_2C_6H_4)$ (M = Ti, Zr).[101,102] Likewise, Pinad *et al.* reported that $Cp'TaCl_4$ reacted with $Li_2[o\text{-}(Me_3SiN)_2C_6H_4]$ to give $Cp'TaCl_2(o\text{-}(Me_3SiN)_2C_6H_4)$.[202]

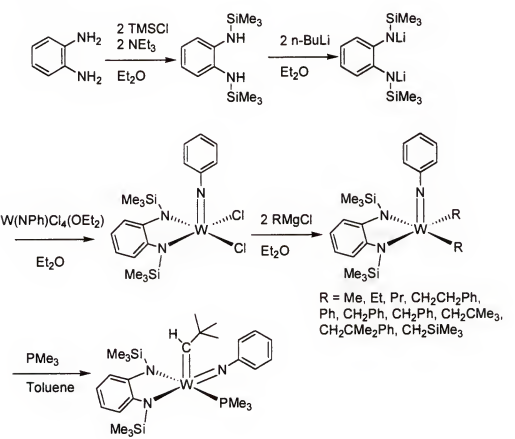

Figure 2.1. Synthesis of W(VI) dialkyl and alkylidene complexes.

The reasons why some diamide ligands can be attached to some metal species while not to others are not immediately obvious. Therefore, a more suitable synthetic scheme and starting material to extend our interests to Mo chemistry had to be found. The starting material that successfully gave Mo(VI) diamides was $Mo(NPh)_2Cl_2(DME)$.[203] This chapter summarizes the initial results concerning the synthesis of Mo(VI) dialkyl species and their derivatives.

Synthesis of Imido-Bridged Dimer

Since our bidentate diamide ligand was bound to W(VI) through the reaction of dilithiated Li_2-*o*-$(Me_3SiN)_2C_6H_4$ with $W(NPh)Cl_4(OEt_2)$[95] (Figure 2.1), the reaction of Li_2-*o*-$(Me_3SiN)_2C_6H_4$ with $Mo(NPh)_2Cl_2DME$[203] was investigated.

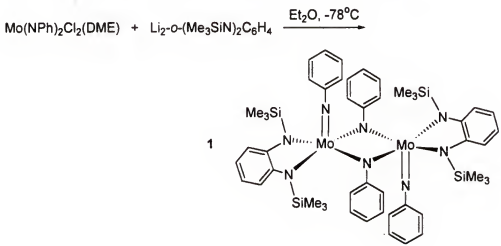

Figure 2.2. Synthesis of imido-bridged dimer **1**.

When Li_2-*o*-$(Me_3SiN)_2C_6H_4$ was prepared *in situ* in Et_2O and cooled to -78°C then added to an -78°C Et_2O slurry of $Mo(NPh)_2Cl_2DME$, a rapid color change from

orange to green occurred as the reaction mixture returned to room temperature. Filtration of the reaction mixture followed by extraction of the remaining solids with toluene and removal of the solvent *in vacuo* produced low yields of forest-green, microcrystalline $[Mo(NPh)(\mu\text{-}NPh)(o\text{-}(Me_3SiN)_2C_6H_4)]_2$ **1**.

The ^1H NMR spectra of **1** are consistent with the dimeric structure shown in Figure 2.2. A sharp singlet was observed at -0.04 ppm (36H) and is assigned to equivalent Me_3Si groups. Signals corresponding to the phenylimido *ortho*-protons were observed as two doublets at 6.55 ppm (4H) and 6.74 ppm, which arise from the inequivalent phenylimido groups. This inequivalency was also confirmed by the observation of a triplet at 6.87 ppm (2H) and a triplet overlapping with the doublet at 6.74 ppm (together integrating to 6H), with both triplets corresponding to the *para*-phenylimido hydrogens. A triplet for a *meta*-phenyl imido hydrogen was observed at 7.00 ppm with its inequivalent counterpart overlapping with one of the pda-ring resonances from 7.07 ppm-7.12 ppm. The other pda-ring resonance was clearly observed at 7.26 ppm (4H).

Further proof of the formulation of **1** was obtained from a single crystal X-ray diffraction study. Unfortunately, a publishable structure refinement was not obtained. However, the data were sufficient to confirm the identity of **1** as an imido-bridged dimer supported by the chelating-diamide group, as shown in Figure 2.3. It is noted that several examples of imido-bridged dimers have been reported, thus the structure of **1** is precedented.[204-214]

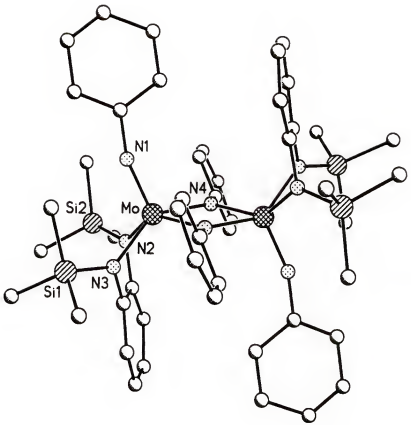

Figure 2.3. Drawing of the crystal structure of **1**. All atoms are shown in isotropic mode.

Attempts to transform **1** into other species were unsuccessful. Addition of excess PMe_3 to a C_6D_6 solution of **1** gave no reaction and only starting materials were observed by ^1H NMR even after heating the mixture to 80°C for 1hr. Furthermore, thermolysis of **1** in a NMR tube heated to 80°C overnight (C_6D_6) gave an intractable mixture.

Synthesis of Chelate-Supported Dichloride Species

When a suspension of brick-red $Mo(NPh)_2Cl_2DME$ in hexanes was mixed with a hexanes solution containing two equivalents of H_2-*o*-$(Me_3SiN)_2C_6H_4$ and stirred overnight, a slow reaction occurred giving a dark green solution along with a blue precipitate. Filtration of the reaction mixture gave a nearly quantitative yield of a hexanes-insoluble, blue-purple powder, **2**.

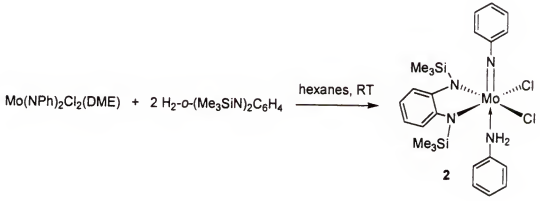

Figure 2.4. Synthesis of aniline adduct **2**.

The NMR spectra of **2** were consistent with the structure shown in Figure 2.4. Proton NMR (C_6D_6) spectra of **2** displayed one resonance due to equivalent Me_3Si groups at 0.40 ppm (18H) and a broad singlet at 3.92 ppm (2H) corresponding to the coordinated aniline N-H protons. Although the aromatic region in the ^1H NMR of **2** was rather complex (three different phenyl rings), the presence of the o-phenylenediamide ring was confirmed by the observation of its two resonances overlapping with signals from the coordinated aniline around 6.6 ppm (m, 8H).

Slightly lower yields of **2** were obtained by refluxing $Mo(NPh)_2Cl_2DME$ and one equivalent of H_2-*o*-$(Me_3SiN)_2C_6H_4$ in hexanes for seven hours followed by cooling to room temperature and filtration. Alternatively, **2** was also isolated by stirring equimolar quantities of starting materials in hexanes at room temperature for two days.

A proposed pathway for the formation of **2** is shown in Figure 2.5. Loss of DME from the starting material is followed by coordination to H_2-*o*-$(Me_3SiN)_2C_6H_4$. Next, a diamine proton is transferred to an imido nitrogen. Following the initial proton transfer there are two conceivable pathways involving H-transfer from the coordinated diamine ligand. In pathway A, **2** is obtained by direct protonation of the anilide ligand. In pathway B, proton transfer to the remaining imido nitrogen to form a dianilide complex could then be followed by formation of aniline and an imido ligand. These types of proton transfer reactions have been postulated to be part of the formation of multiply bonded ligands in related complexes.[69, 70]

For example, Danopoulos *et al.* reported that the reaction of $Cr(NBu^t)_2Cl_2$ and excess NH_2Bu^t resulted in the formation of $Cr(NBu^t)_2(NHBu^t)Cl$ with loss of Bu^tNH_3Cl.[215] Chan *et al.* have reported that W(N-t-Bu)$_2$(HN-t-Bu)$_2$ reacts with substituted vicinal diols to form chelated-glycolate compounds W(N-t-Bu)$_2$(X)(NH_2-t-Bu) (X = pinacolate, benzopinacolate, perfluoropinacolate) with loss of aniline.[216] In addition, Morrison and Wigley reported that $[Mo(NAr)_3Cl]^-$ is converted to $Mo(NAr)_2(NHAr)_2$ when in the presence of NH_2Ar.[217]

Because of possible side reactions with coordinated aniline during alkylation reactions, species of the type $Mo(NPh)Cl_2$(*o*-$(Me_3SiN)_2C_6H_4$)L (L = PMe_3 **3**, THF **4**) were prepared from **2**. Compound **3** was prepared by dissolving **2** in Et_2O at room

temperature followed by addition of excess PMe_3 with stirring. Blue-purple micro-crystals of **3** were obtained by concentrating the reaction mixture and cooling to -78°C. Proton and ^{13}C NMR spectra suggest that **3** has pseudo octahedral coordination geometry with the phenylimido and PMe_3 ligands occupying mutually *trans* positions, as shown in Figure 2.6. Proton NMR spectra showed equivalent Me_3Si groups which give rise to one resonance at 0.44 ppm (18H). A doublet centered at 0.73 ppm (9H, J_{PH} = 8.7Hz) was assigned to the PMe_3 methyl groups. The pda ligand showed its characteristic set of resonances centered at 6.90 ppm (m, 4H). In addition, two triplets and a doublet corresponding to the imido ligand were also observed (6.77 ppm (t), 7.04 ppm (t), and 7.83 ppm (d)).

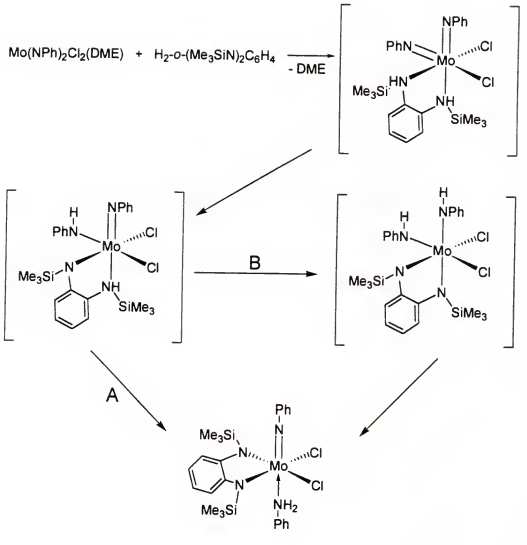

Figure 2.5. Two possible pathways for the synthesis of **2**.

The THF adduct $Mo(NPh)Cl_2(o\text{-}(Me_3SiN)_2C_6H_4)THF$, **4**, was prepared by stirring **2** in THF for 1hr followed by precipitation with pentane and filtration. Proton NMR (Figure 2.7) spectra in C_6D_6 confirmed the presence of coordinated THF as two multiplets at 1.06 ppm (4H) and 3.56 ppm (4H). In addition, the singlet at 0.44 ppm

corresponding to the equivalent Me_3Si methyl groups was consistent with octahedral coordination geometry shown in Figure 2.6.

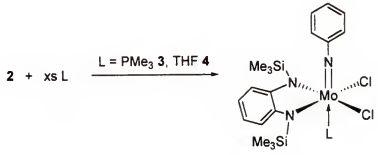

Figure 2.6. Syntheses of PMe3 adduct **3**, and THF adduct **4**.

Crystals of **3** were obtained by cooling a concentrated Et_2O solution to -20°C for several days. As Figure 2.8 shows, **3** has a distorted octahedral geometry with the PMe_3 and phenylimido ligands in mutually *trans* positions. The molybdenum metal center is raised 0.307(1) Å above the plane containing the chloride and amido N atoms. A long Mo-P(1) bond length of 2.7240(6) Å[218-225] is indicative of a weak interaction between the metal center and the phosphorus atom. A search of the Cambridge Database (October, 1998 release) revealed that **3** has a Mo-P bond that is more that 0.2 Å longer than the average Mo-P bond in six-coordinate molecules (2.507 Å).[225] The Mo-N3 bond length of 1.745(2) Å is consistent with a Mo≡N triple bond.[226-231] The Mo-N1 [2.018(2) Å] and

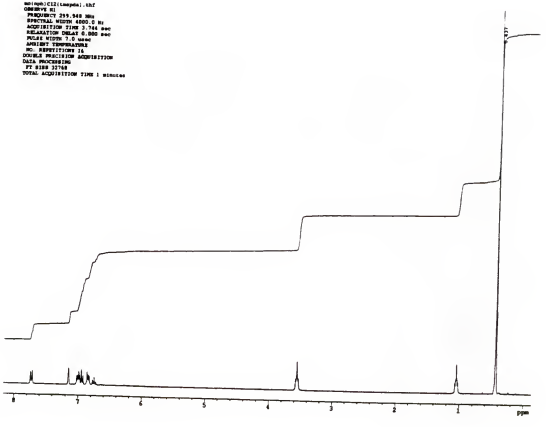

Figure 2.7. Proton NMR spectrum (C_6D_6) of $Mo(NPh)Cl_2(o\text{-}(Me_3SiN)_2C_6H_4)THF$.

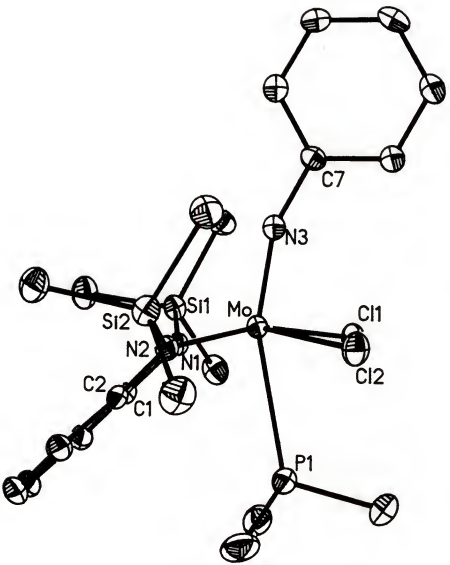

Figure 2.8. Thermal ellipsoids drawing of **3**. Ellipsoids have been drawn at 40% probability and hydrogens have been removed for clarity.

Mo-N2 [2.017(2) Å] bond lengths are within normal values for Mo-N single bonds as are the Mo-Cl1 and Mo-Cl2 distances.

Synthesis of Dialkyl Complexes

The reaction of **4** with two equivalents of RMgCl (R = Me **5**, R = Me_3CCH_2 **7**, $PhCH_2$ **8**, Me_3SiCH_2 **9**) in Et_2O at -78°C gave orange-red mixtures within 1hr. The reaction of **4** with two equivalents of RMgBr (R = Ph **6**) produced a purple mixture within 1hr. Removal of the solvent followed by extraction with pentane or toluene separated the desired dialkyl products $Mo(NPh)R_2(o\text{-}(Me_3SiN)_2C_6H_4)$ from the magnesium salts. Complexes **5**, **7**, and **9** were crystallized by cooling concentrated acetonitrile solutions to 0°C, while compounds **6** and **8** were recrystallized from toluene and pentane solutions cooled to -78°C, respectively.

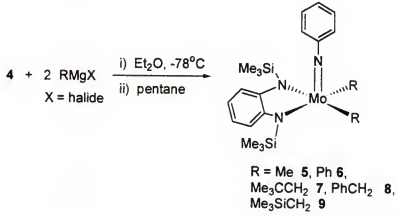

Figure 2.9. Synthesis of dialkyl compounds **5**-**9**.

Proton NMR spectra of **5** in C_6D_6 revealed the presence of two methyl groups as a singlet at 1.13 ppm (6H). Both the methyl and Me_3Si groups, respectively, were equivalent at room temperature. This suggests that the coordination geometry of this compound is square pyramidal with the phenylimido group occupying the apical position (Figure 2.9). Carbon-13 NMR spectra in $CDCl_3$ showed the methyl carbons to be at 31.28 ppm with a coupling constant of $^1J_{CH}$ = 126.4Hz. This coupling constant indicates that agostic interactions[232-238] between the methyl hydrogens and the metal center in **5** are unlikely, at least at room temperature, despite the formal 14e$^-$ electron count at the metal center.

Proton NMR spectra of **6** in C_6D_6 solution showed equivalent Me_3Si groups at 0.11 ppm (18H) which suggested the symmetric square pyramidal structure shown in Figure 2.9. There are two triplets in a 2:1 ratio at 6.82 ppm (2H) and 6.90 ppm (1H), which were assigned to the phenyl-group hydrogens *para* to the metal center and *para* to the imido nitrogen, respectively. Another set of resonances which confirmed the identity of **6** are two doublets in a 4:2 ratio at 7.40 ppm and 7.61 ppm which are assigned to the phenyl group protons *ortho* to the metal center and *ortho* to the imido nitrogen, respectively. One of the resonances attributed to the pda ring protons was observed but it is partially overlapping with the doublet at 7.40 ppm. However, these two resonances, integrate to six total hydrogens.

Singlets corresponding to equivalent Me_3Si methyl groups and to equivalent neopentyl methyl groups in the ^1H NMR (C_6D_6) spectrum of bis-neopentyl complex **7** appear at 0.55 ppm (18H) and 0.95 ppm (18H), respectively. This is consistent with a

square pyramidal coordination around the Mo(VI) metal center, as is observed for **5** and **6**. A set of doublets is observed at 2.58 ppm (2H) and 2.77 ppm (2H), which are assigned to the diastereotopic protons attached to the neopentyl α-carbon and integrate accordingly. The phenylimido resonances appear at 6.90 ppm (t, 1H), 7.09 ppm (t, 2H), and 7.75 ppm (d, 2H) while broadened pda-ring protons are observed at 6.96 ppm (m, 2H) and 7.30 ppm (m, 2H).

Similar resonances to those in spectra of **5**, **6**, and **7** were observed in the ^1H NMR spectra of dibenzyl complex **8** and bis-trimethylsilylmethyl complex **9**. The relevant features of the ^1H NMR (C_6D_6) spectra of **8** were a singlet at 0.09 ppm (18H) corresponding to equivalent Me_3Si methyl groups, and an AB quartet at 2.91 ppm (2H, $J_{H\text{-}H}$ = 11.1 Hz) and 2.85 ppm (2H, $J_{H\text{-}H}$ = 11.1 Hz) corresponding to the diastereotopic methylene protons of the benzyl groups. Proton NMR spectra of **9** in C_6D_6 solution at room temperature showed equivalent Me_3Si methyl groups from the diamide ligand at 0.03 ppm (s, 18H) and equivalent Me_3Si methyl groups from the trimethylsilylmethyl alkyl ligands at 0.46 ppm (s, 18H). Two resonances were observed at 1.81 ppm (d, 2H) and 2.19 ppm (br, 2H) corresponding to the diastereotopic methylene protons.

The solid-state structure of $W(NPh)(CH_2CMe_3)_2(o\text{-}(Me_3SiN)_2C_6H_4)$ is a trigonal bipyramid[96] while solution VT NMR studies show that it rapidly interconverts with the square pyramidal isomer at room temperature, as shown in Figure 2.10 for the Mo(VI) analogs. Other bulky dialkyl complexes behave similarly. Variable temperature ^1H NMR studies showed that **7** and **9** are also fluxional in solution and that decoalescence of the Me_3Si- peak, corresponding to the diamide Me_3Si group occurs at -18°C and -30°C,

respectively. A ^{1}H NMR of **7** (d_8-toluene) taken at -40°C is shown in Figure 2.11. The two site exchange approximation gives $\Delta G^{\ddagger}_{+} = 12.61$ kcal/mol for this process for **7** and $\Delta G^{\ddagger}_{+} = 11.90$ kcal/mol for **9**.[239] Thus, the structures of **7** and **9** are trigonal bipyramids with the imido group and one -NSiMe$_3$ group occupying the axial positions. It appears that this geometry is preferred, over the square pyramid with an apical imido group, for steric reasons.

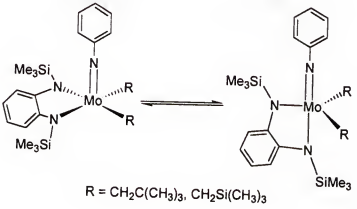

Figure 2.10. Square-pyramidal and trigonal-bipyramidal equilibrium observed in solution by ^{1}H NMR for **7** and **9**.

Reactivity of **2** With Alkylating Agents

When **2** was allowed to react with two equivalents of RMgCl (R = Me_3CCH_2, or Me_3SiCH_2) in diethyl ether at -78°C an unexpected mixture of products was obtained. As shown in Figure 2.12, the mixture contained the chelate supported Mo(NPh)R_2(*o*-$(Me_3SiN)_2C_6H_4$) (**7**, **9**) species as well as the bis-imido species of the type Mo(NPh)$_2R_2$ (**10**, and **11**, respectively). Formation of dimeric **1** was not observed.

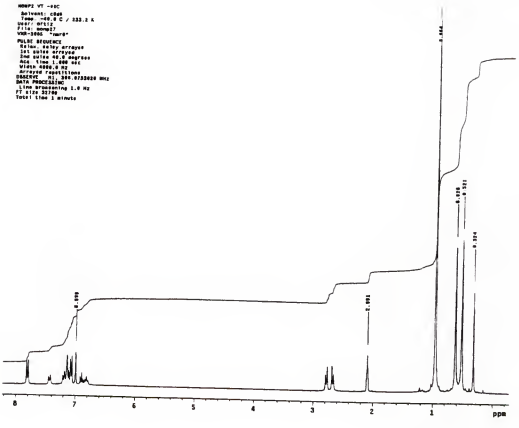

Figure 2.11. Proton NMR spectrum (d_8-toluene) of **7** taken at -40°C.

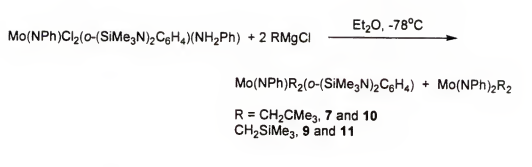

Figure 2.12. The reaction of **2** with alkylating agents.

We have independently prepared **10** and **11** by reaction of $Mo(NPh)_2Cl_2DME$ with two equivalents of RMgCl (R = Me_3CCH_2, and Me_3SiCH_2) in Et_2O at -78°C (Figure 2.13). Both **10** and **11** were obtained in high yields and purity in this manner. Similar compounds have been reported by Oskam *et al.*[240] and Schoettel *et al.*[241] as intermediates in the syntheses of Mo(VI) alkylidenes with alkoxide or triflate ancillary ligands. However, they did not report these complexes (presumably because of the unexpected insolubility of **10** and **11** in aliphatic hydrocarbon solvents). Proton NMR spectra (C_6D_6) of **10** showed the neopentyl methyl resonance as a sharp singlet at 1.19 ppm (18H) and the methylene protons as a singlet at 2.06 ppm (4H). Proton NMR (C_6D_6) of **11** showed a sharp singlet at 0.17 ppm (18H) corresponding to the Me_3Si methyl protons and a singlet at 1.58 ppm (4H) for the methylene protons. The aromatic region showed the normal resonances for equivalent phenyl imido groups.

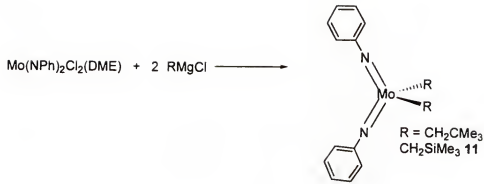

Figure 2.13. Synthesis of molybdenum bis-phenylimido dialkyls.

One possible explanation for the reactivity observed in the reaction of **2** with alkylating agents is shown in Figure 2.14. If **2** is equilibrating with **12**, alkylation of **12** would lead to **10** and **11** while alkylation of **2** would give **7** and **9**. In separate NMR-scale experiments, samples of **7** and **10** were combined with aniline and H_2-*o*-$(Me_3SiN)_2C_6H_4$, respectively. No reaction was observed in either case. This eliminates the possibility that in the presence of aniline or H_2-*o*-$(Me_3SiN)_2C_6H_4$ the dialkyl species interconvert. We were, however, unable to detect further evidence for an equilibrium between **12** and **2** other than the reactivity observed with the alkylating agents. Proton NMR samples of **2** (d_8-toluene) do not show evidence for proton exchange even when cooled to -85°C.

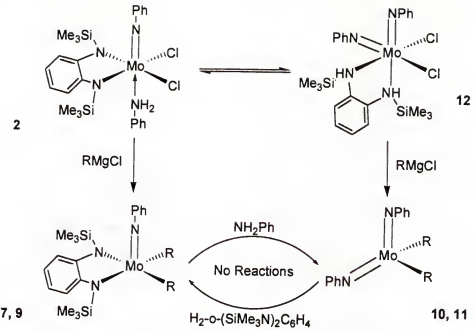

Figure 2.14. Possible equilibrium that would cause the isolation of **10** and **11** along with **7** and **9**.

Synthesis of Chelate Supported Alkylidenes

The alkylidene complex **13** was obtained when a toluene solution of **7** was heated to 80°C for 0.5hr in the presence of excess PMe_3 (Figure 2.15). Proton NMR spectra of this purple solid revealed a singlet at 0.37 ppm (18H) assigned to Me_3Si methyl groups, a broadened doublet at 0.85 ppm corresponding to coordinated PMe_3, and a singlet at 1.32 ppm (9H) which was assigned to the alkylidene tert-butyl group. A small, broad singlet was observed at 12.13 ppm (1H) and is assigned to the alkylidene hydrogen.

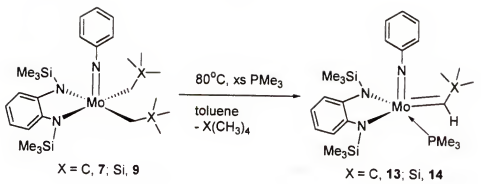

Figure 2.15. Syntheses of alkylidenes **13** and **14**.

In a similar reaction, when **9** was heated to 85°C in d_8-toluene in the presence of excess PMe_3, formation of the corresponding alkylidene was observed (Figure 2.15). The formation of alkylidene **14**, was confirmed by a singlet at 13.62 ppm attributed to the alkylidene proton and a singlet near 0.0 ppm for TMS. This alkylidene, however, has proven difficult to isolate in pure form.

Alkylidene **13** demonstrated fluxional behavior while in solution. A coalesced resonance was observed at room temperature for the Me_3Si- groups of the diamide ligand which decoalesced at -37°C ($\Delta G^{\ddagger}$ = 12.51 kcal/mol). The mechanism for this equilibration is proposed to involve the reversible dissociation of phosphine from the metal center, as shown in Figure 2.16. This dissociation induces a plane of symmetry in the intermediate **15**, which makes the Me_3Si groups equivalent.[242]

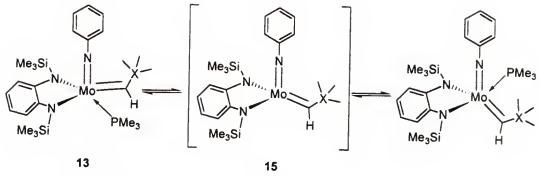

Figure 2.16. Equilibrium of alkylidenes that induces a plane of symmetry in the intermediate.

Polymerization Reactions

The activity of several of the compounds described above towards olefin polymerization was examined. Dimethyl **5** was added to an ethylene-saturated MAO solution in toluene. After 10 minutes no polyethylene was obtained. However, the polymerization of norbornene was achieved by preparing alkylidenes *in situ*. In separate experiments, small samples of the dialkyls **7**, **8**, and **9** were heated to 85°C in toluene for 0.5hr. To these reaction mixtures, toluene solutions of freshly sublimed norbornene were added and stirred without heat for 1hr. Moderate quantities of polynorbornene were isolated in both cases as white solids.

Conclusions

In this chapter, the syntheses and characterization of Mo(VI) dichloride and dialkyl complexes supported by ancillary phenylimido and chelating diamide co-ligands are presented.

The synthesis of **2**, while unexpected, represents an opportunity for our group to study the chemistry of Mo(VI) alkyls and alkylidenes supported by dianionic chelating ligands. It is of great interest to see how the reactivity of these compounds compares to that of their W(VI) analogs.

CHAPTER 3
SYNTHESIS AND REACTIVITY OF MOLYBDENUM(IV) OLEFIN COMPLEXES SUPPORTED BY A CHELATING ANCILLARY LIGAND.

In recent years, members of our research group synthesized a series of stable dialkyl complexes, $W(NPh)R_2(o\text{-}(Me_3SiN)_2C_6H_4)$ containing β-hydrogen atoms.[98,242,243] These complexes were resistant to decomposition indefinitely as long as they were stored under an inert atmosphere. It was found that upon addition of PMe_3 to $W(NPh)R_2(o\text{-}(Me_3SiN)_2C_6H_4)$ (R = Et, CH_2CH_2Ph), η^2-olefin complexes were isolated in essentially quantitative yield.[243]

In general, mechanistic studies into β-H transfer chemistry have defined a dissociative mechanism for the decomposition of β-H containing alkyl complexes.[4] A dissociative mechanism would imply that an open coordination site must be created before H-transfer can occur. However, β-H transfer chemistry of $W(NPh)R_2(o\text{-}(Me_3SiN)_2C_6H_4)$ complexes was induced by adding a ligand to the metal center. It was proposed that the observation of a large kinetic isotope effect, negative entropy of activation, and no deuterium label scrambling were consistent with a β-hydrogen/abstraction mechanism for the conversion of $W(NPh)Et_2(o\text{-}(Me_3SiN)_2C_6H_4)$ into $W(NPh)(\eta^2\text{-ethylene})(o\text{-}(Me_3SiN)_2C_6H_4)(PMe_3)_2$.

The study of β-hydride containing molybdenum complexes related to $W(NPh)R_2(o\text{-}(Me_3SiN)_2C_6H_4)$ was undertaken. The results are presented in this chapter

and show that the behavior of the Mo(VI) dialkyl complexes differs greatly from what is observed in the W(VI) analogs.

Formation of Mo(VI) Metallacyclopentane

The reaction of $Mo(NPh)Cl_2(o\text{-}(Me_3SiN)_2C_6H_4)THF$ (**4**) with one equivalent of $BrMgCH_2CH_2CH_2CH_2MgBr$ in Et_2O (-78°C) resulted in the formation of red-orange metallacyclopentane **16**, as shown in Figure 3.1. The equivalency of the pda Me_3Si-groups (s, 0.31 ppm (18H)) in ^1H NMR spectra of **2** suggested a square pyramidal geometry around the metal in which the phenyl imido ligand occupies the apical position while the two pda-nitrogens and the two α-carbons occupy the basal plane.

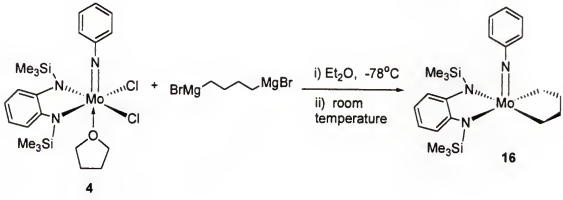

Figure 3.1. Synthesis of metallacyclopentane **16** using $BrMgCH_2CH_2CH_2CH_2MgBr$.

As shown in Figure 3.2, four multiplets (1.53 ppm (2H), 2.01 ppm (2H), 2.64 ppm (2H), and 3.13 ppm (2H)) were observed for the metallacycle hydrogens as predicted by the square pyramidal geometry. The plane of symmetry that bisects the N-Mo-N and C_α-

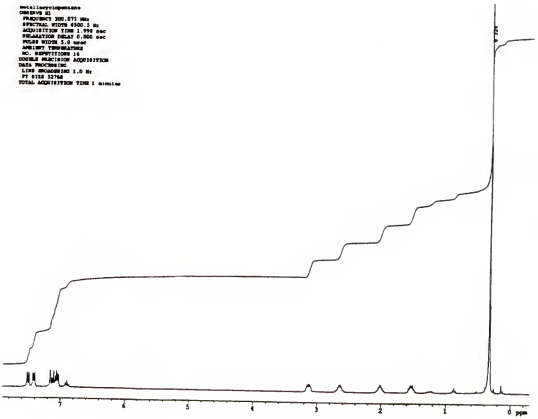

Figure 3.2. Proton NMR spectrum of **16** (C_6D_6).

Mo-C_α angles makes each group of α- and β-hydrogens equivalent to each other. However, hydrogens sitting above and below the basal plane are inequivalent, thus each α-hydrogen couples to its geminal hydrogen and to both vicinal β-hydrogens. Likewise, each β-hydrogen couples to its geminal β-hydrogen and to both α-hydrogens. Single-crystal X-ray studies of $W(NPh)(CH_2CH_2CH_2CH_2)(o\text{-}(Me_3SiN)_2C_6H_4)$ confirmed its structure to be a square pyramid.[99] The same solid-state structure is proposed for the molybdenum analog **16**.

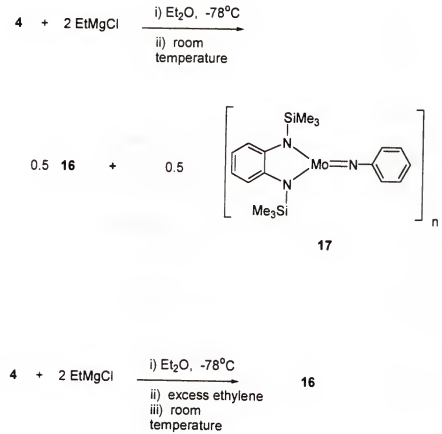

Figure 3.3. i) Reaction of ethylmagnesium chloride with molybdenum dichloride **4**. ii) Synthesis of metallacyclopentane **16** in the presence of ethylene.

Metallacyclopentane **16** was also obtained if **4** was allowed to react with two equivalents of EtMgCl (Et_2O, -78°C) and the reaction mixture was allowed to warm to room temperature (Figure 3.3i). The yield of this reaction was much lower as some "Mo(IV)" is proposed to be lost when two ethylene molecules couple to make the metallacycle. The identity of the remaining Mo(IV) species is not known, but it is proposed to be $[Mo(\mu\text{-}NPh)(o\text{-}(Me_3SiN)_2C_6H_4)]_n$ (**17**) (n = 1, 2) or species derived from such an intermediate. Proton NMR spectra of **17** showed a singlet corresponding to equivalent Me_3Si groups at 0.85 ppm (18H), and five multiplets in the aromatic region [6.25 (m, 2H); 7.58 (m, 2H); 8.00 (m, 2H); 8.05 (t, 1H); 8.45 (m, 2H)]. Our best results for the synthesis of **16** were obtained when **4** was treated with two equivalents of EtMgCl (Et_2O, -78°C) in the presence of excess dry ethylene (Figure 3.3ii).

We propose that the formation of **16** occurs via the mechanism shown in Figure 3.4. Upon addition of EtMgCl to **4**, the bright orange-red color of the dialkyl complex appears. Upon warming, the solution darkens to a dark brown color. Slowly, the solution returns to an orange-red color which remains. Beta-hydride elimination from a Mo(VI) diethyl complex would result in a Mo(IV) ethylene complex. This ethylene complex would then disproportionate, in the absence of excess ethylene to make **16** and a proposed three coordinate intermediate of the form $[Mo(NPh)(o\text{-}(Me_3SiN)_2C_6H_4)]$. This three coordinate, coordinatively unsaturated and electron poor intermediate could then dimerize, or react further to give the final side-product **17**. However, in the presence of excess ethylene the coupling of the coordinated ethylene molecule and a free ethylene molecule gives **16** quantitatively.

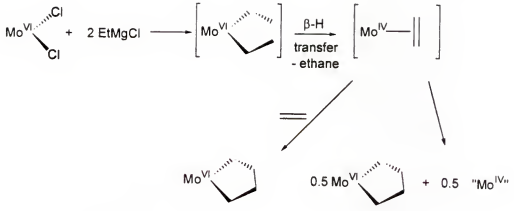

Figure 3.4. Scheme detailing the proposed pathway by which **16** and **17** are made. The ancillary ligands have been removed for clarity.

A lot of interest has been shown in early-transition metallacyclopentanes species due to their role in the dimerization and trimerization of ethylene as a means for catalytically preparing butene[244,245] and hexene,[246,247] respectively. We did not observe formation of metallacycloheptane species nor of hexene when **16** was exposed to excess ethylene. When a C_6D_6 solution of **16** was heated to 80°C under ethylene pressure (1-2 atm), the only identifiable products were butene and free H_2-*o*-$(Me_3SiN)_2C_6H_4$. The observation of H_2-pda suggests that the butene formed is more likely a result of the decomposition of **16** than of the catalytic dimerization of ethylene.

Formation of Mo(IV) Ethylene Complex

When a small excess (2.2 eq.) of PMe_3 was added to a C_6D_6 solution of **16** and heated to 80°C, formation of Mo(NPh)(η^2-ethylene)(*o*-$(Me_3SiN)_2C_6H_4$)$(PMe_3)_2$ (**18**) was observed (Figure 3.5i). No reaction was observed if the reagents were mixed at room temperature. Alternatively, **18** was prepared by reacting two equivalents of EtMgCl with **4** (Et_2O, -78°C) while in the presence of slightly more than two equivalents of PMe_3 (Figure 3.5ii).

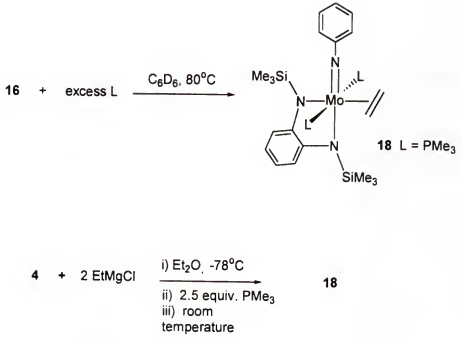

Figure 3.5. i) NMR scale reaction of metallacyclopentane **16** and excess PMe_3. ii) Synthesis of Mo(NPh)(η^2-ethylene)(*o*-$(Me_3SiN)_2C_6H_4$) **18** from **4**.

Proton NMR spectra of **18** showed a broad singlet (0.46 ppm, 18H) in the trimethylsilyl region and a broadened singlet (0.95 ppm, 18H) in the trimethylphosphine

region. Two broadened doublets at 2.22 ppm (2H) and 2.66 ppm (2H) were assigned to the ethylene protons. The broadness of these signals suggests fluxionality of the structure proposed for **18**.

The equilibrium between metallacyclopentanes and bis-ethylene species has been extensively studied in the past.[248-250] Thus, the need for heat in the preparation of **18** from **16** suggests that **16** can be better described as a metallacyclopentane than as a bis-ethylene complex (Figure 3.6). A bis-ethylene species, like **16a**, could conceivably be part of an equilibrium, which lies towards **16**. Addition of PMe_3, accompanied by heat, would then shift this equilibrium towards the right and produce **18**.

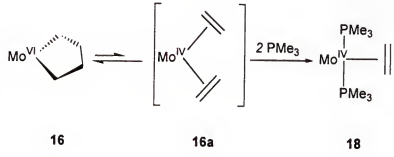

16 **16a** **18**

Figure 3.6. Equilibrium between metallacyclopentane species and bis-ethylene species. Substitution of ethylene by PMe_3 is proposed to drive the reaction to the right. Ancillary ligands have been removed for clarity.

Synthesis of η^2-Olefin Complexes

The reaction of **4**, in Et_2O at -78°C, with two equivalents of RMgCl (R = CH_2CH_2Ph (**19**), *n*-Pr (**20**), *i*-Bu (**21**)) initially resulted in a color change from blue to purple. As the temperature of the reaction was raised to room temperature, an orange-red solution was obtained (believed to be a dialkyl intermediate) which slowly (1-2hrs.)

changed to a forest green color that remained. As Figure 3.7 shows, monomeric η^2-olefin complexes **19-21** were obtained from pentane extractions as either dark-green solids or oils (**21**).

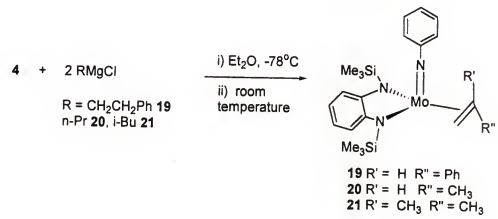

Figure 3.7. Synthesis of Mo(NPh)(η^2-olefin)(*o*-$(Me_3SiN)_2C_6H_4$) complexes.

NMR experiments revealed that **19** is a four coordinate η^2-styrene complex and that two isomers are present in solution in a 1:1 ratio. As Figure 3.8 shows, the ^1H NMR of **19** showed four singlets (0.09 ppm (9H), 0.29 ppm(9H), 0.359 ppm (9H), 0.41 ppm (9H)) corresponding to two sets of inequivalent trimethylsilyl groups. Other resonances, due to the coordinated styrene, were observed in the 1-5 ppm region. Through a COSY 2D NMR experiment (in C_6D_6), two sets of olefinic resonances were identified for **19**. Isomer A had resonances at 1.16 ppm (m, 1H), 3.34 ppm (m, 1H), and 4.90 ppm (br t, 1H). Isomer B showed signals at 1.05 ppm (m, 1H), 2.22 ppm (t, 1H), and 3.54 ppm (m, 1H). Furthermore, the $^{13}C\{^1H\}$ NMR (C_6D_6) spectrum of **19** showed four signals due to coordinated styrene carbons (50.81 ppm, 52.61 ppm, 67.38 ppm, 74.27 ppm).

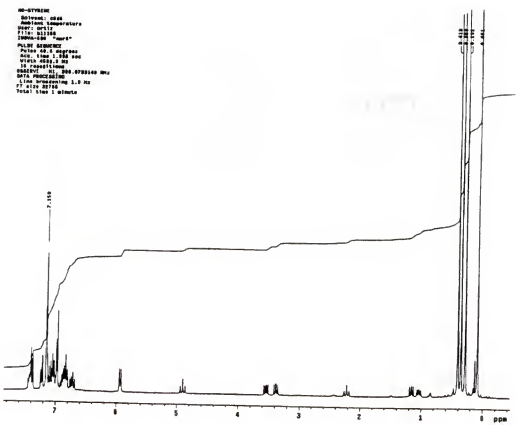

Figure 3.8. Proton NMR spectrum (C_6D_6) of Mo(η^2-styrene) complex **19**.

A single-crystal X-ray diffraction experiment revealed that the structure of one of the isomers of **19** is a pseudo-tetrahedral η^2-styrene complex wherein the styrene phenyl ring is oriented away from the phenyl-imido ligand (Figure 3.9). Single crystals of **19** were grown from a concentrated pentane solution of **19** at room temperature, overnight.

A short Mo-imido nitrogen bond length[251-254] of 1.7361(18)Å is indicative of triple-bond character despite the Mo-N1-C9 bond angle of 167.82(17)°. The Mo-N2 and Mo-N3 bond distances [2.0099(16)Å and 2.0181(16)Å, respectively] are within the normal range. The Mo-C1 and Mo-C2 bond distances are 2.146(2)Å and 2.190(2)Å, respectively. This small difference in the Mo-C1, C2 bond lengths can be attributed to steric interactions of the styrene-phenyl ring with the pda ring. The relatively long C1-C2 bond length of 1.455(3)Å is indicative of a metallacyclopropane[255,256] interaction of the styrene olefinic carbons and the Mo metal center [1.33(1)Å for free ethylene[257]]. The average C=C distance in metal-coordinated styrenes is 1.41(9)Å.[258]

It is noteworthy that the *ortho* protons of the coordinated styrene in the structure of **19** are situated approximately 2.3Å directly above the pda ring. In ^{1}H NMR experiments, these protons were observed as a doublet centered at 5.91 ppm (2H) and assigned to Isomer A. This shift in the upfield direction is attributed to the shielding effect that the ring current of the pda ring has on these two protons. With this proton assigned, nOe experiments were used to assign the rest of the protons in the two isomers. An nOe was observed between the ortho protons of the styrene (5.91 ppm) and the signals centered at 4.90 ppm and 1.16 ppm. These signals were then assigned to the olefinic hydrogen *cis* to the phenyl ring and the hydrogen geminal to the phenyl ring. An

additional nOe was observed for the signal at 3.38 ppm, assigned to the proton *trans*- to the styrene phenyl ring.

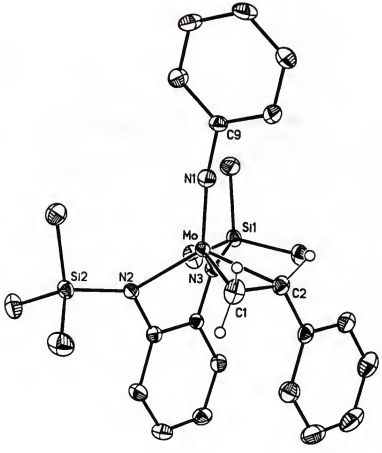

Figure 3.9. Thermal ellipsoid drawing of the crystal structure of **19**. Atoms are drawn at 40% probability and most hydrogens have been removed for clarity.

We propose that the second isomer of **19** (isomer B) has a very similar structure to the isomer A, shown in Figure 3.9. In the second isomer, however, the styrene phenyl group is oriented towards the phenylimido ligand. By analogy to isomer A, the resonances corresponding to isomer B can be assigned. The multiplet observed at 1.05 ppm (1H) corresponds to the olefinic proton *trans* to the styrene phenyl ring, the triplet at

2.22 ppm (1H) to the proton geminal to the phenyl ring, and the multiplet at 3.54 ppm (1H) to the *cis* olefinic proton. There is precedent in the literature for transition-metal olefin complexes having these types of rotational isomers.[251-253,259,260]

We have also observed that the two isomers of **19** do not interconvert with each other, on the NMR timescale. A C_6D_6 solution of **19** was heated to 80°C in a NMR tube and no interconvertion was observed. This large barrier for rotation of the olefin along the metal-olefin axis is consistent with a high degree of backbonding in the fragment. This agrees with the long C1-C2 bond length observed in the crystal structure of **19**.[153]

Propene complex **20** can also be observed to possess two isomeric forms. Although proton NMR spectra of **20** showed only two singlets [0.31 ppm (27H), 0.36 ppm (9H)] due to the trimethylsilyl groups, two doublets, assigned to the propene-methyl groups, were observed at 0.90 ppm (3H) and 2.40 ppm (3H), respectively. Six multiplets, corresponding to olefinic protons, were also observed (0.45 ppm (1H), 0.91 ppm (1H), 1.24 ppm (1H), 2.81 ppm (1H), 3.31 ppm (1H), 4.00 ppm(1H)).

Proton NMR spectra of isobutene complex **21** showed signals corresponding to inequivalent trimethylsilyl groups at 0.29 ppm (s, 9H), and 0.35 ppm (s, 9H). In addition, two singlets assigned to the isobutene-methyl groups were observed at 0.73 ppm (4H), and 2.60 ppm (3H). However, one of the doublets due to the olefinic hydrogens was obscured by the methyl resonance at 0.73 ppm. The remaining olefinic hydrogen was observed at 2.99 ppm (1H). The isolation of **21** represents one of the few number of early-transition metal isobutene complexes.[135,152] This small number of examples is mainly due to poor coordination capabilities of isobutene to early-transition metal complexes due to the steric hindrance of the methyl groups.

When **4** was allowed to react with two equivalents of *n*-BuMgCl or with two equivalents of *sec*-BuMgCl (Et_2O, -78°C), a green oil was obtained after the appropriate work-up. This green oil was identified, by NMR experiments, to be a mixture of butene complexes (**22a-b**). The same mixture was observed to be the product of the reaction of **4** with one equivalent of Bu_2Mg.

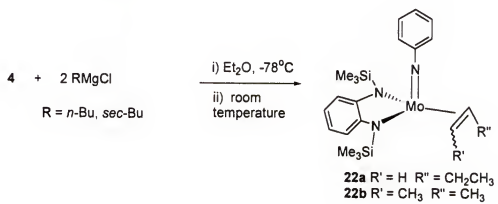

Figure 3.10. Synthesis of Mo(η^2-butene) complexes **22a-b**.

Due to the complexity of the ^1H NMR spectra of **22a-b**, ^{13}C and APT experiments were used to confirm the identities of the complexes in this mixture. Five signals due to trimethylsilyl groups were observed near 1.32 ppm in the C_6D_6 solution of **22**. Three resonances due to olefinic methyl groups were observed at 18.96 ppm, 19.52 ppm, and 25.58 ppm. We can only assume that more signals are obscured by the signals observed, since five $-CH_3$ groups were expected from the mixture of olefin complexes. We were also able to observe two resonances which were assigned to the aliphatic $-CH_2-$ groups of the two 1-butene isomers, 27.49 ppm and 34.32 ppm. Two resonances observed at 55.73 ppm and 56.64 ppm were assigned to the terminal olefin $H_2C=$ groups of the 1-butene

complexes. The internal olefin signals for the 1-butene and 2-butene complexes were observed at 66.26 ppm, 71.50 ppm, 72.32 ppm, 76.11 ppm, and 81.05 ppm.

As Figure 3.11 shows, we propose that 1-butene and 2-butene complexes are present in these mixtures due to isomerization of the coordinated olefin through allylic C-H activation. Allylic activation has been known for some time and has been proposed to be involved in the mechanism for making allyl and allyl-hydride complexes.[261-267] First, the reaction of **4** with *sec*-BuMgCl should give the di-*sec*-butyl complex **22d** which, through β-hydride transfer, decomposes to both 1-butene and 2-butene complexes **22a** and **22b**, respectively. However, di-*n*-butyl complex **22c** can only decompose to the 1-butene complex. At this point, allylic activation would produce an allyl hydride intermediate (**22e**), which can reversibly be converted into a 2-butene complex by insertion/migration into the opposite carbon.

Reactions of Olefin Complexes With σ-Donor Ligands

We had previously observed that W(NPh)(η^2-styrene)(*o*-($Me_3SiN)_2C_6H_4$) reacted with donor ligands like PMe_3 to give W(NPh)(η^2-styrene)(*o*-($Me_3SiN)_2C_6H_4$)($PMe_3)_2$ as the sole product.[243] This is not the case when Mo(NPh)(η^2-styrene)(*o*-($Me_3SiN)_2C_6H_4$) reacts with donor ligands like *t*-butyl-isocyanide or trimethylphosphine.

When **19-22** were allowed to react with excess C≡N(*t*-Bu) or excess PMe_3 at room temperature, a fast color change from green to purple occurred. Purple microcrystals precipitated from the solution after concentration and **23-24** were easily isolated by filtration.

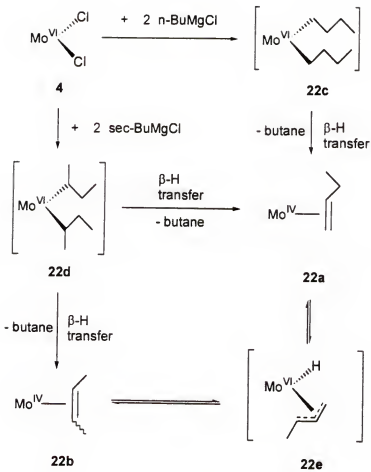

Figure 3.11. Isomerization of Mo(η^2-butene) complexes **22a-b** through allylic C-H activation. Ancillary ligands have been removed for clarity.

The pseudo-octahedral structure shown in Figure 3.12 was proposed on the basis of the observed NMR data and confirmed by X-ray crystallography. Resonances corresponding to inequivalent trimethylsilyl groups in **23** were observed at 0.58 ppm (br s, 9H) and 0.77 ppm (br s, 9H). The broadness of these signals was attributed to fluxional behavior while in solution (see below). Two broad singlets at 0.93 ppm (18H) and 1.17 (9H) were assigned to inequivalent *t*-butyl isocyanide peaks. A plane of symmetry

containing the imido nitrogen, pda nitrogens, and one of the isocyanide ligands makes the remaining isocyanide ligands chemically equivalent.

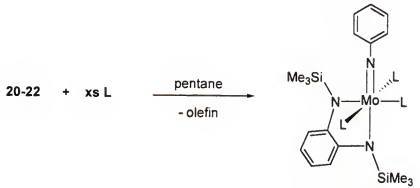

Figure 3.12. Synthesis of tris-*t*-butyl isocyanide (**23**) and tris-trimethylphosphine (**24**).

The proton NMR (C_6D_6) spectrum of **24** showed a broadened singlet at 0.38 ppm(18H) corresponding to the trimethylsilyl group and a broadened singlet centered at 0.99 ppm(27H) that was assigned to the trimethylphosphine ligands. The resonances found in the aromatic region were also broad. The $^{13}C\{^1H\}$ spectrum also confirms the formulation of **24**.

The broadening observed in the NMR spectra of **23** and **24** has been correlated to an equilibrium involving fast, and reversible ligand dissociation. As Figure 3.13 shows, loss of L (L = PMe_3, CN-*t*-Bu) induces a plane of symmetry in the $Mo^{IV}L_2$ species that is formed (**25**). Thus, the remaining L ligands in **25** become equivalent, as do the trimethylsilyl groups. For **23** coalesced silyl groups were observed at 34°C. For **24**, decoalescence of the silyl peaks was observed at -36°C. Using the two site exchange

approximation, the activation barrier for ligand dissociation was estimated to be $\Delta G^{\ddagger}$ = 15.0 and 11.3 kcal/mol for **23** and **24**, respectively.[239]

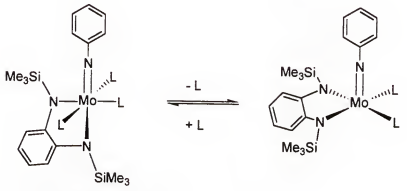

L = CN(*t*-Bu) **23**, PMe_3 **24**

25

Figure 3.13. Dissociative equilibrium observed for **23** and **24**.

Crystal Structure of Mo(NPh)(C≡N(t-Bu))$_3$(*o*-$(Me_3SiN)_2C_6H_4$) (**23**)

Single crystals of **23** were obtained from slow evaporation of a concentrated pentane solution of **23**. As Figure 3.14 shows, **23** was found to have a distorted octahedral geometry. Three isocyanide ligands were found to occupy meridianal positions. The imido-nitrogen was found to be *trans* to one of the pda-nitrogens while the other pda-nitrogen was *trans* to one of the isocyanide groups. Angles around the metal center do not deviate too far from the idealized octahedral angles (smallest was N5-Mo-N6 [77.08(13) °] and largest was N4-Mo-N5 [106.92(14) °]). The acute N5-Mo-N6 angle arises because of the rigid bite angle of the pda chelate-ring.

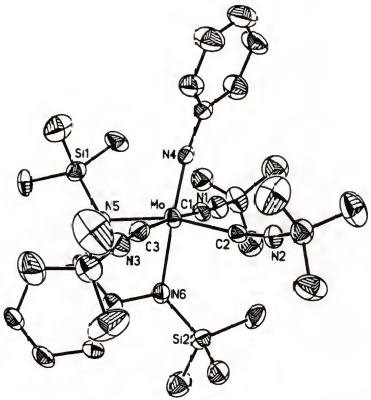

Figure 3.14. Thermal ellipsoid drawing of **23**. Atoms are drawn to 40% probability and hydrogens have been removed for clarity.

The Mo-imido bond length [1.804(4) Å] was found to be longer than in other complexes we have prepared[251-254] and the Mo-N4-C16 bond angle was found to be 172.0(5)°. This can be correlated to more double bond character in the Mo-N bond of **23**. This however was not surprising since a short Mo-N6 length [2.127(5) Å] is indicative of N4 and N6 competing for p_{π}-d_{π} electron donation to the metal center. On the other hand, the elongated Mo-N5 bond [2.169(3) Å] can be attributed to better σ-donation from the isocyanide ligand bound in the *trans* position.

The Mo-C1, C2, and C3 distances of the isocyanide ligands were found to be 2.157(5) Å, 2.072(5) Å, and 2.137(5) Å, respectively. The shorter bond length of the Mo-C2 bond was attributed to the effect of the π-back-donation from the metal to the isocyanide. This was also observed in the elongated C2-N2 bond length [1.182(6) Å] compared and the bent nature of that isocyanide group (C2-N2-C8 [152.8(5)°]) when **23** is compared to related d^2-isocyanide complexes.[289, 290]

Crystal Structure of $Mo(NPh)(PMe_3)_3(o\text{-}(Me_3SiN)_2C_6H_4)$ (**24**)

Single crystals of **24** were grown by slow evaporation of a concentrated pentane solution of **24** over the course of several days. Figure 3.15 shows a drawing of the molecular structure of **24**. Like **23**, **24** was found to have a distorted octahedral geometry. All of the angles around the Mo metal center were found to be close to 90° with the smallest being the N2-Mo-N3 angle [78.08(6)°] and the largest the N1-Mo-N2 angle [104.96(6)°]. As in the structure of **23**, the small N2-Mo-N3 angle is due to the bite angle of the chelate ring.

The Mo-imido bond length [1.7847(15) Å], like in most of our imido compounds, is short and indicative of a Mo≡N interaction.[251-254] The Mo-P bond lengths [2.5280(5) Å, 2.5459(5) Å, and 2.5532(5) Å] are all within normal values for six-coordinate Mo complexes.[268] However, the distances from the Mo to one of the pda nitrogens is unusual since Mo-N2 [2.2334(15) Å] is much longer than Mo-N3 [2.1405(15) Å]. This was correlated to a *trans*-influence due to better σ-donation from the phosphine ligand P2 that is *trans* to N2.

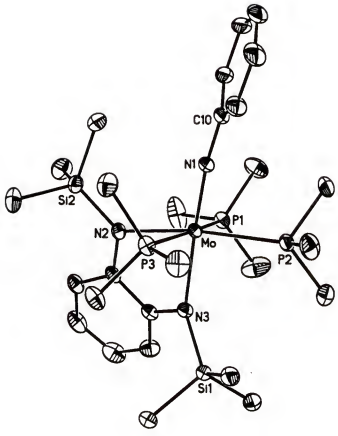

Figure 3.15. Thermal ellipsoids drawing of **24**. Atoms are drawn to 40% probability and hydrogens were removed for clarity.

Other Reactions of Mo(NPh)(η^2-olefin)(*o*-($Me_3SiN)_2C_6H_4$) Complexes

A common reaction for early transition metal d^2-olefin complexes is the coupling of the olefin with a free olefin to form metallacyclopentane species.[269] As described above, this was the case for the synthesis of **16**. In addition, coupling of double bonds has been used to synthesize complex metallacycles which can be used for the synthesis of rare organic molecules. Similarly, the reaction of olefin complexes with acetylenic

species to form metallacyclopentene species[270] is very common. We have not observed this for the η^2-olefin complexes **19-22**.

As Figure 3.16 shows, when a C_6D_6 solution of **19** was exposed to a slight pressure of ethylene, the only species observed were free styrene and metallacyclopentane **16**, i.e. no coupling of ethylene and styrene. Likewise, no coupling was observed when a C_6D_6 solution of **19** was charged with 15 equivalents of styrene. Also, when **19** was reacted with 1,7-octadiene no metallacyclic species were observed, only starting materials. Unfortunately, an intractable mixture of products was formed when a C_6D_6 solution of **4a** was exposed to a slight pressure of CO.

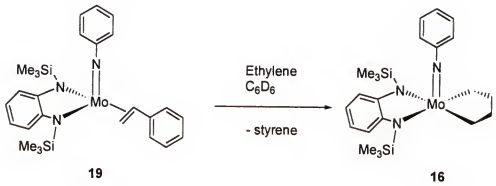

Figure 3.16. Conversion of Mo(η^2-styrene) complex **19** into metallacyclopentane **16** under a slight pressure of ethylene.

However, when a C_6D_6 solution of **19** was mixed with an excess of 2-propyne, phenylacetylene, or diphenylacetylene, a gel-like polymer was obtained although none of the species in solution were identifiable. We are still in the process of identifying the species formed in this reaction as well as characterizing the polymer formed, but we believe that the polymer is the corresponding polyacetylene.

Conclusions

The chemistry of d^2-metal centers has been well documented in the past. In this chapter the results in the study of β-hydride containing alkyl complexes supported by a diamide ligand were presented. It was found that the reactivity of the Mo(VI) complexes presented in this chapter differed from what was observed for their W analogs. In addition, the reactivity of the resulting Mo(IV)-olefin complexes also differed from their W analogs and from related d^2- Ti, Zr, Hf, Ta, and Nb species.

CHAPTER 4
LOW-PRESSURE HYDROGENOLYSIS OF MOLYBDENUM(IV) AND MOLYBDENUM(VI) COMPLEXES.

Transition metal complexes containing M-H bonds are of great interest because of their unusual reactivity in stoichiometric reactions and their potential as homogeneous catalysts.[1-5, 271-279] This prompted members of our group to attempt to synthesize hydride species of group 6 metal complexes in high oxidation states.

Hydride species can be synthesized in different ways, such as utilizing hydride reagents like *n*-BuSnH, hydrogen transfer reagents like KH, or oxidative addition of H_2.[1-5] Oxidative addition is particularly important due to its role in catalytic processes like the hydrogenation of unsaturated organic substrates.

In years prior to this dissertation, the reactivity of tungsten(VI) dialkyl complexes of the type $W(NPh)R_2(o\text{-}(Me_3SiN)_2C_6H_4)$ was studied in our laboratories.[242,243] It was found that a mixture of hydridic species formed upon the reaction of $W(NPh)R_2(o\text{-}(Me_3SiN)_2C_6H_4)$ (R = Et, CH_2CMe_3) with dihydrogen. The identities of the components of this mixture could not be confirmed. Attempts to produce hydride species by reacting of $W(NPh)Cl_2(o\text{-}(Me_3SiN)_2C_6H_4)$ with KH or $LiAlH_4$ lead to inseparable mixtures. The existence of hydride species in these mixtures was, however, unquestionable. If $W(NPh)(R)_2(o\text{-}(Me_3SiN)_2C_6H_4)$ (R = Et, CH_2CMe_3, CH_2CH_2Ph) was allowed to react with hydrogen in the presence of PMe_3, a seven coordinate dihydride, $W(NPh)_2H_2(o\text{-}(Me_3SiN)_2C_6H_4)(PMe_3)_2$ was isolated in high yield (Figure 4.1). It was also found that

olefin complexes of the type W(NPh)(η^2-olefin)(*o*-($Me_3SiN)_2C_6H_4$) (olefin = ethylene, styrene) could be converted to W(NPh)$_2H_2$(*o*-($Me_3SiN)_2C_6H_4$)($PMe_3)_2$ upon addition of H_2.

This chapter presents the results obtained to date concerning the reaction of both Mo(VI) and Mo(IV) diamide supported complexes with molecular hydrogen (H_2).

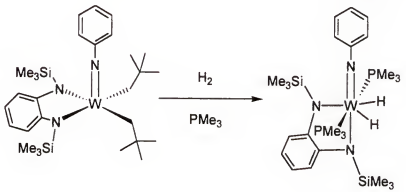

Figure 4.1. Hydrogenolysis of W(VI) bis-neopentyl complex.

Hydrogenolysis of Mo(IV) Olefin Complexes

We first explored the reactivity of olefin complexes of the type Mo(NPh)(η^2-olefin)(*o*-($Me_3SiN)_2C_6H_4$) with hydrogen. When a pentane solution of Mo(NPh)(η^2-styrene)(*o*-($Me_3SiN)_2C_6H_4$) was exposed to a slight pressure of H_2 (1-2 atm), the forest-green color of the solution changed to blue-green in a matter of minutes. The compound formed was easily isolated as a solid by concentrating the solution followed by cooling (-78°C) and filtration.

Through NMR experiments we identified the product of this reaction to be Mo(NPh)(η^6-ethylbenzene)(*o*-($Me_3SiN)_2C_6H_4$) (**26**), with the proposed structure shown in

Figure 4.2. Figure 4.3 shows a ^{1}H NMR spectrum of **26**. Equivalent trimethylsilyl groups were observed at 0.36 ppm (s, 18H) while the aromatic ring protons of the diamide ligand appeared as two multiplets at 6.71 ppm (2H) and 6.91 ppm (2H). Unexpectedly, the imido-group protons appeared as a multiplet centered at 7.05 ppm. In other complexes, these usually resonate as two triplets and a doublet in a 1:2:2 ratio. Nevertheless, all of the signals gave the corresponding integral values for the formulation of **26**.

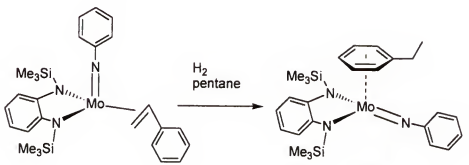

26

Figure 4.2. Hydrogenolysis of Mo(IV) η^2-styrene complex.

It has been proposed that the coordination of an arene ring to a transition metal disrupts the deshielding effect created by the ring-electron flow on aromatic protons.[4] For this reason, the NMR resonances for aromatic-ring protons coordinated to metals usually shift upfield by 2-3 ppm. This arises from the depletion of π-electron density from the ring upon coordination to the metal center. In complex **26**, the resonances for the aromatic protons appeared as two triplets and a doublet at 4.56 ppm (t, 1H), 4.92 ppm(d, 2H), and 5.03 ppm (t, 2H). The resonances corresponding to the alkyl hydrogens in the

coordinated ethylbenzene were also shifted upfield and appeared at 0.54 ppm (t, 3H) and 1.53 ppm (q, 2H).

The isolation and characterization of **26** as a η^6-ethylbenzene complex was rather surprising. As discussed in Chapter 1, the examples of d^2-arene complexes are rather scarce. Yet, **26** can be isolated easily and in high yield. Thus, we became interested in obtaining more η^6-arene complexes of Mo(IV) by hydrogenolysis of η^2-olefin complexes and testing the generality of this reaction as a synthetic tool.

Syntheses of Other Arene Complexes

Molybdenum(IV) complexes of the type Mo(NPh)(η^2-olefin)(*o*-$(Me_3SiN)_2C_6H_4$) (olefin = propene **20**, isobutene **21**, butene **22**) were used as precursors to other η^6-arene complexes. As shown in Figure 4.4, the low-pressure (1-2 atm) hydrogenolysis of **20-22** in pentane and in the presence of 10-15 equivalents of arene gave complexes **26-33** in high yield (80-85%).

The resonances observed in ^{1}H NMR spectra of these complexes are summarized in Table 4.1. All of these complexes exhibit similar chemical shifts for the trimethylsilyl, phenylimido, and phenylenediamide protons.

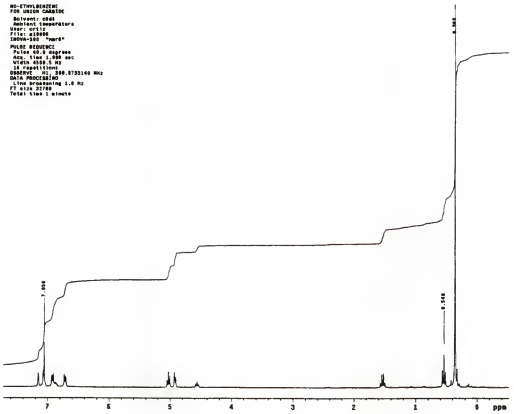

Figure 4.3. Proton NMR of Mo(NPh)(η^6-ethylbenzene)(*o*-$(Me_3SiN)_2C_6H_4$) (**26**).

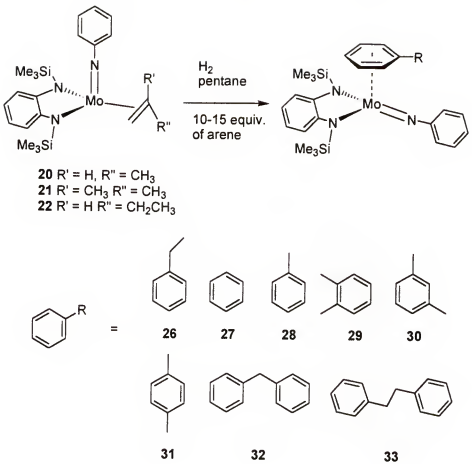

Figure 4.4. Syntheses of arene complexes **26-33** through the hydrogenolysis of Mo(IV) olefin complexes in the presence of excess arenes.

Both steric and electronic effects seem to play a role in what arene complexes can be synthesized. Syntheses of other complexes analogous to **26-33** with biphenyl, naphthalene, mesitylene, and pentamethylbenzene as the coordinating arene ligand were attempted. None of these arenes showed coordination to the metal center. It was proposed that this was due to steric interactions of the arene-ring substituents with the ancillary ligands of the molybdenum metal center. Likewise, α,α',α"-trifluoro-toluene did not show coordination to Mo(IV). This lack of arene coordination was probably

observed because trifluoro-toluene is too electron poor to offer the electron density needed by the metal center to be stabilized.

Table 4.1. Summary of ^{1}H NMR chemical shifts for compounds **26-33**. All spectra were obtained in C_6D_6 solutions and chemical shifts are reported in ppm downfield of TMS. Aromatic proton signals for **32** and **33** were obscured by excess arene.

Arene complex	**26**	**27**	**28**	**29**	**30**	**31**	**32**	**33**
Me_3Si-	0.36, s	0.33, s	0.35, s	0.36, s	0.37, s	0.36, s	0.35,	0.35, s
Arene aliphatic groups	0.54, t 1.53, q		1.15, s	1.10, s	1.19, s	1.21, s	1.38, s	1.88, t 2.43, t
Arene Aromatic protons	4.56, t 4.92, d 5.03, t	4.80, s	4.55, t 4.80, d 4.98, t	4.56, m 5.29, m	4.45, d 5.04, s 5.49, t	4.85, s	4.65, t 4.87, d 5.05, t 6.57, d	4.61, t 4.92, d 5.04, t
Diamide aromatic protons	6.71, m 6.91, m	6.74, m 6.93, m	6.71, m 6.94, m	6.71, m 6.92, m	6.72, m 6.94, m	6.72, m 6.93, m	6.77, m	
Imido protons	7.05, m	6.88, m 7.05, d	7.03, m	6.86, m 7.05, m	6.87, t 7.00, d 7.08, t	6.86, t 7.05- 7.10, m		

Crystal Structure of Mo(NPh)(*m*-xylene)(*o*-$(Me_3SiN)_2C_6H_4$) (**30**)

Crystals of **30** suitable for X-ray diffraction structural studies were grown from a concentrated pentane solution of **30** cooled to -20°C for weeks. Figure 4.5 shows a drawing of the crystal structure of **30**.

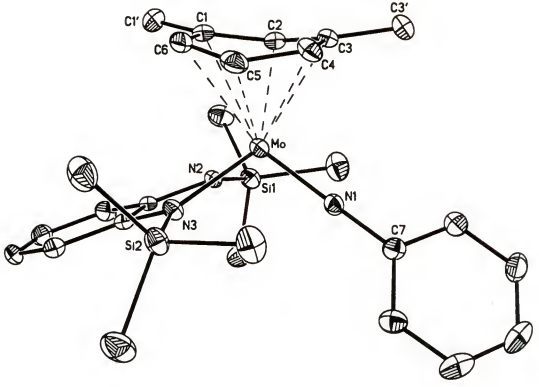

Figure 4.5. Thermal ellipsoids drawing of Mo(NPh)(*m*-xylene)(o-(Me_3SiN)$_2C_6H_4$) (**30**). Atoms are drawn to 40% probability and all hydrogens were removed for clarity.

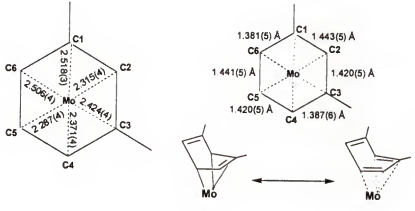

Figure 4.6. Mo-C distances in **30**, C-C distances within the arene ligand of **30**, and the proposed interaction of the ring with the metal center.

A pseudo-tetrahedral coordination geometry was found for **30** in which, the arene ligand coordinates in a nearly η^4-manner. A considerable ring distortion of 17.4(3)° was found between the planes formed by C2-C1-C6-C5 and C2-C3-C4-C5 while small torsion angles [0.9(5)° and 2.8(5)°] were found within these planes. Molybdenum to ring-carbon distances of 2.315(4) Å, 2.424(4) Å, 2.371(4) Å, and 2.287(4) Å were found for C2, C3, C4, and C5, respectively. Carbons C1 and C6 were considerably farther from the metal center [2.518(3) Å and 2.506(4) Å], which suggest that the ring interaction with the metal center is mostly through C2, C3, C4, and C5. The ring C-C distances are summarized in Figure 4.6. The shorter bondlengths for C3-C4 and C1-C6 suggest that double bonds can be assigned between these carbons. Thus, the structural data suggests that the interaction of the arene ligand with the molybdenum metal center is much like a 1,3-butadiene-metal interaction, as shown in Figure 4.6.[4,158]

The molybdenum to imido-nitrogen bond length [1.761(3) Å] is comparable to similar complexes and is indicative of a Mo-N triple bond interaction [Mo-N1-C7 angle (178.9(3)°)].[251-254] Bond lengths from the metal center to the amido nitrogens are within normal values for Mo-N single bonds [2.070(3) Å and 2.075 (3) Å].

Crystal Structure of Mo(NPh)(*p*-xylene)(*o*-$(Me_3SiN)_2C_6H_4$) (**31**)

Crystals of **31** suitable for X-ray diffraction structural studies were grown from a concentrated pentane solution of **31** cooled to -20°C for two days. Figure 4.7 shows a drawing of the crystal structure of **31**.

A pseudo-tetrahedral coordination geometry was found for **31** in which the arene ligand coordinates in a nearly η^4-manner. A considerable ring distortion of 17.1(1)° was

found between the planes formed by C1-C2-C3-C6 and C3-C4-C5-C6 while small torsion angles (0.8(3)° and 1.4(3)°) were found within these planes. Molybdenum to ring-carbon distances of 2.391(2) Å, 2.387(2) Å, 2.325(2) Å, and 2.298(2) Å were found for C1, C2, C3, and C6, respectively. Carbons C4 and C5 were considerably farther from the metal center [2.564(2) Å and 2.537(2) Å], which suggests that the ring interaction with the metal center is mostly through C1, C2, C3, and C6. The ring C-C distances are summarized in Figure 4.7. The shorter bondlengths for C1-C2 and C5-C4 suggest that double bonds can be assigned between these carbons. Thus, the structural data suggests that the interaction of the arene ligand with the molybdenum metal center in **31**, like in **30**, is much like a 1,3-butadiene-metal interaction, as shown in Figure 4.7.

The molybdenum to imido-nitrogen bond length [1.775(1) Å] is comparable to similar complexes and is indicative of a Mo-N triple bond despite the small Mo-N1-C7 angle [145.5(1)°]. Bond lengths from the metal center to the amido nitrogens are within normal values for Mo-N single bonds [2.047(1) Å and 2.067 (1) Å].

Substitution of the Coordinated Arene Ligands

A coordinated arene ligand can be an spectator ligand, a labile ligand, a catalyst poison, and a substrate ligand.[4] For these reasons, the coordination and displacement of arene ligands is of great importance in catalysis.[280] The mechanisms by which an arene displaces ligands or is displaced by other ligands have been studied in the past.[280-282]

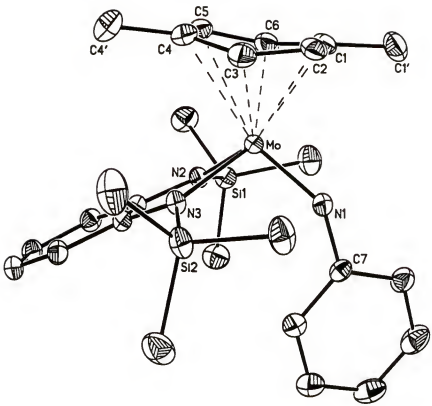

Figure 4.7. Thermal ellipsoids diagram of Mo(NPh)(*p*-xylene)(*o*-$(Me_3SiN)_2C_6H_4$) **31**. Atoms are drawn to 40% probability and all hydrogens were removed for clarity.

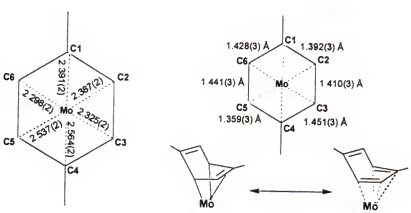

Figure 4.7. Mo-C distances in **31**, C-C distances within the arene ligand of **31**, and the proposed interaction of the ring with the metal center.

In the case of **26-33**, it was noticed that these arene complexes do undergo exchange of the arene ligand. It was found that the C_6D_6 in NMR samples of **26-33** exchanged with the coordinated arene to produce free arene and $Mo(NPh)(C_6D_6)(o\text{-}(Me_3SiN)_2C_6H_4)$ (**34**). Figure 4.8 shows a portion of a $^{13}C\{^1H\}$ NMR spectrum of **26** (C_6D_6) in which a triplet corresponding to coordinated C_6D_6 can be observed at 108.68 ppm.

The coordinated arenes in **26-33** were also substituted by excess CN(*t*-Bu) and PMe_3 to give **23** and **24**, respectively. Pentane solutions of **26-33** were allowed to react with three equivalents of L (L = PMe_3 **23**, CN(*t*-Bu) **24**), and compounds **23** and **24** were isolated from these reactions with equal purity to their preparation from Mo-olefin complexes **19-22** (Chapter 3).

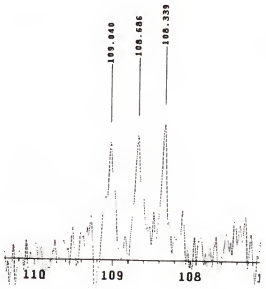

Figure 4.8. Portion of a $^{13}C\{^1H\}$ spectrum of **26** where substitution by C_6D_6 can be observed.

Substitution of the coordinated arene by olefins also occurs. When a C_6D_6 solution of **26** was charged with a slight pressure of ethylene (1-2 atm), formation of metallacyclopentane **16** was observed to occur quantitatively (by NMR). In addition, the ethylbenzene in **26** was rapidly substituted by styrene to give **19** quantitatively (by NMR).

Catalytic Hydrogenation and Isomerization of Olefins

Preliminary results show that compounds **26-33** are active towards the hydrogenation and the isomerization of olefins. The hydrogenations of styrene, neohexene, and *trans*-stilbene were achieved by reacting C_6D_6 solutions of **26** and the corresponding olefin with 1-2 atm of molecular hydrogen. Slow conversions to the respective alkanes occurred (36.9% conversion of styrene to ethylbenzene over the course of two days and two additions of H_2). Raising the temperature of the reaction from room temperature to 50°C proved to increase the rate of the hydrogenation of neohexene, using 1 mol% **28**, from 16.7% conversion overnight to 62.5% over 8 hours (TOF~7/hr).

The W(IV) compound analogous to **26** also showed catalytic activity towards the hydrogenation of olefins. However, W(NPh)(η^6-ethylbenzene)(*o*-$(Me_3SiN)_2C_6H_4$) hydrogenated styrene under 1000 psi of hydrogen (50°C) at a rate of 40 turnovers per hour (>5000 TON).[243]

A catalytic cycle for the hydrogenation of olefins by arene complexes like **26-33** was proposed and is shown in Figure 4.9. As mentioned above, styrene substitutes the coordinated ethylbenzene molecule in **26** to form **19**. The reaction of **19** with hydrogen should hydrogenate the coordinated styrene and produce three coordinate **35**. This

coordinatively and electronically unsaturated molecule (**35**) should bind styrene readily to regenerate **19**.

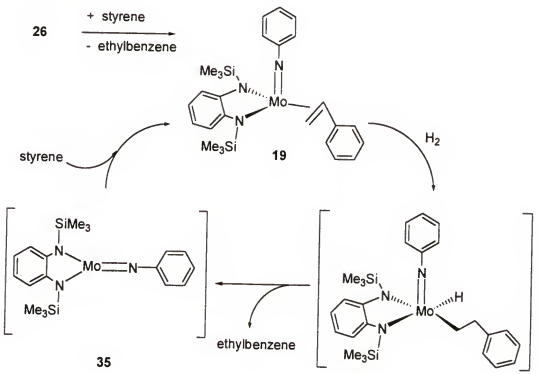

Figure 4.9. Proposed pathway for the catalytic hydrogenation of styrene by **26**.

Compounds **26-33** were shown to be active towards the isomerization of terminal olefins into internal olefins. The isomerizations of 1-butene, 1-pentene, 1-hexene, and 1,7-octadiene were observed to occur in C_6D_6 solutions of the olefins and **26-33**. At 50°C, a 5 mol% C_6D_6 solution of **26** isomerized 60% of 1-pentene to 2-pentene in 8 hrs (TON~12, TOF~1.5/hr). After 20 hrs, 87% of the 1-pentene had been converted to 2-pentene and after 51hrs the reaction was practically over. Heat improved the performance of the catalyst as after 8hrs a 1 mol% sample of **26** at 80°C isomerized 1-pentene to 2-pentene with 93% yield (TOF~11/hr).

For 1-hexene, the isomerization stopped at 2-hexene and did not produce any 3-hexene (TON = 15 after 8hrs, TOF~1.8/h, 5 mol% **26** at 50°C).

A proposed pathway for the isomerization of terminal olefins into internal olefins is shown in Figure 4.10. Resonances due to olefin complexes have been observed in NMR samples of 1-pentene and **26**. Therefore, we can assume that the first step towards the isomerization of the terminal olefin is coordination to the metal. This is followed by allylic C-H activation to give an allyl hydride species. This allyl hydride could then be converted into a new Mo-internal-olefin complex that can undergo exchange with free olefin. Allylic activation has been previously proposed as a way of isomerizing olefins.[4, 261-267, 283-286]

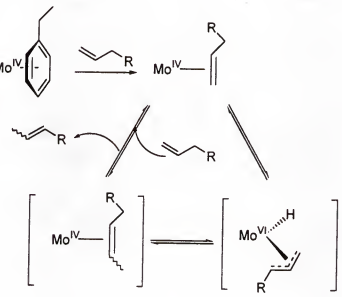

Figure 4.10. Proposed catalytic pathway for the isomerization of olefins by Mo(IV) centers.

Hydrogenolysis of Mo(IV) Olefin Complexes in the Absence of Arene Ligands

While the hydrogenolysis of Mo(IV) olefin complexes in the presence of non-bulky and electron-rich arene substrates gave Mo(IV) arene complexes, we became interested in identifying the fate of the metal species when the arene cannot coordinate to yield a stable specie or when no arene is added to the reaction mixture.

When pentane solutions of olefin complexes **20-22** were pressurized with dihydrogen (1-2 atm) at room temperature, within minutes, the forest-green color of the olefin complexes changed to dark-brown. Proton NMR spectra of the isolated brown solid showed multiple small singlets in the aliphatic region (0-1.5 ppm). These signals could only be attributed to decomposition products. A large singlet was observed 0.85 ppm (18H). The aromatic region showed several resonances [6.25 (m, 2H); 7.58 (m, 2H); 8.00 (m, 2H); 8.05 (t, 1H); 8.45 (m, 2H)]. No resonances that could be attributed to metal-hydrides were observed.

Upon further examination, it was found that this compound was also present as a side-product in the reaction of $Mo(NPh)Cl_2(o\text{-}(Me_3SiN)_2C_6H_4)THF$ **4** with two equivalents of EtMgCl to make metallacyclopentane $Mo(NPh)(CH_2CH_2CH_2CH_2)(o\text{-}(Me_3SiN)_2C_6H_4)$ (**16**) (Chapter 3). During the reaction to make **16**, in the absence of ethylene, it was proposed that a molybdenum-ethylene complex is an intermediate which disproportionates to **16** and a Mo(IV) species. The identity of this Mo(IV) species was proposed to be $[Mo(\mu\text{-}NPh)(o\text{-}(Me_3SiN)_2C_6H_4)]_n$ (**17**) (n = 1 or 2) or a product of decomposition of such a species. Thus both the hydrogenolysis of Mo(IV)-olefin complexes **20-22** in the absence of arene ligands and the alkylation of $Mo(NPh)Cl_2(o\text{-}$

$(Me_3SiN)_2C_6H_4)THF$ (**4**) with two equivalents of EtMgCl produce **17** as shown in Figure 4.11.

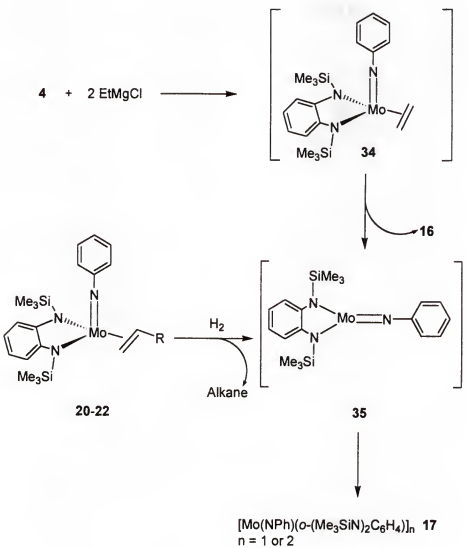

Figure 4.11. Synthesis of **17** from olefin complexes **20-22** and dichloride **4**.

Attempts to react **17** with excess PMe_3 or CN(*t*-Bu), or ethylene in C_6D_6 have not shown any appreciable changes even when heated (80°C). Poor reactivity would be expected if the formulation of **17** as a dimer is correct. Robbins *et al.* have reported the isolation and structure of $[Mo(\mu\text{-}NAr)(O\text{-}t\text{-}Bu)_2]_2$ from the decomposition of

metallacyclobutane $Mo(NAr)(CH_2CH_2CH_2)(O\text{-}t\text{-}Bu)_2$ which does not react with simple olefins or with PMe_3.[144]

Hydrogenolysis of Mo(VI) Dialkyl Complexes

Like $W(NPh)Me_2(o\text{-}(Me_3SiN)_2C_6H_4)$, $Mo(NPh)Me_2(o\text{-}(Me_3SiN)_2C_6H_4)$ (**5**) showed no reactivity under pressure of H_2 (1-2 atm). Other dialkyl complexes did react with hydrogen. When a pentane solution of bis-neopentyl complex $Mo(NPh)(CH_2CMe_3)_2(o\text{-}(Me_3SiN)_2C_6H_4)$ (**7**) was stirred for 1hr under hydrogen (1-2 atm), the orange-red color of the solution slowly changed to dark-brown. From this reaction mixture, after concentration followed by cooling (-78°C) and filtration, the Mo(IV) species **17** was isolated. In this case, the same type of aliphatic impurities as in its preparation from Mo(IV)-olefin complexes **20-22** and THF-adduct **4** were observed (by NMR).

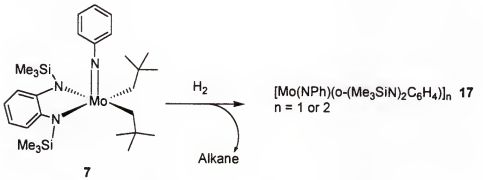

Figure 4.12. Hydrogenolysis of bis-neopentyl complex **7** to give **17**.

The hydrogenolysis of W(VI)-dialkyl complexes and W(IV)-olefin complexes produced hydride species which could be isolated but not characterized.[242,243] However,

in the case of the Mo(VI) analogs no evidence for hydride species could be found. Hydride species could still be intermediates in the hydrogenolysis of both Mo(VI) dialkyl complexes and Mo(IV) olefin complexes. Yet, no hydride species could be isolated in either case.

Hydrogenolysis of Mo(VI)-Dialkyl Complexes in the Presence of PMe_3

In an attempt to isolate any intermediate species in the hydrogenolysis of bis-neopentyl complex **7**, the reaction was carried out in the presence of excess PMe_3. Stirring a benzene solution containing **7** and PMe_3 for 5 days under a slight pressure of hydrogen afforded purple solid **36**. However, **36** was not a hydride species but a diamide-supported tris-trimethylphosphine complex analogous to **24** (Figure 4.13).

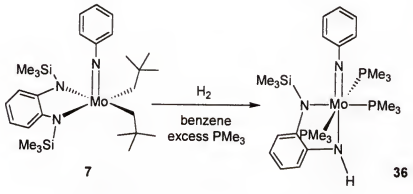

7 36

Figure 4.13. Hydrogenolysis of **7** in the presence of excess PMe_3.

Proton NMR spectra of **36** showed a sharp singlet at 0.70 ppm (9H) assigned to the $SiMe_3$ group and two broadened singlets at 0.83 ppm (9H) and 0.87 ppm (18H) corresponding to inequivalent PMe_3 groups. A broad singlet at 4.10 ppm (1H) was assigned to the amide proton.

Compound **36** was also obtained from the hydrogenolysis in benzene of tris-phosphine adduct **24** (Figure 4.14). When a benzene solution of **24** was stirred for five days under 1-2 atm of hydrogen, **36** was obtained.

Figure 4.14. Reaction of **24** with H_2 to give **36**.

A possible pathway for the formation of **36** from **7** was proposed and is shown in Figure 4.15. Throughout the five days that the reaction mixtures were allowed to stir, there were several color changes, which suggested different intermediates in this reaction. The identities of these intermediates are not yet known, though intermediacy of hydride species is possible. NMR scale monitoring of the reaction (C_6D_6) allowed us to observe a broadened triplet at 3.59 ppm within 1hr of reaction. That signal later disappeared (~18hr) and the formation of H-$SiMe_3$ was observed. If we consider these molybdenum complexes to initially behave like their tungsten analogs, then from bis-neopentyl complex **7**, hydrogenolysis should give two molecules of alkane and "Mo(IV)" **35**. This intermediate could coordinate PMe_3 to give **24** or bis-phosphine **25**. Oxidative addition of H_2 to either **24** or **25** could then produce a hydride species like **37**. The broadened triplet observed at 3.59 ppm after ~1hr of reaction could be due to such species as **37**. From **37**, H-$SiMe_3$ could be lost from the molecule by an α-abstraction-like mechanism

to give bis-imido intermediate **38**. The remaining hydride in **38** could then migrate to produce **36**.

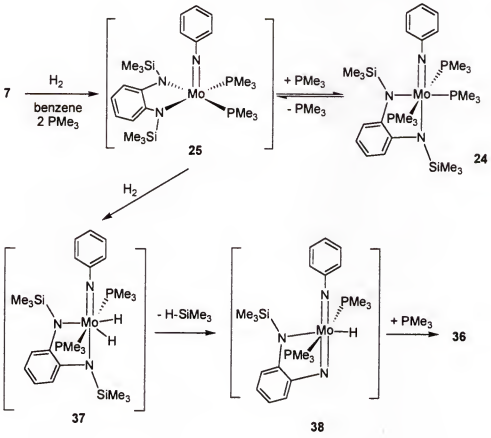

Figure 4.15. Possible mechanism for the conversion of **7** and **24** to **36** upon hydrogenolysis.

Another possible mechanism for the formation of **36** would be the addition of H_2 across the N-Si bond of the diamide ligand. Further studies into this reaction are underway.

Crystal Structure of Mo(NPh)(*o*-(Me_3SiN)(HN)C_6H_4)(PMe_3)$_3$ (**36**)

Single crystals of **36** were grown by cooling a concentrated toluene solution of **36** to -20°C for several weeks. Figure 4.16 shows an ORTEP diagram of the molecular structure of **36**. Like **23** and **24**, **36** was found to have a distorted octahedral geometry. All of the angles around the Mo metal center were found to be close to 90° with the smallest being the N2-Mo-N3 angle [75.17(6)°] and the largest the N1-Mo-N2 angle [109.48(6)°]. As in the structure of **23**, the small N2-Mo-N3 angle is due to the rigid bite angle of the chelate ring.

The Mo-imido bond length [1.797 (1) Å], like in most of our imido compounds, is short and indicative of a Mo≡N interaction.[251-254] The Mo-P bond lengths [2.4612(6) Å, 2.5204(5) Å, and 2.5385(6) Å] are all within normal values for six-coordinate Mo complexes.[268] Like in the structure of **24**, the distances from the Mo to the pda nitrogens are unusual since Mo-N2 [2.2176(15) Å] is much longer than Mo-N3 [2.0872(15) Å]. For **24** this was correlated to a *trans*-influence due to better σ-donation from the phosphine ligand P2 that is *trans* to N2. This effect should also come into play for **36**. However, the fact that a much smaller group is bound to N3 decreases the Mo-N3 bond length even further because of reduced steric hindrance.

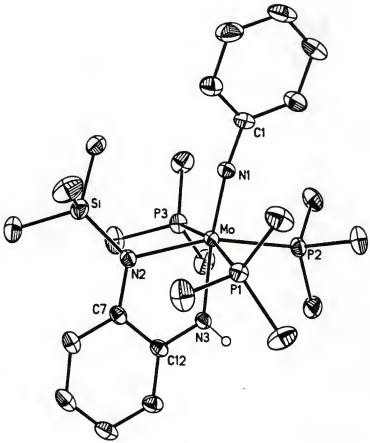

Figure 4.16. Drawing of the crystal structure of Mo(NPh)(*o*-(Me_3SiN)(HN)C_6H_4)(PMe_3)$_3$ (**36**). Ellipsoids are drawn to 40% probability. Most hydrogens have been removed for clarity.

Conclusions

The chemistry of d^2-metal centers has been well documented in the past. In this chapter the results in the study of hydrogenolysis of d^2-olefin complexes and d^0-dialkyl complexes supported by a diamide ligand were presented. It was found that when olefin complexes **19-22** reacted with hydrogen the ligated olefin was hydrogenated and that when free aromatic molecules were present, arene complexes **26-33** were produced. If no free arene was present, a compound thought to be [Mo(NPh)(*o*-(Me_3SiN)$_2C_6H_4$)]$_n$ (n = 1

or 2) was isolated. This compound was also found to be the product of the reaction of $Mo(NPh)(CH_2CMe_3)_2(o\text{-}(Me_3SiN)_2C_6H_4)$ (7) with dihydrogen. If 7 was reacted with hydrogen in the presence of PMe_3, the activation of a N-Si bond of the diamide occurred.

The work presented in chapter 2, 3, and 4 show that the behavior of molybdenum compounds supported by the diamide ligand $[o\text{-}(Me_3SiN)_2C_6H_4]^{-2}$ differs considerably from the chemistry related with the analogous tungsten complexes. However, these differences provide us with the opportunity to explore new areas of organometallic chemistry from which new applications may be revealed for these complexes.

CHAPTER 5
EXPERIMENTAL

General Methods

All reactions were conducted under a dry argon atmosphere using standard Schlenk techniques and all compounds were handled in a nitrogen-filled dry box. Diethyl ether, dimethoxyethane, tetrahydrofuran, toluene, pentane, hexane, and hexamethyldisiloxane were distilled under nitrogen from sodium or sodium benzophenone ketyl, stored over molecular sieves, and degassed prior to use. Acetonitrile was dried over P_2O_5, vacuum-transferred into a storage flask, stored over molecular sieves, and degassed prior to use. Ethylene was pre-dried through molecular sieves prior to use and hydrogen was pre-dried through activated alumina.

NMR spectra were obtained on Varian Gemini 300, VXR 300, or Mercury 300 instruments in C_6D_6, $CDCl_3$, or d_8-toluene solutions, referenced to residual solvent peaks, and reported relative to TMS.

The compounds $Mo(NPh)_2Cl_2DME$[203] and bis-trimethylsilyl-*o*-phenylenediamine[242,243] were prepared according to literature procedures. All other reagents were obtained from Aldrich Chemicals and used as received.

Atlantic Microlab, Inc., Norcross, Georgia, performed the elemental analyses. The Mass Spectrometry Laboratory at the Department of Chemistry, University of Florida, performed mass spectrometry experiments.

Synthesis of $[Mo(\mu\text{-}NPh)(NPh)(o\text{-}(Me_3SiN)_2C_6H_4)]_2$ **1**

A sample of bis-trimethylsilyl-*o*-phenylenediamine (0.574g, 2.27 mmol) was dissolved in 20 ml of diethyl ether and cooled to -78°C. With stirring, two equivalents of n-BuLi (1.82ml, 4.55 mmol) were added. The yellow solution was stirred at -78°C for 20 min. and then at room temperature for 30 minutes. This yellow solution was then combined with a slurry of $Mo(NPh)_2Cl_2(DME)$ (1.0 g, 2.27 mmol) in Et_2O (20 ml) at –78°C. The reaction mixture turned to a forest green color within a few minutes and was then stirred at room temperature for 1hr. The solution was then filtered and the precipitate dried under reduced pressure. Extraction with toluene (30ml) produced a green solution that was then pumped to dryness giving **1** as green microcrystals in low yield (0.27 g, 23% yield). Washing the product four times with cold ether and twice with pentane provided analytically pure **1**. Anal. Calcl. for $C_{48}H_{64}N_8Si_4Mo_2$: C, 54.52; H, 6.10; N, 10.60 . Found: C, 54.37; H, 6.16; N, 10.44. ^1H NMR (C_6D_6): δ -0.04 (s, 36H, NSi*Me*$_3$), 6.55 (d, 4H, aromatic), 6.75 (m, 6H, aromatic), 6.87 (t, 2H, aromatic), 7.01 (t, 4H, aromatic), 7.1 (m, 8H, aromatic), 7.26 (m, 4H, aromatic). ^{13}C NMR ($CDCl_3$): δ 1.273, 122.03, 122.27, 122.53, 123.71, 124.20, 125.67, 128.22, 128.84, 141.76, 156.28, 171.96.

Synthesis of $Mo(NPh)Cl_2(o\text{-}(Me_3SiN)_2C_6H_4)(NH_2Ph)$ **2**

Using Two Equivalents of Diamine

A hexanes solution (30 ml) of bis-trimethylsilyl-*o*-phenylenediamine (5.74 g, 22.7 mmol) was added to a slurry of $Mo(NPh)_2Cl_2(DME)$ (5.0 g, 11.3 mmol) in hexanes (40ml). The dark-red mixture was stirred for 24hrs and filtered giving a blue-purple powder. Washing the powder twice with hexanes (20ml) followed by washing with cold diethyl ether (20ml) gave pure compound in 91% yield (6.23g). Analytically pure **2** was obtained by washing twice with cold diethyl ether. Anal. Calcl. for $C_{24}H_{34}Si_2N_4Cl_2Mo$: C, 47.91; H, 5.69; N, 9.31. Found: C, 47.89; H, 5.66; N, 9.24. ^1H NMR (C_6D_6): δ 0.39 (s, 18H, NSi*Me*$_3$), 3.95 (s, 2H, N*H*$_2$Ph), 6.24 (m, 2H, aromatic), 6.54-6.80 (m, 8H, aromatic), 6.98 (t, 2H, aromatic), 7.82 (d, 2H, aromatic). ^{13}C NMR ($CDCl_3$): δ 1.28, 119.75, 120.99, 122.93, 125.08, 126.91, 128.49, 128.56, 129.47, 140.57, 146.03, 155.63.

Using One Equivalent of Diamine

The above procedure was repeated using 0.5g (1.13 mmol) of $Mo(NPh)_2Cl_2(DME)$ and 0.287g (1.13 mmol) of bis-trimethylsylil-*o*-phenylenediamine. The reaction mixture was allowed to stir for ca. 2 days at room temperature or refluxed in hexanes for 7hrs. From either procedure blue-purple $Mo(NPh)Cl_2(o\text{-}(Me_3SiN)_2C_6H_4)(NH_2Ph)$ was obtained in high yield and purity.

Synthesis of $Mo(NPh)Cl_2(o\text{-}(Me_3SiN)_2C_6H_4)(PMe_3)$ **3**

A sample of **2** (3.0g, 4.98mmol) was slurried in diethyl ether (25ml) and stirred at room temperature. A small excess of PMe_3 (0.417g, 5.48 mmol) was added via syringe. The reaction mixture immediately formed a royal blue solution, which was stirred for 1hr. Concentration (ca. 15ml) followed by cooling (-78°C) and filtration gave 2.7g of microcrystalline **3** (92%). Recrystallization of **3** from diethyl ether provided analytically pure compound. Melting point: 140-145°C. Anal. Calcl. for $C_{21}H_{36}Si_2N_3Cl_2PMo$: C, 43.15; H, 6.21; N, 7.19. Found: C, 43.03; H, 6.14; N, 7.23. ^1H NMR (C_6D_6): δ 0.44 (s, 18H, NSi*Me*$_3$), 0.74 (d, 9H, $J_{P\text{-}H}$ = 8.7Hz, P*Me*$_3$), 6.77 (t, 1H, phenylimido *para*-proton), 6.83 (m, 2H, diamine ring *meta*-protons), 6.99(m, 2H, diamine ring *ortho*-protons), 7.04 (t, 2H, phenylimido *meta*-protons), 7.83 (m, 2H, phenylimido *ortho*-protons). ^{13}C NMR ($CDCl_3$): δ 1.41, 11.50 (d, 18.17 Hz), 120.70, 125.55, 128.34, 128.77, 129.11, 129.47. ^{31}P NMR (C_6D_6): δ -22.48.

Synthesis of $Mo(NPh)Cl_2(o\text{-}(Me_3SiN)_2C_6H_4)(THF)$ **4**

At room temperature a sample (5.0g, 8.31mmol) of **2** was dissolved in tetrahydrofuran (30ml) and stirred for 1hr. Upon addition of THF the reaction mixture acquired a royal blue color. Concentration (ca. 20 ml) followed by addition of pentane (ca. 150ml) caused precipitation of **4** which was isolated by filtration and dried *in vacuo* (5.21g, 76 %). Analytically pure **4** was obtained after washing the product with cold pentane (ca. 20ml) three times. Anal. Calcl. for $C_{22}H_{35}ON_3Si_2Cl_2Mo$: C, 45.51; H,

6.08; N, 7.24. Found: C, 45.53; H, 6.10; N, 7.18. ^{1}H NMR (C_6D_6): δ 0.44 (s, 18H, NSi*Me*$_3$), 1.07 (m, 4H, -OCH$_2$C*H*$_2$C*H*$_2$CH$_2$-), 3.56 (m, 4H, -OC*H*$_2$CH$_2$CH$_2$C*H*$_2$-), 6.74 (t, 1H, phenylimido *para*-proton), 6.82 (m, 2H, diamine ring *meta*-protons), 6.94 (t, 2H, phenylimido *meta*-protons), 7.01 (m, 2H, diamine ring *ortho*-protons), 7.73 (d, 2H, phenylimido *ortho*-protons). ^{13}C NMR ($CDCl_3$): δ 1.18, 25.34, 68.58, 120.07, 120.92, 125.02, 127.26, 128.41, 128.59, 129.44.

Synthesis of Mo(NPh)Me$_2$(*o*-(Me$_3$SiN)$_2$C$_6$H$_4$) **5**

A diethyl ether solution (25ml) of **4** (1.0g, 1.72mmol) was cooled to -78°C. Two equivalents of 3.0M MeMgCl (1.15ml, 3.45mol) in Et_2O was added in a dropwise fashion and the mixture was allowed to warm to room temperature. The blue solution quickly turned to an orange-red solution. After 1hr of stirring, the mixture was pumped to dryness and extracted with pentane once (50ml). The volume of the filtrate was then reduced ca. 10ml. Acetonitrile was then added (30ml) to precipitate the product which was isolated by filtration at 0°C. (0.59g, 74%). Further purification of **5** was attained by recrystallization (five times) from concentrated pentane/acetonitrile (20/80) solutions cooled to 0°C. Melting point: 96-100°C. Anal. Calcl. for $C_{20}H_{33}N_3Si_2Mo$: C, 51.36; H, 7.11; N, 8.98. Found: C, 49.11; H, 7.02; N, 8.34. Mass Spec. Calcl. for $[M - CH_3]^+$: 454.1035 m/e. Found (FAB): 454.1096 m/e. ^{1}H NMR (C_6D_6): δ 0.36 (s, 18H, NSi*Me*$_3$), 1.14 (s, 6H, Mo*Me*$_2$), 6.84 (t, 1H, phenylimido *para*-proton), 6.98 (m, 2H, diamine ring *meta*-protons), 7.02 (t, 2H, phenylimido *meta*-protons), 7.34 (m, 2H, diamine ring *ortho*-

protons), 7.42 (d, 2H, phenylimido *ortho*-protons). ^{13}C NMR ($CDCl_3$): δ 1.22, 31.29 (s, Mo-Me_2, J_{C-H} = 126.4Hz), 122.05, 124.38, 124.83, 124.91, 128.45, 134.77, 156.45.

Synthesis of Mo(NPh)Ph_2(*o*-$(Me_3SiN)_2C_6H_4$) **6**

A diethyl ether solution (25ml) of **4** (0.5g, 0.862mmol) was cooled to -78°C and charged with 2 equivalents of PhMgBr in Et_2O (.86 ml, 1.72mmol). After 1hr of stirring at room temperature the mixture was stripped of solvent and dried (*in vacuo*). Extraction with toluene (25ml) followed by concentration (10ml) and cooling (-78°C) produced red-purple microcrystals in good yield (0.35g, 70%). Further purification of the product was attained after washing the crude product with cold pentane three times. Melting point: 114-117°C. Anal. Calcl. for $C_{30}H_{37}N_3Si_2Mo$: C, 60.89; H, 6.30; N, 7.10. Found: C, 58.54; H, 6.33; N, 6.87. Mass Spec. Calcl. for $[M + H]^+$: 594.1664 m/e. Found (FAB): 594.1669 m/e. ^1H NMR (C_6D_6): δ 0.12 (s, 18H, NSiMe_3), 6.78-6.98 (m, aromatics), 7.06-7.12 (m, aromatics), 7.34-7.43(m, 6H, aromatics), 7.60 (d, 2H, phenylimido *ortho*-protons). ^{13}C NMR ($CDCl_3$): δ 0.46, 123.23-134.784 (aromatic, overlapping).

Synthesis of Mo(NPh)$(CH_2CMe_3)_2$(*o*-$(Me_3SiN)_2C_6H_4$) **7**

A diethyl ether (40ml) solution of **4** (0.5g, 0.862mmol) was cooled to -78°C. Two equivalents of 0.54M neopentylmagnesium chloride (3.19ml, 1.72mmol) in Et_2O were added in a dropwise fashion and the reaction mixture was allowed to warm to room temperature. The blue solution quickly turned to a red-brown solution. After 1hr of

stirring, the mixture was pumped to dryness and extracted with pentane (50 ml). The filtrate was stripped of solvent *in vacuo* and **7** was isolated as a viscous oil. Recrystallization from acetonitrile (15ml) at 0°C yielded **7** as a red solid in high yield (0.41g, 79%). Further purification of **7** was attained by recrystallization (five times) from concentrated acetonitrile solutions cooled to 0°C. Anal. Calcl. for $C_{28}H_{49}N_3Si_2Mo$: C, 58.00; H, 8.52; N, 7.25. Found: C, 57.10; H, 8.61; N, 7.17. ^{1}H NMR (C_6D_6): δ 0.56 (s, 18H, NSi*Me*$_3$), 0.95 (s, 18H, CH_2C*Me*$_3$), 2.57 (d, 2H, C*H*$_2$CMe$_3$), 2.77 (d, 2H, C*H*$_2$CMe$_3$), 6.90 (t, 1H, phenylimido *para*-proton), 6.96 (m, 2H, diamine ring *meta*-protons), 7.09 (t, 2H, phenylimido *meta*-protons), 7.30 (m, 2H, diamine ring *ortho*-protons), 7.75 (d, 2H, phenylimido *ortho*-protons). ^{13}C NMR ($CDCl_3$): δ 4.17, 33.66, 38.58, 82.52, 117.97, 126.43, 128.60, 145.17, 154.44.

Synthesis of Mo(NPh)(CH_2Ph)$_2$(*o*-(Me$_3$SiN)$_2$C$_6$H$_4$) **8**

Two equivalents of a 1M benzylmagnesium chloride solution in THF (1.72ml, 1.72mmol) were added to a stirring diethyl ether (30ml) solution of **4** (0.5g, 0.862mmol) at -78°C. After 1hr of stirring at room temperature, the mixture was pumped to dryness and extracted with pentane (50 ml). The filtrate was then concentrated (ca. 10ml), cooled to -78°C, and filtered giving red-orange crystals of **8** (0.37g, 69%). Further purification of **8** was attained by recrystallization (five times) from concentrated pentane solutions cooled to -78°C. Melting point: 112-116°C. Anal. Calcl. for $C_{32}H_{41}N_3Si_2Mo$: C, 62.01; H, 6.67; N, 6.78. Found: C, 61.17; H, 6.59; N, 6.63. Mass Spec. Calcl. for $[M + H]^+$: 622.1995 m/e. Found (FAB): 622.2 m/e. ^{1}H NMR (C_6D_6): δ 0.09 (s, 18H,

NSi*Me*$_3$), 2.91 (d, 2H, C*H*$_2$Ph, $J_{H\text{-}H}$ = 11.1 Hz), 2.85 (d, 2H, C*H*$_2$Ph, $J_{H\text{-}H}$ = 11.1 Hz), 6.86 (m, 3H, aromatics), 7.07 (m, 4H, aromatics), 7.09 (m, 8H, aromatics), 7.35 (m, 4H, aromatics). ^{13}C NMR ($CDCl_3$): δ 1.083, 54.43, 122.32, 123.34, 125.56, 126.47, 127.53, 127.80, 128.57, 134.31, 152.79, 156.33.

Synthesis of Mo(NPh)(CH_2SiMe_3)$_2$(*o*-(Me_3SiN)$_2C_6H_4$) **9**

A diethyl ether solution (30ml) of **4** (0.5g, 0.862mmol) was cooled to -78°C with stirring. Two equivalents of 1.28M trimethylsilylmethylmagnesium chloride (1.34ml, 1.72mmol) in Et_2O were added in a dropwise fashion and the reaction mixture was allowed to warm to room temperature. The blue solution quickly turned to a red-orange solution. After 1hr of stirring, the mixture was pumped to dryness and extracted with pentane (40ml). The pentane filtrate was then pumped to dryness to yield **9** as a green solid in good yield (0.42g, 80%). The compound was purified further by recrystallization from acetonitrile at 0°C (five times). Anal. Calcl. for $C_{26}H_{49}N_3Si_4Mo$: C, 51.03; H, 8.07; N, 6.87. Found: C, 49.95; H, 7.91; N, 6.82. ^{1}H NMR (C_6D_6): δ 0.03 (s, 18H, CH_2Si*Me*$_3$), 0.47 (s, 18H, NSi*Me*$_3$), 1.82 (d, 2H, C*H*$_2$SiMe_3), 2.19 (br, 2H, C*H*$_2$SiMe_3), 6.87 (t, 1H, phenylimido *para*-proton), 6.81 (m, 2H, diamine ring *meta*-protons), 7.08 (t, 2H, phenylimido *meta*-protons), 7.27 (m, 2H, diamine ring *ortho*-protons), 7.71 (d, 2H, phenylimido *ortho*-protons). ^{13}C NMR ($CDCl_3$): δ 2.27, 3.73, 58.01, 118.83, 126.81, 127.60, 128.72, 154.50.

Reaction of **2** With Alkylating Agents

To a diethyl ether (30ml) solution of **2** (0.45g, 0.758mmol) cooled to -78°C, two equivalents of 0.54M neopentylmagnesium chloride in Et_2O (2.80ml, 1.51mmol) was added with stirring. The solution was then allowed to stir at room temperature for 1hr. The solvent was removed *in vacuo* and pentane used to extract the product. The pentane was then removed *in vacuo* and the solid dried. Proton NMR spectra showed a mixture of **7** and **10** in a 1.18 : 1 ratio.

The 0.45g of **2** was reacted with a 1.28M solution of trimethylsilylmethylmagnesium chloride (1.18ml, 1.51mmol) following the same reaction procedure as described above. Proton NMR spectra revealed a 1.09 : 1 mixture of **9** and **11.**

Synthesis of $Mo(NPh)_2(CH_2CMe_3)_2$ **10**

Two equivalents of 0.54M neopentylmagnesium chloride in Et_2O (8.43ml, 4.55mmol) were added to a stirring slurry of $Mo(NPh)_2Cl_2DME$ (1.0g, 2.27mmol) in Et_2O (40ml) at -78°C and stirred for 2hr at room temperature. The solvent was removed *in vacuo* and then toluene (30ml) added to extract a light-orange solution. After removal of the solvent *in vacuo* crystalline **10** was isolated in good yield (0.81g, 85%) and high purity. Further purification was attained from cooling concentrated toluene/diethylether (~20/80) solutions of **10** to -78°C (five times). Anal. Calcl. for $C_{22}H_{32}N_2Mo$: C, 62.84; H, 7.67; N, 6.66. Found: C, 61.63; H, 7.54; N, 6.56. ^1H NMR (C_6D_6): δ 1.19 (s, 36H,

CH_2CMe_3), 2.04 (s, 4H, CH_2CMe_3), 6.80 (t, 2H, phenylimido *para*-proton), 6.99 (t, 4H, phenylimido *meta*-protons), 7.28 (d, 4H, phenylimido *ortho*-protons). ^{13}C NMR (C_6D_6): δ 33.79, 81.99, 123.75, 125.24, 128.96, 157.20.

Synthesis of $Mo(NPh)_2(CH_2SiMe_3)_2$ **11**

Two equivalents of a 1.28M trimethylsilylmethylmagnesium chloride in diethyl ether (2.54ml, 3.26mmol) were added to a stirring slurry of $Mo(NPh)_2Cl_2DME$ (0.72g, 1.63mmol) in Et_2O (40ml) at -78°C and stirred for 2hr at room temperature. The solvent was removed *in vacuo* and then pentane (ca. 25 ml) was added to extract a dark-orange solution, which after filtration and removal of the pentane *in vacuo* gave crystalline **11** as a red solid in good yield (0.62g, 84%). Further purification was attained from cooling concentrated pentane solutions of **11** to -78°C (five times). Anal. Calcl. for $C_{20}H_{32}N_2Si_2Mo$: C, 53.07; H, 7.12; N, 6.19. Found: C, 51.45; H, 7.10; N, 6.05. ^1H NMR (C_6D_6): δ 0.05 (s, 36H, CH_2SiMe_3), 1.62 (s, 4H, CH_2SiMe_3), 7.06 (t, 2H, phenylimido *para*-proton), 7.13 (d, 4H, phenylimido *meta*-protons), 7.24 (t, 4H, phenylimido *ortho*-protons). ^{13}C NMR ($CDCl_3$): δ 1.96, 56.52, 123.58, 124.89, 128.54, 156.34.

Synthesis of $Mo(NPh)(C(H)C(CH_3)_3)(o\text{-}(Me_3SiN)_2C_6H_4)(PMe_3)$ **13**

In a re-sealable ampule a toluene (30ml) solution of **7** (1.12g, 1.92mmol) was combined with an excess of trimethylphosphine (1.46g, 19.2mmol) and heated to 80°C

for 0.5hr. The color of the solution changed form red-orange to a dark purple color. The toluene was removed *in vacuo*. Microcrystals of **13** were obtained from a concentrated pentane (ca. 5ml) solution. Isolated yield, 0.70g (63%). Compound **13** was recrystallized three times from pentane (ca. 5ml) at -78°C. Anal. Calcl. for $C_{26}H_{46}N_3Si_2PMo$: C, 53.49; H, 7.94; N, 7.19. Found: C, 51.11; H, 7.66; N, 7.23. ^1H NMR (C_6D_6): δ 0.378 (s, 18H, NSi*Me*$_3$), 0.871 (d, 9H, $J_{P\text{-}H}$= 8.1Hz, P*Me*$_3$) 1.32 (s, 9H, C(C*H*$_3$)$_3$), 6.6-7.2 (m, aromatic), 12.14 (s, 1H, C(*H*)C(CH$_3$)$_3$). ^{13}C NMR (C_6D_6): δ 4.0, 17.5, 35.7, 43.4, 116.2, 120.8, 123.0, 124.6, 125.9, 128.6, 148.6, 275.3.

Synthesis of Mo(NPh)(C(H)Si(CH$_3$)$_3$)(*o*-(Me$_3$SiN)$_2$C$_6$H$_4$)(PMe$_3$) **14**

In an NMR tube a toluene-d_8 solution of **9** was charged with an excess of PMe_3 and heated to 80°C for 12hrs. Formation of **14** was observed by NMR. Efforts to isolate this compound have proven difficult.

Synthesis of Mo(NPh)(CH$_2$CH$_2$CH$_2$CH$_2$)(*o*-(Me$_3$SiN)$_2$C$_6$H$_4$) **16**

Method 1

One equivalent of 0.99M BrMgCH$_2$CH$_2$CH$_2$CH$_2$MgBr (0.862mmol) was added to a diethyl ether solution of **4** (0.5g, 0.862) cooled to -78°C. The blue solution quickly turned to a purple solution upon addition of the alkylating agent. As the reaction mixture was allowed to warm-up to room temperature, the color of the solution slowly turned into a red-orange. The red-orange solution was stirred for 1 hr. and pumped to dryness (*in*

vacuo). The remaining solids were extracted with pentane and filtered. The red-orange filtrate was pumped to dryness an dried of overnight (*in vacuo*). By NMR, metallacyclopentane **16** was obtained in low purity and yield.

Method 2

To a cooled (-78°C) diethyl ether solution of **4** (0.5g, 0.862 mmol), two equivalents of EtMgCl in Et_2O (1.72 mmol, 2.0M) was added. Reaction work-up, similar to that described in method 1, provided metallacyclopentane **16** and dimeric **17** in low purity.

Method 3

To a schlenk tube containing a cooled (-78°C) diethyl ether solution of **4** (1.0g, 0.862mmol), two equivalents of EtMgCl in Et_2O (3.45 mmol, 2.0M) was added dropwise. The solution quickly changed color from blue to purple. This purple solution was frozen and the vessel evacuated. Subsequently, the solution was allowed to thaw while the neck of the vessel was degassed for five minutes using dry ethylene. Ethylene was added to the schlenk tube (1-2 atm) and the solution stirred for 1hr at room temperature. The resulting red-orange solution was pumped to dryness (*in vacuo*) followed by extraction with pentane. The volume of the filtrate was reduced and the concentrated solution cooled to -78°C. This yielded dark red crystals that were isolated by filtration. Isolated yield 0.58g (69%). Further purification of **16** was done by recrystallization from pentane (five times) at -78°C. Anal. Calcl. for $C_{22}H_{35}N_3Si_2Mo$:

C, 53.52; H, 7.14; N, 8.51. Found: C, 52.67; H, 7.11; N, 8.44. ^{1}H NMR (C_6D_6): δ 0.32 (s, 18H, NSi*Me*$_3$), 1.53 (m, 2H, C*H*$_2$CH$_2$CH$_2$C*H*$_2$), 2.01 (m, 2H, CH$_2$C*H*$_2$C*H*$_2$CH$_2$), 2.64 (m, 2H, CH$_2$C*H*$_2$C*H*$_2$CH$_2$), 3.13 (m, 2H, C*H*$_2$CH$_2$CH$_2$C*H*$_2$), 6.90 (t, 1H, phenylimido *para*-proton), 7.05 (m, 2H, diamine ring *meta*-protons), 7.10 (t, 2H, phenylimido *meta*-protons), 7.42 (m, 2H, diamine ring *ortho*-protons), 7.50 (m, 2H, phenylimido *ortho*-protons). ^{13}C NMR (C_6D_6): δ 1.03, 36.27, 57.31, 123.32, 124.45, 125.10, 125.56, 128.98, 133.36.

Synthesis of η^2-Olefin Complexes (**19-22**)

To an Et_2O solution containing 0.5g (0.862mmol) of **4**, cooled to -78°C, two equivalents of a 2.0M Et_2O solution of RMgCl (R = $CH_2CH_2C_6H_5$ **19**, $CH_2CH_2CH_3$ **20**, $CH_2CH(CH_3)_2$ **21**, $CH_2CH_2CH_2CH_3$ **22**, $CH(CH_3)CH_2CH_3$ **22**) or one equivalent of But_2Mg (**22**) (1M in heptane) was added dropwise, with stirring. The mixture quickly turned from a blue-purple mixture to a red-purple mixture. Then the reaction mixture was allowed to stir at room temperature for about 2hr. During this time the red-purple solution changed to an orange-red solution and then to a forest green solution. After this time, the diethylether was removed (*in vacuo*) and the solids dried for 1hr. Pentane (40ml) was then used to extract the products by filtration.

R = $CH_2CH_2C_6H_5$ (**19**)

The volume of the pentane extract was reduced ca. 10ml. (*in vacuo)* and then cooled to -78°C for two hours. Forest-green crystals appeared at the bottom of the flask

after which the mixture was filtered to yield Mo(NPh)(η^2-styrene)(*o*-($Me_3SiN)_2C_6H_4$) (**19**) as a crystalline solid. Yield 77%. Recrystallization from concentrated pentane (-78°C) solutions of **19** allowed for further purification (x5). Melting point: 110-113°C. Anal. Calcd. for $C_{26}H_{35}N_3Si_2Mo$: C, 57.65; H, 6.51; N, 7.76. Found: C, 52.27; H, 6.25; N, 7.90. Mass Spec. Calcl. for $[M + H]^+$: 544.1506 m/e. Found (FAB): 544.1569 m/e. ^1H NMR (C_6D_6): δ 0.09 (s, 9H, NSi*Me*$_3$), 0.29 (s, 9H, NSi*Me*$_3$), 0.36 (s, 9H, NSi*Me*$_3$), 0.41 (s, 9H, NSi*Me*$_3$), 1.05 (m, 1H, C*H*$_2$CHPh), 1.16 (m, 1H, C*H*$_2$CHPh), 2.22 (t, 1H, CH$_2$C*H*Ph), 3.38 (m, 1H, C*H*$_2$CHPh), 3.54 (m, 1H, C*H*$_2$CHPh), 4.90 (t, 1H, CH$_2$C*H*Ph), 5.94 (d, 1H, styrene *ortho*-proton), 6.6-7.5 (aromatics). ^{13}C NMR (C_6D_6): δ 1.19, 1.44, 1.61, 50.81, 52.62, 67.38, 74.27, 123.24-129.05 (aromatics).

R = $CH_2CH_2CH_3$ (**20**)

The volume of the pentane extract was reduced ca. 10ml. (*in vacuo*) and then cooled to -78°C for two hours. Dark-green microcrystals appeared and after filtration, Mo(NPh)(η^2-propene)(*o*-($Me_3SiN)_2C_6H_4$) (**20**) was obtained as microcrystals. Yield 68%. Recrystallization from concentrated pentane (-78°C) solutions of **20** allowed for further purification (x5). Anal. Calcd. for: C, 52.59; H, 6.94; N, 8.76. Found: C, 48.26; H, 6.481; N, 8.33. ^1H NMR (C_6D_6): δ 0.32 (s, 27H, NSi*Me*$_3$), 0.36 (s, 9H, NSi*Me*$_3$), 0.45 (m, 1H, C*H*$_2$CHCH$_3$), 0.90 (m, 4H, CH$_2$CHC*H*$_3$), 1.34 (m, 1H, CH$_2$C*H*CH$_3$), 2.40 (d, 3H, CH$_2$CHC*H*$_3$), 2.81 (m, 1H, C*H*$_2$CHCH$_3$), 3.32 (m, 1H, CH$_2$C*H*Ph), 4.01 (m, 1H, C*H*$_2$CHCH$_3$), 6.8-7.5 (aromatics). ^{13}C NMR (C_6D_6): δ 0.90-1.60, 19.65, 25.94, 56.55, 57.68, 64.02, 73.83, 123.0-125.5 (aromatics), 128.9.

R = $CH_2CH(CH_3)_2$ (**21**)

The pentane solution was pumped to dryness (*in vacuo*). This allowed Mo(NPh)(η^2-isobutene)(*o*-$(Me_3SiN)_2C_6H_4$) (**21**) to be isolated as a thick, dark-green oil. Further attempts to obtain **21** as a solid were not successful. Isolated yield 56%. ^1H NMR (C_6D_6): δ 0.29 (s, 9H, NSi*Me*$_3$), 0.36 (s, 9H, NSi*Me*$_3$), 0.73 (m, 4H, CH_2C(CH_3)$_2$), 2.60 (s, 3H, $CH_2C(CH_3)_2$), 2.99 (d, 1H, CH_2C$(CH_3)_2$), 6.88 (t, 1H, phenylimido *para*-proton), 7.00 (m, 2H, diamine ring *meta*-protons), 7.07 (t, 2H, phenylimido *meta*-protons), 7.41 (m, 4H, diamine ring *ortho*-protons and phenylimido *ortho*-protons). ^{13}C NMR (C_6D_6): δ 1.11, 1.72, 25.94, 27.58, 33.50, 59.101, 81.00, 123.14, 123.59, 124.03, 124.37, 124.68, 124.98, 129.06, 131.90, 132.80, 157.90.

R = $CH_2CH_2CH_2CH_3$, $CH(CH_3)CH_2CH_3$, or $(CH_3CH_2CH_2CH_2)_2Mg$ (**22**)

The pentane solution was pumped to dryness (*in vacuo*). This allowed Mo(NPh)(η^2-1-butene)(*o*-$(Me_3SiN)_2C_6H_4$) (**22**) and Mo(NPh)(η^2-2-butene)(*o*-$(Me_3SiN)_2C_6H_4$) (**22**) to be isolated in a mixture and as a dark-green oil. Further attempts to obtain either of these compounds as solids and purify them were unsuccessful.

Synthesis of Mo(NPh)(C≡NC$(CH_3)_3)_3$(*o*-$(Me_3SiN)_2C_6H_4$) (**23**)

To a Et_2O solution of **20** (1.0g, 1.83mmol), 0.62ml (5.53mmol), tert-butylisocyanide was added at room temperature, with stirring. The reaction mixture quickly turned from green to purple and was then stirred for 1hr. at room temperature. Small crystals of **23** started forming in solution after this time. Subsequently, the volume

of the reaction was reduced and cooled for 1hr. (-78°C). Purple microcrystals of **23** were obtained by filtration at -78°C. The solids were then dried overnight, *in vacuo*. Yield 82%. Cooling concentrated pentane solutions to -78°C (five times) attained further purification. Melting point: 118-122°C. Mass Spec. Calcl. for $C_{32}H_{52}N_6Si_2Mo$ [M – CH_3]$^+$: 674.2852 m/e. Found (FAB): 674.2795 m/e. ^{1}H NMR (C_6D_6): δ 0.58 (s, 9H, NSi*Me*$_3$), 0.77 (s, 9H, NSi*Me*$_3$), 0.93 (s, 18H, CN(C(C*H*$_3$)$_3$), 1.17 (s, 9H, CN(C(C*H*$_3$)$_3$), 6.81 (t, 1H, imido *para*-H), 6.92 (m, 2H, pda), 7.05 (t, 2H, imido *meta*-H), 7.31 (d, 2H, imido *ortho*-H), 7.42 (m, 2H, pda). ^{13}C NMR (d_8-toluene, -10°C): δ 4.02, 4.84, 30.02, 30.82, 56.26, 58.35, 112.63, 116.39, 116.53, 118.12, 120.52, 121.16, 122.60, 122.96, 150.86, 155.98, 157.72, 160.28.

Synthesis of Mo(NPh)(PMe$_3$)$_3$(*o*-(Me$_3$SiN)$_2$C$_6$H$_4$) (**24**)

To a Et_2O solution of **20** (1.0g, 1.83mmol), 0.57ml (5.53mmol) of trimethylphosphine was added at room temperature, with stirring. The reaction mixture quickly turned from green to purple and was then stirred for 1hr. at room temperature. Small crystals of **24** started forming in solution after this time. Subsequently, the volume of the reaction was reduced and cooled for 1hr. (-78°C). Purple microcrystals of **24** were obtained by filtration at -78°C. The solids were then dried overnight, *in vacuo*. Yield 84%. Anal. Calcd. for. ^{1}H NMR (d_8-toluene, -60°C): δ 0.31 (s, 9H, NSi*Me*$_3$), 0.57 (s, 9H, NSi*Me*$_3$), 0.93 (s, 18H, *PMe*$_3$), 1.22 (s, 9H, P*Me*$_3$), 6.6-6.8 (m, aromatics), 6.8-6.9 (m, aromatics), 7.44 (d, 2H, imido *ortho*-H). ^{13}C NMR (d_8-toluene, -70°C): δ -0.13, 17.77, 23.60, 110.54, 117.64, 118.07, 120.05, 120.10, 150.50, 153.69, 156.82.

Reaction of **19** With Ethylene

In an NMR tube equipped with a Young valve, a small sample of **19** was dissolved in C_6D_6. To this solution, 10psi of dry ethylene was added at room temperature. Instantly, the green color of the solution of **19** changed a red-orange color. By NMR, the quantitative conversion of **19** to **16** was confirmed.

Reaction of Mo(NPh)(η^2-styrene)(*o*-$(Me_3SiN)_2C_6H_4$) (**19**) With H_2, Synthesis of Mo(NPh)(η^6-ethylbenzene)(*o*-$(Me_2SiN)_2C_6H_4$)

In a schlenk tube, a pentane solution (25ml) containing 0.25g of **19** (0.46mmol) was frozen and evacuated. The vessel was then closed and the mixture thawed. The neck of the vessel was flushed with dry H_2 for three minutes. Hydrogen gas was then added (10psi) to the solution and the mixture was allowed to stir for 0.5hr. The solution quickly turned to a blue-green color from the forest-green of **19**. The volume was reduced *in vacuo* (ca. 10ml) and cooled to -78°C. Green microcrystals quickly precipitated from the solution and **26** was isolated in 71% yield (0.17g) by filtration. Mass Spec. Calcl. for $C_{26}H_{38}N_3Si_2Mo$ $[M + H]^+$: 546.1663 m/e. Found (FAB): 546.1652 m/e. ^1H NMR (C_6D_6): δ 0.36 (s, 18H, NSi*Me*$_3$), 0.54 (t, 3H, $C_6H_5CH_2CH_3$), 1.53 (q, 2H, $C_6H_5CH_2CH_3$), 4.56 (t, 1H, *o*-$C_6H_5CH_2CH_3$), 4.92 (d, 2H, *m*-$C_6H_5CH_2CH_3$), 5.03 (t, 2H, *p*-$C_6H_5CH_2CH_3$), 6.71 (m, 2H, *o*-pda), 6.91 (m, 2H, *m*-pda), 7.05 (m, 5H, Mo≡NC_6H_5). ^{13}C NMR (C_6D_6): δ 3.98, 12.17, 27.54, 104.86, 105.73, 114.72, 116.27, 117.60, 119.19, 125.75, 129.13, 133.60, 155.35, 159.93.

Synthesis of Mo(NPh)(η^6-arene)(*o*-$(Me_3SiN)_2C_6H_4$) (**26-33**)

Arene complexes **26-33** were prepared from pentane solutions of freshly Mo(NPh)(η^2-propene)(*o*-$(Me_3SiN)_2C_6H_4$) (**20**).

To an Et_2O solution (25ml, -78°C) containing 0.5g of **4** (0.862mmol), two equivalents of *n*-PrMgCl (2.0M in Et_2O, 0.862ml) was added dropwise. The reaction mixture was then allowed to stir at room temperature for 1hr. The solvent was removed *in vacuo* and pentane (30ml) was used to extract **20** into a schlenk tube. To this pentane solution of **20**, 15 equivalents (relative to **4**) of the appropriate arene was added and the mixture was frozen and evacuated. The stopcock to the vessel was then closed and the frozen mixture was thawed. The neck to the vessel was then flushed with dry H_2 for three minutes. Hydrogen (10psi) was added to the solution, which was stirred at room temperature for 0.5hr.

Arene = Ethylbenzene (**26**)

Ethylbenzene (1.37g, 12.9mmol) was added to the pentane solution of **20** prior to adding H_2. After stirring under H_2, the volatiles were removed and the green solid (**26**) was dried (*in vacuo*). Pentane (10ml) was then added to redissolve **26**. The mixture was then cooled to -78°C until green microcrystals of **26** appeared. These microcrystals were then filtered and dried (*in vacuo*). Yield 0.47g of **26** (72%).

Arene = Benzene (**27**)

Benzene (1.01g, 12.9mmol) was added to the pentane solution of **20** prior to adding H_2. After stirring under H_2, the volatiles were removed and the green solid (**27**) was dried (*in vacuo*). Pentane (10ml) was then added to redissolve **27**. The mixture was then cooled to -78°C until green microcrystals of **27** appeared. These microcrystals were then filtered and dried (*in vacuo*). Yield 0.32g of **27** (74%). Mass Spec. Calcl. for $C_{24}H_{34}N_3Si_2Mo$ $[M + H]^+$: 518.1349 m/e. Found (FAB): 518.1310 m/e. ^1H NMR (C_6D_6): δ 0.33 (s, 18H, NSi*Me*$_3$), 4.80 (s, 6H,C_6H_6), 6.74 (m, 2H, *o*-pda), 6.93 (m, 2H, *m*-pda), 6.88 (m, 3H, Mo≡NC$_6$*H*$_5$), 7.05 (d, 2H, imido *ortho*-H). ^{13}C NMR (d_8-toluene, -20°C): δ 3.76, 108.82, 115.97, 117.48, 118.79, 125.58, 155.08, 159.50.

Arene = Toluene (**28**)

Toluene (1.19g, 12.9mmol) was added to the pentane solution of **20** prior to adding H_2. After stirring under H_2, the volatiles were removed and the green solid (**28**) was dried (*in vacuo*). Pentane (10ml) was then added to redissolve **28**. The mixture was then cooled to -78°C until green microcrystals of **28** appeared. These microcrystals were then filtered and dried (*in vacuo*). Yield 0.37g of **28** (81%). ^1H NMR (C_6D_6): δ 0.35 (s, 18H, NSi*Me*$_3$), 1.15 (s, 3H, $C_6H_5CH_3$), 4.55 (t, 1H, *o*-$C_6H_5CH_3$), 4.80 (d, 2H, *m*-$C_6H_5CH_3$), 4.98 (t, 2H, *p*-$C_6H_5CH_3$), 6.71 (m, 2H, *o*-pda), 6.94 (m, 2H, *m*-pda), 7.03 (m, 5H, Mo≡NC$_6$*H*$_5$).

Arene = *o*-Xylene (**29**)

Ortho-xylene (1.36g, 12.9mmol) was added to the pentane solution of **20** prior to adding H_2. After stirring under H_2, the volatiles were removed and the green solid (**29**) was dried (*in vacuo*). Pentane (10ml) was then added to redissolve **29**. The mixture was then cooled to -78°C until green microcrystals of **29** appeared. These microcrystals were then filtered and dried (*in vacuo*). Yield 0.37g of **29** (79%). ^{1}H NMR (C_6D_6): δ 0.36 (s, 18H, NSi*Me*$_3$), 1.10 (s, 6H, C_6H_5-*o*-(CH_3)$_2$), 4.56 (m, 2H, C_6H_5-*o*-(CH_3)$_2$), 5.29 (m, 2H, C_6H_5-*o*-(CH_3)$_2$), 6.71 (m, 2H, *o*-pda), 6.92 (m, 2H, *o*-pda), 6.86 (m, 1H, Mo≡NC_6H_5), 7.05 (m, 4H, Mo≡NC_6H_5).

Arene = *m*-Xylene (**30**)

Meta-xylene (1.36g, 12.9mmol) was added to the pentane solution of **20** prior to adding H_2. After stirring under H_2, the volatiles were removed and the green solid (**30**) was dried (*in vacuo*). Pentane (10ml) was then added to redissolve **30**. The mixture was then cooled to -78°C until green microcrystals of **30** appeared. These microcrystals were then filtered and dried (*in vacuo*). Yield 0.36g of **30** (78%). Mass Spec. Calcl. for $C_{26}H_{38}N_3Si_2Mo$ $[M + H]^+$: 546.1663 m/e. Found (FAB): 546.1656 m/e. ^{1}H NMR (C_6D_6): δ 0.37 (s, 18H, NSi*Me*$_3$), 1.19 (s, 6H, C_6H_5-*m*-(CH_3)$_2$), 4.45 (d, 2H, C_6H_5-*m*-(CH_3)$_2$), 5.04 (s, 1H, C_6H_5-*m*-(CH_3)$_2$), 5.49 (t, 1H, C_6H_5-*m*-(CH_3)$_2$), 6.72 (m, 2H, *o*-pda), 6.94 (m, 2H, *o*-pda), 6.87 (t, 1H, imido-*p*-proton), 7.00 (d, 2H, imido-*o*-protons), 7.08 (t, 2H, imido-*m*-protons). ^{13}C NMR (d_8-toluene, -40°C): δ 4.07, 94.04, 96.93, 113.95, 116.38, 117.43, 119.41, 125.61, 154.79, 159.77.

Arene = *p*-Xylene (**31**)

Para-xylene (1.36g, 12.9mmol) was added to the pentane solution of **20** prior to adding H_2. After stirring under H_2, the volatiles were removed and the green solid (**31**) was dried (*in vacuo*). Pentane (10ml) was then added to redissolve **31**. The mixture was then cooled to -78°C until green microcrystals of **31** appeared. These microcrystals were then filtered and dried (*in vacuo*). Yield 0.36g of **31** (78%). Mass Spec. Calcl. for $C_{26}H_{38}N_3Si_2Mo$ $[M + H]^+$: 546.1663 m/e. Found (FAB): 546.1641 m/e. ^1H NMR (C_6D_6): δ 0.36 (s, 18H, NSi*Me*$_3$), 1.21 (s, 6H, C_6H_5-*p*-(CH_3)$_2$), 4.85 (s, 4H, C_6H_5-*p*-(CH_3)$_2$), 6.72 (m, 2H, *o*-pda), 6.93 (m, 2H, *o*-pda), 6.86 (t, 1H, imido-*p*-proton), 7.05-7.10 (m, 4H, imido protons). ^{13}C NMR (d_8-toluene, -40°C): δ 4.04, 106.21, 116.49, 117.49, 119.43, 125.64, 154.73, 159.92.

Arene = Diphenylmethane (**32**)

Diphenylmethane (2.17g, 12.9mmol) was added to the pentane solution of **20** prior to adding H_2. After stirring under H_2, the volatiles were removed and a dark-green solid was dried (*in vacuo*). Pentane (10ml) was then added to redissolve the products. The mixture was then cooled to -78°C until a green solid appeared. This solid was then filtered and dried (*in vacuo*). By NMR, this solid was a mixture of **32** and uncoordinated diphenylmethane. Attempts to purify this mixture further by sublimation or recrystallization were not successful. ^1H NMR (C_6D_6): δ 0.35 (s, 18H, NSi*Me*$_3$), 1.38 (s, 2H, η^6–C_6H_5-C*H*$_2$-C_6H_5), 4.65 (t, 1H, η^6–C_6H_5-CH_2-C_6H_5), 4.87 (d, 2H, η^6–C_6H_5-CH_2-C_6H_5), 5.05 (t, 2H, η^6–C_6H_5-CH_2-C_6H_5), 6.57 (d, 1H, η^6–C_6H_5-CH_2-C_6H_5), 6.77 (m, 2H,

o-pda). Other aromatic resonances in the 6.7-7.4 ppm region were obscured by the excess diphenylmethane resonances.

Arene = Bibenzyl (**33**)

Bibenzyl (2.35g, 12.9mmol) was added to the pentane solution of **20** prior to adding H_2. After stirring under H_2, the volatiles were removed and a dark-green solid was dried (*in vacuo*). Pentane (10ml) was then added to redissolve the products. The mixture was then cooled to -78°C until a green solid appeared. This solid was then filtered and dried (*in vacuo*). By NMR, this solid was a mixture of **33** and uncoordinated bibenzyl. Attempts to purify this mixture further by sublimation or recrystallization were not successful. ^{1}H NMR (C_6D_6): δ 0.35 (s, 18H, NSi*Me*$_3$), 1.88 (t, 2H, η^6–C_6H_5-C*H*$_2$CH$_2$-C_6H_5), 2.43 (t, 2H, η^6–C_6H_5-CH$_2$C*H*$_2$-C_6H_5), 4.61 (t, 1H, η^6–C_6*H*$_5$-CH$_2$CH$_2$-C_6H_5), 4.92 (d, 2H, η^6–C_6*H*$_5$-CH$_2$CH$_2$-C_6H_5), 5.04 (t, 2H, η^6–C_6*H*$_5$-CH$_2$CH$_2$-C_6H_5). Other resonances in the aromatic region were obscured by the excess bibenzyl resonances.

Reaction of **26** With Excess C≡NC(CH$_3$)$_3$ to Make **23**

To a pentane solution of **26** (0.5g, 0.9mmol), 0.31ml (2.7mmol), tert-butylisocyanide was added at room temperature, with stirring. The reaction mixture quickly turned from green to purple and was then stirred for 1hr. at room temperature. Small crystals of **23** started forming in solution after this time. Subsequently, the volume of the reaction was reduced and cooled for 1hr. (-78°C). Purple microcrystals of **23** were

obtained by filtration at -78°C. The solids were then dried overnight, *in vacuo*. Yield 82%.

Reaction of **26** With Excess PMe_3 to Make **24**

To a pentane solution of **26** (0.5g, 0.9mmol), 0.28ml (2.7mmol) of trimethylphosphine was added at room temperature, with stirring. The reaction mixture quickly turned from green to purple and was then stirred for 1hr. at room temperature. Small crystals of **24** started forming in solution after this time. Subsequently, the volume of the reaction was reduced and cooled for 1hr. (-78°C). Purple microcrystals of **24** were obtained by filtration at -78°C. The solids were then dried overnight, *in vacuo*. Yield 84%.

Reaction of **26** With Ethylene.

In an NMR tube equipped with a Young valve, a small sample of **26** was dissolved in C_6D_6. To this solution, 10psi of dry ethylene were added at room temperature. Instantly, the green color of the solution of **26** changed a red-orange color. The quantitative conversion of **26** to **16** was confirmed by NMR.

Reaction of **26** With Styrene

In an NMR tube, a small sample of **26** was dissolved in C_6D_6. To this solution, one drop of styrene was added at room temperature. The quantitative conversion of **26** to **19** was confirmed by NMR.

Reaction of **7** With H_2

In a NMR tube equipped with a Young valve, a small sample of **7** was dissolved in C_6D_6. To this solution, 10psi of dry hydrogen were added at room temperature. Within minutes, the red-orange color of the solution of **7** dark brown. After five days, the brown color of the solution remained and NMR confirmed the conversion of **7** to **17**.

Reaction of Mo(NPh)(η^2-propene)(*o*-$(Me_3SiN)_2C_6H_4$) (**20**) With Hydrogen to Make **17**

Compound **17** was prepared from pentane solutions of freshly Mo(NPh)(η^2-propene)(*o*-$(Me_3SiN)_2C_6H_4$) (**20**).

To an Et_2O solution (25ml, -78°C) containing 0.5g of **4** (0.862mmol), two equivalents of *n*-PrMgCl (2.0M in Et_2O, 0.862ml) was added dropwise. The reaction mixture was then allowed to stir at room temperature for 1hr. The solvent was removed *in vacuo* and pentane (30ml) was used to extract **20** into a schlenk tube. The stopcock to the vessel was then closed and the frozen mixture was thawed. The neck to the vessel was then flushed with dry H_2 for three minutes. Hydrogen (10psi) was added to the solution, which was stirred at room temperature for 0.5hr. A fast color change from the

forest green of **20** to a dark brown occurred. Small solid particles precipitated from the solution. The volume of the solution was reduced (*ca.* 10ml) *in vacuo*. The concentrated mixture was then cooled to -78°C, and then filtered. Compound **17** was isolated in low purity. Attempts to purify this mixture further by recrystallization were not successful. ^{1}H NMR (C_6D_6): δ 0.85 (s, 18H, NSi*Me*$_3$), 6.25 (m, 2H), 7.58 (m, 2H), 8.00 (m, 2H), 8.05 (t, 1H), 8.45 (m, 2H).

Reaction of **7** With H_2 in the Presence of Excess PMe_3 to Make Mo(NPh)(*o*-(Me_3SiN)(HN)C_6H_4)(PMe_3)$_3$ (**36**)

In a NMR tube equipped with a Young valve, a small sample of **7** was dissolved in C_6D_6 along with two drops of PMe_3. To this solution, 10psi of dry hydrogen were added at room temperature. Within minutes, the red-orange color of the solution of **7** changed to a green color. This green color then changed to brown and finally purple. After five days, the purple color of the solution remained and NMR confirmed the quantitative conversion of **7** to **36**.

Synthesis of **36** from the Reaction of **24** and H_2

In a Schlenk tube, a benzene (30ml) solution of **24** was frozen and evacuated. The stopcock to the vessel was then closed and the mixture thawed. Purging with dry hydrogen for five minutes degassed the neck of the flask. Then, 10psi of hydrogen were added at room temperature, with stirring. The reaction mixture quickly turned from purple to green and then (~2hr) to brown. It was then stirred for five days at room

temperature after which a purple solution remained. The solvent was then removed *in vacuo*. Pentane (10ml) was then added followed by the cooling of the solution to -78°C. Purple microcrystals of **36** were obtained by filtration at -78°C. The solids were then dried overnight, *in vacuo*. ^{1}H NMR (C_6D_6): δ 0.71 (s, 9H, NSi*Me*$_3$), 0.91 (br s, 27H, PMe_3), 4.04 (br s, 1H, N*H*), 6.71 (d, 1H, *o*-pda), 6.87 (m, 3H, aromatics), 7.03 (m, 4H, aromatics), 7.52 (d, 1H, *o*-pda). ^{13}C NMR (C_6D_6): δ 5.38, 19.75, 113.84, 116.34, 117.03, 120.98, 121.43, 122.44, 125.61, 150.02, 152.11, 157.84. ^{31}P NMR (C_6D_6): δ -12.26.

X-ray Experimental for Mo(NPh)Cl_2(*o*-$(Me_3SiN)_2C_6H_4$)(PMe_3) **3**

Suitable crystals of **3** were obtained by cooling a concentrated Et_2O solution to -20°C for several days. Data were collected at 173 K on a Siemens SMART PLATFORM equipped with a CCD area detector and a graphite monochromator utilizing MoK_α radiation (λ = 0.71073 Å). Cell parameters were refined using 8192 reflections. A hemisphere of data (1381 frames) was collected using the ω-scan method (0.3° frame width). The first 50 frames were remeasured at the end of data collection to monitor instrument and crystal stability (maximum correction on I was < 1 %). Psi scan absorption corrections were applied based on the entire data set.

The structure was solved by the Direct Methods in *SHELXL-97*,[287] and refined using full-matrix least squares. The non-H atoms were treated anisotropically, whereas the hydrogen atoms were calculated in ideal positions and were riding on their respective carbon atoms. A total of 461 parameters were refined in the final cycle of refinement

using 6045 reflections with $I > 2\sigma(I)$ to yield R_1 and wR_2 of 2.83% and 6.76%, respectively. Refinement was done using F^2.

X-ray Experimental for Mo(NPh)(η^2-styrene)(*o*-$(Me_3SiN)_2C_6H_4$) (**19**)

Suitable crystals of **19** were obtained from concentrated pentane solution at room temperature, overnight. Data were collected at 173 K on a Siemens SMART PLATFORM equipped with A CCD area detector and a graphite monochromator utilizing MoK_α radiation (λ = 0.71073 Å). Cell parameters were refined using 8192 reflections. A hemisphere of data (1381 frames) was collected using the ω-scan method (0.3° frame width). The first 50 frames were remeasured at the end of data collection to monitor instrument and crystal stability (maximum correction on I was < 1 %). Absorption corrections were applied based on measured indexed faces.

The structure was solved by the Direct Methods in *SHELXTL*,[288] and refined using full-matrix least squares. The non-H atoms were treated anisotropically, whereas the hydrogen atoms were calculated in ideal positions and were riding on their respective carbon atoms. A total of 290 parameters were refined in the final cycle of refinement using 5129 reflections with $I > 2\sigma(I)$ to yield R_1 and wR_2 of 2.88 and 6.84, respectively. Refinement was done using F^2.

X-ray Experimental for $Mo(NPh)(C{\equiv}NC(CH_3)_3)_3(o\text{-}(Me_3SiN)_2C_6H_4)$ (**23**)

Suitable crystals of **23** were obtained by slow evaporation of a pentane solution. Data were collected at 173 K on a Siemens SMART PLATFORM equipped with A CCD area detector and a graphite monochromator utilizing MoK_α radiation (λ = 0.71073 Å). Cell parameters were refined using 2919 reflections. A hemisphere of data (1381 frames) was collected using the ω-scan method (0.3° frame width). The first 50 frames were remeasured at the end of data collection to monitor instrument and crystal stability (maximum correction on I was < 1 %). Psi scan absorption corrections were applied based on the entire data set.

The structure was solved by the Direct Methods in *SHELXL-97*,[287] and refined using full-matrix least squares. The non-H atoms were treated anisotropically, whereas the hydrogen atoms were calculated in ideal positions and were riding on their respective carbon atoms. A total of 415 parameters were refined in the final cycle of refinement using 5197 reflections with $I > 2\sigma(I)$ to yield R_1 and wR_2 of 4.94% and 9.04%, respectively. Refinement was done using F^2.

X-ray Experimental for $Mo(NPh)(PMe_3)_3(o\text{-}(Me_3SiN)_2C_6H_4)$ (**24**)

Suitable crystals of **24** were obtained by slow evaporation of a pentane solution. Data were collected at 173 K on a Siemens SMART PLATFORM equipped with A CCD area detector and a graphite monochromator utilizing MoK_α radiation (λ = 0.71073 Å). Cell parameters were refined using 8192 reflections. A hemisphere of data (1381 frames)

was collected using the ω-scan method (0.3° frame width). The first 50 frames were remeasured at the end of data collection to monitor instrument and crystal stability (maximum correction on I was < 1 %). Absorption corrections were applied based on measured indexed faces.

The structure was solved by the Direct Methods in *SHELXTL5*,[288] and refined using full-matrix least squares. The non-H atoms were treated anisotropically, whereas the hydrogen atoms were calculated in ideal positions and were riding on their respective carbon atoms. A total of 326 parameters were refined in the final cycle of refinement using 6606 reflections with $I > 2\sigma(I)$ to yield R_1 and wR_2 of 2.64 and 6.52, respectively. Refinement was done using F^2.

X-ray Experimental for Mo(NPh)(η^6-*m*-xylene)(*o*-$(Me_3SiN)_2C_6H_4$) (**30**)

Suitable crystals of **30** were obtained by cooling a concentrated pentane solution to -20°C for several days. Data were collected at 173 K on a Siemens SMART PLATFORM equipped with A CCD area detector and a graphite monochromator utilizing MoK_α radiation (λ = 0.71073 Å). Cell parameters were refined using 4043 reflections. A hemisphere of data (1381 frames) was collected using the ω-scan method (0.3° frame width). The first 50 frames were remeasured at the end of data collection to monitor instrument and crystal stability (maximum correction on I was < 1 %). Absorption corrections were applied based on measured indexed faces.

The structure was solved by the Direct Methods in *SHELXTL5*,[288] and refined using full-matrix least squares. The non-H atoms were treated anisotropically, whereas

the hydrogen atoms were calculated in ideal positions and were riding on their respective carbon atoms. A total of 297 parameters were refined in the final cycle of refinement using 4124 reflections with $I > 2\sigma(I)$ to yield R_1 and wR_2 of 4.53 and 9.17, respectively. Refinement was done using F^2.

X-ray Experimental for Mo(NPh)(η^6-*p*-xylene)(*o*-$(Me_3SiN)_2C_6H_4$) (**31**)

Suitable crystals of **31** were obtained by cooling a concentrated pentane solution to -20°C for several days. Data were collected at 173 K on a Siemens SMART PLATFORM equipped with A CCD area detector and a graphite monochromator utilizing MoK_α radiation (λ = 0.71073 Å). Cell parameters were refined using 8192 reflections. A hemisphere of data (1381 frames) was collected using the ω-scan method (0.3° frame width). The first 50 frames were remeasured at the end of data collection to monitor instrument and crystal stability (maximum correction on I was < 1 %). Absorption corrections by integration were applied based on measured indexed crystal faces.

The structure was solved by the Direct Methods in *SHELXTL5*,[288] and refined using full-matrix least squares. The non-H atoms were treated anisotropically, whereas the hydrogen atoms were calculated in ideal positions and were riding on their respective carbon atoms. A total of 298 parameters were refined in the final cycle of refinement using 5112 reflections with $I > 2\sigma(I)$ to yield R_1 and wR_2 of 2.37% and 5.90%, respectively. Refinement was done using F^2.

X-ray Experimental for $Mo(NPh)(PMe_3)_3(o\text{-}(Me_3SiN)(HN)C_6H_4)$ (**36**)

Suitable crystals of **36** were obtained by cooling a concentrated toluene solution to -20°C for several weeks. Data were collected at 173 K on a Siemens SMART PLATFORM equipped with a CCD area detector and a graphite monochromator utilizing MoK_α radiation (λ = 0.71073 Å). Cell parameters were refined using 8192 reflections. A hemisphere of data (1381 frames) was collected using the ω-scan method (0.3° frame width). The first 50 frames were remeasured at the end of data collection to monitor instrument and crystal stability (maximum correction on I was < 1 %). Absorption corrections by integration were applied based on measured indexed crystal faces.

The structure was solved by the Direct Methods in *SHELXTL5*,[288] and refined using full-matrix least squares. The non-H atoms were treated anisotropically, whereas the hydrogen atoms were calculated in ideal positions and were riding on their respective carbon atoms. A toluene molecule was found disordered around a center of inversion thus only a half toluene was refined in the asymmetric unit. Because of symmetry, the methyl group and its *para* proton are disordered and thus their site occupation factors were fixed at 0.5. A total of 298 parameters were refined in the final cycle of refinement using 5112 reflections with $I > 2\sigma(I)$ to yield R_1 and wR_2 of 2.37% and 5.90%, respectively. Refinement was done using F^2.

APPENDIX A
NUCLEAR MAGNETIC RESONANCE SPECTRA

This appendix is a collection of ^{1}H and ^{13}C NMR spectra for all the compounds prepared during the course of this study.

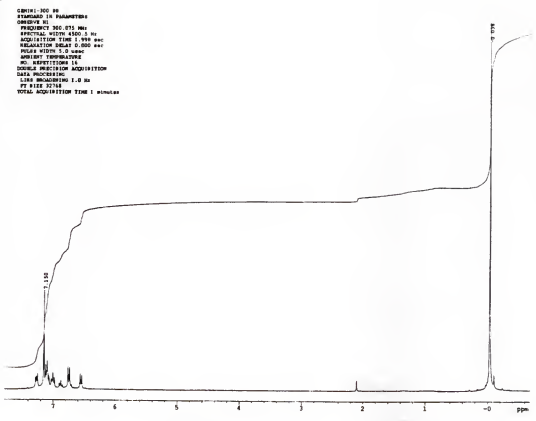

Figure A.1. Proton NMR of $[Mo(NPh)(\mu\text{-}NPh)(o\text{-}(Me_3SiN)_2C_6H_4)]_2$ (**1**) in C_6D_6.

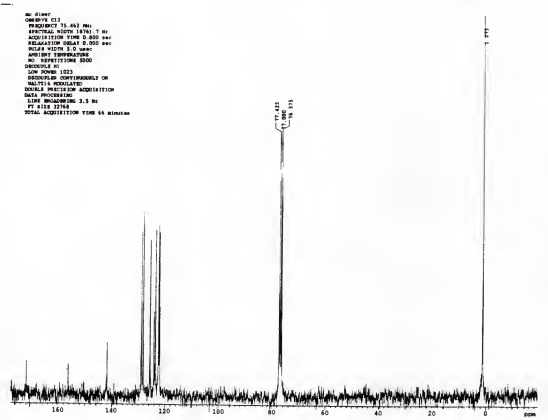

Figure A.2. Carbon[13] NMR of $[Mo(NPh)(\mu\text{-}NPh)(o\text{-}(Me_3SiN)_2C_6H_4)]_2$ (**1**) in $CDCl_3$.

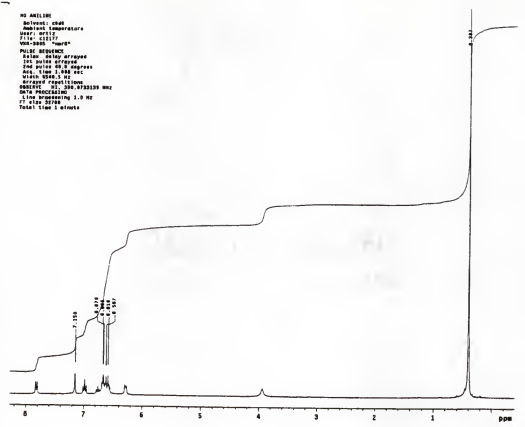

Figure A.3. Proton NMR of $Mo(NPh)Cl_2(o\text{-}(Me_3SiN)_2C_6H_4)(NH_2Ph)$ (**2**) in C_6D_6.

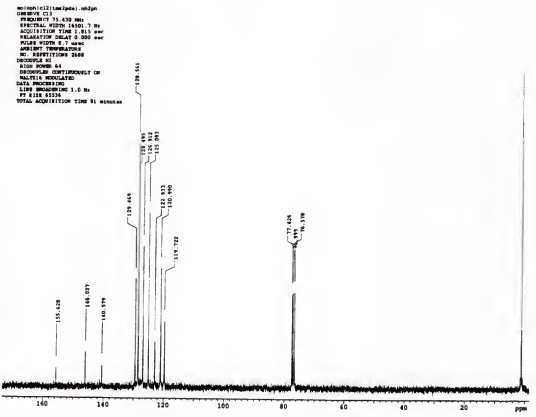

Figure A.4. Carbon[13] NMR of $Mo(NPh)Cl_2(o\text{-}(Me_3SiN)_2C_6H_4)(NH_2Ph)$ (**2**) in $CDCl_3$.

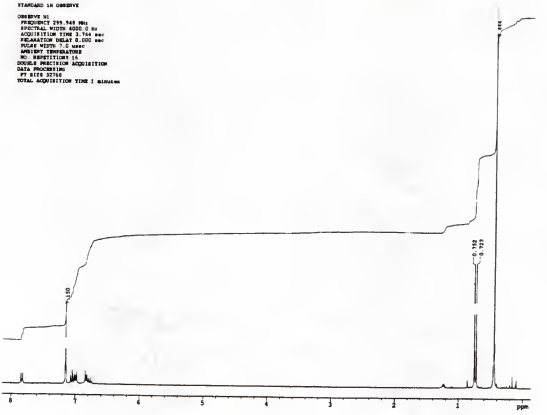

Figure A.5. Proton NMR of $Mo(NPh)Cl_2(o\text{-}(Me_3SiN)_2C_6H_4)(PMe_3)$ (**3**) in C_6D_6.

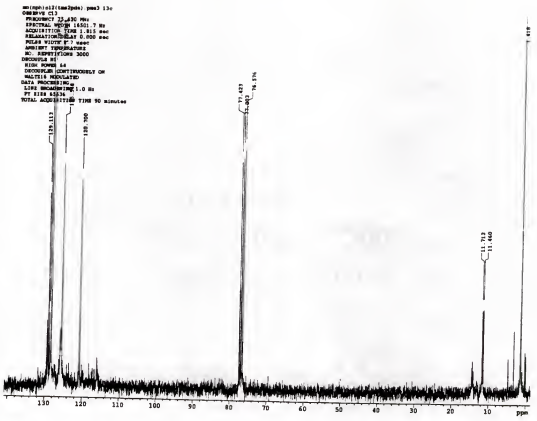

Figure A.6. Carbon[13] NMR of $Mo(NPh)Cl_2(o\text{-}(Me_3SiN)_2C_6H_4)(PMe_3)$ (**3**) in $CDCl_3$.

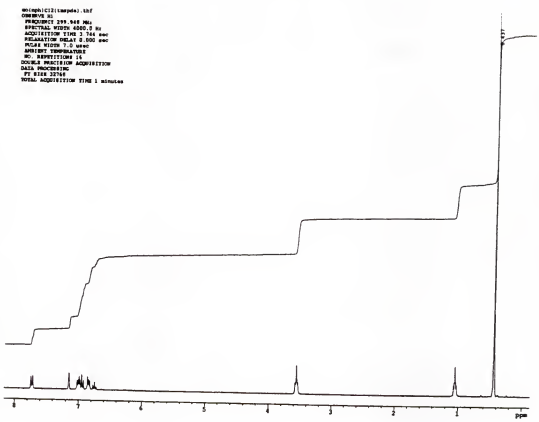

Figure A.7. Proton NMR of $Mo(NPh)Cl_2(o\text{-}(Me_3SiN)_2C_6H_4)(THF)$ (**4**) in C_6D_6.

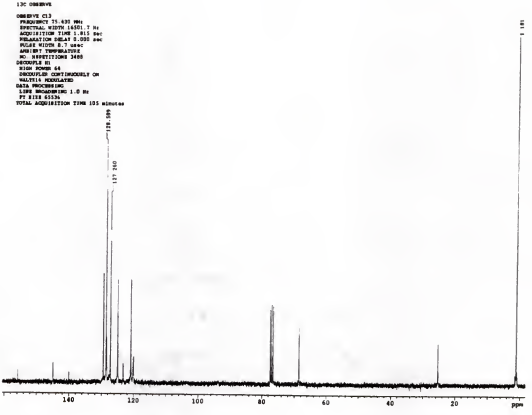

Figure A.8. Carbon[13] NMR of $Mo(NPh)Cl_2(o\text{-}(Me_3SiN)_2C_6H_4)(THF)$ (**4**) in $CDCl_3$.

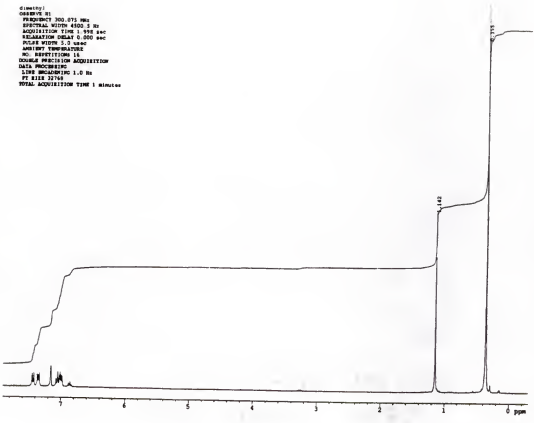

Figure A.9. Proton NMR of $Mo(NPh)Me_2(o\text{-}(Me_3SiN)_2C_6H_4)$ (**5**) in C_6D_6.

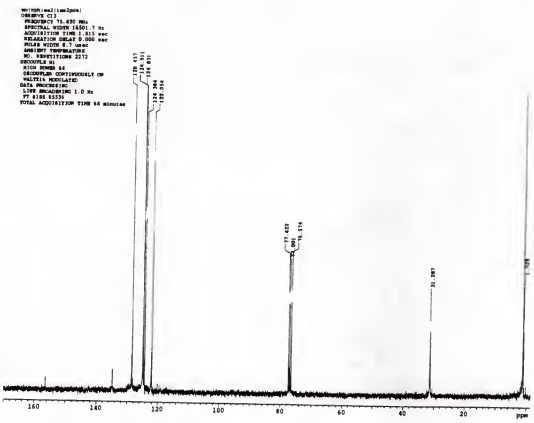

Figure A.10. Carbon-13 NMR of $Mo(NPh)Me_2(o\text{-}(Me_3SiN)_2C_6H_4)$ (**5**) in $CDCl_3$.

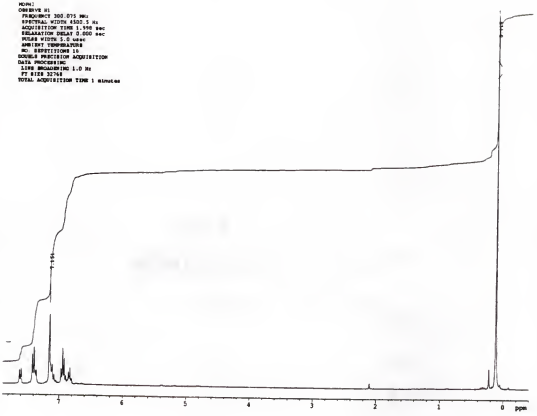

Figure A.11. Proton NMR of $Mo(NPh)Ph_2(o\text{-}(Me_3SiN)_2C_6H_4)$ (**6**) in C_6D_6.

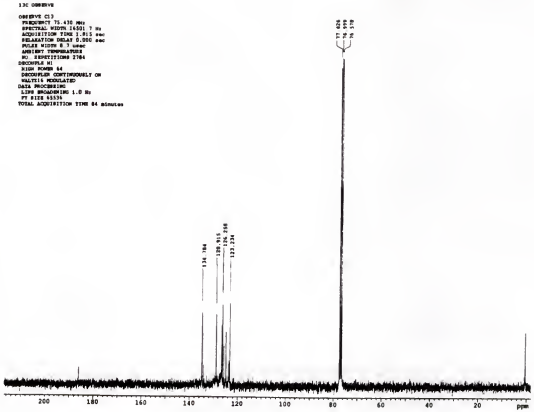

Figure A.12. Carbon-13 NMR of $Mo(NPh)Ph_2(o\text{-}(Me_3SiN)_2C_6H_4)$ (**6**) in $CDCl_3$.

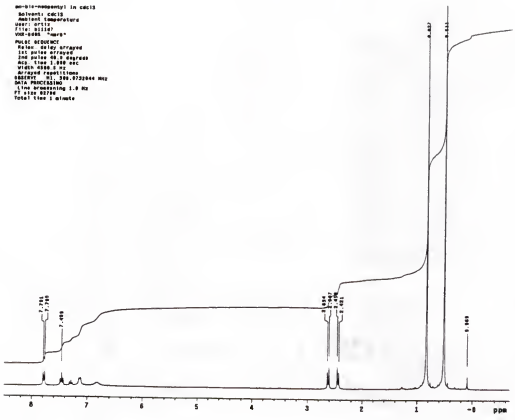

Figure A.13. Proton NMR of $Mo(NPh)(CH_2C(CH_3)_3)_2(o\text{-}(Me_3SiN)_2C_6H_4)$ (7) in $CDCl_3$.

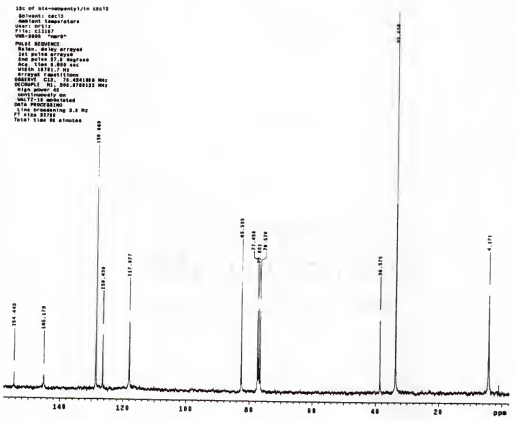

Figure A.14. Carbon-13 NMR of $Mo(NPh)(CH_2C(CH_3)_3)_2(o\text{-}(Me_3SiN)_2C_6H_4)$ (**7**) in $CDCl_3$.

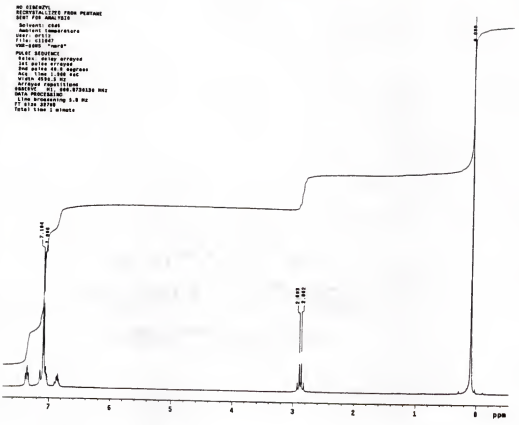

Figure A.15. Proton NMR of $Mo(NPh)(CH_2Ph)_2(o\text{-}(Me_3SiN)_2C_6H_4)$ (**8**) in C_6D_6.

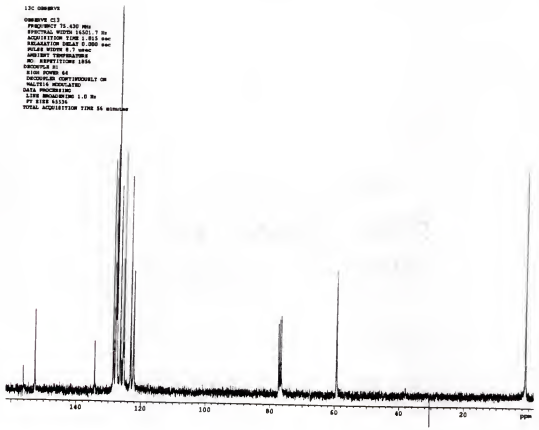

Figure A.16. Carbon-13 NMR of $Mo(NPh)(CH_2Ph)_2(o\text{-}(Me_3SiN)_2C_6H_4)$ (**8**) in $CDCl_3$.

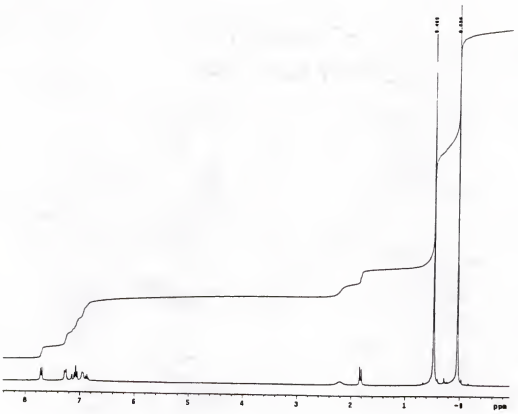

Figure A.17. Proton NMR of $Mo(NPh)(CH_2Si(CH_3)_3)_2(o\text{-}(Me_3SiN)_2C_6H_4)$ (**9**) in C_6D_6.

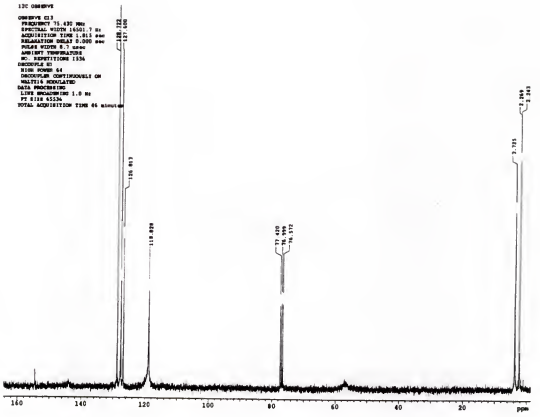

Figure A.18. Carbon-13 NMR of $Mo(NPh)(CH_2Si(CH_3)_3)_2(o\text{-}(Me_3SiN)_2C_6H_4)$ (**9**) in $CDCl_3$.

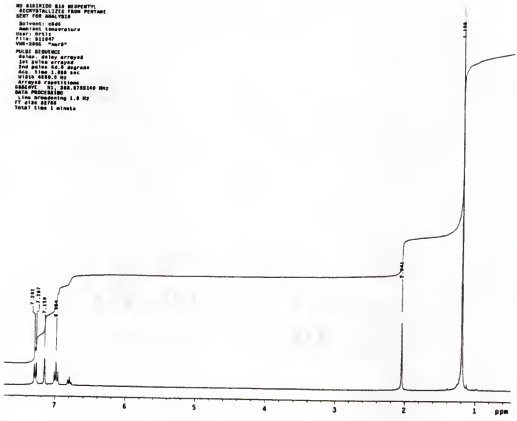

Figure A.19. Proton NMR of $Mo(NPh)_2(CH_2C(CH_3)_3)_2$ (**10**) in C_6D_6.

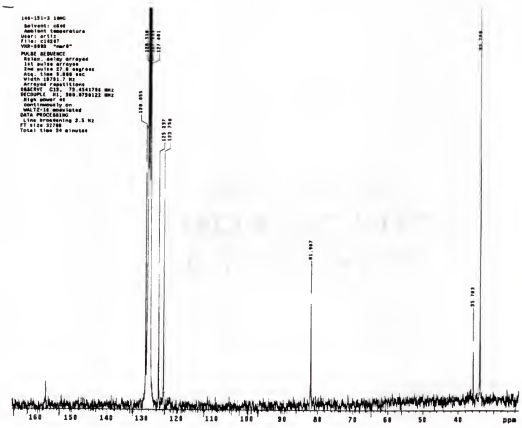

Figure A.20. Carbon-13 NMR of $Mo(NPh)_2(CH_2C(CH_3)_3)_2$ (**10**) in C_6D_6.

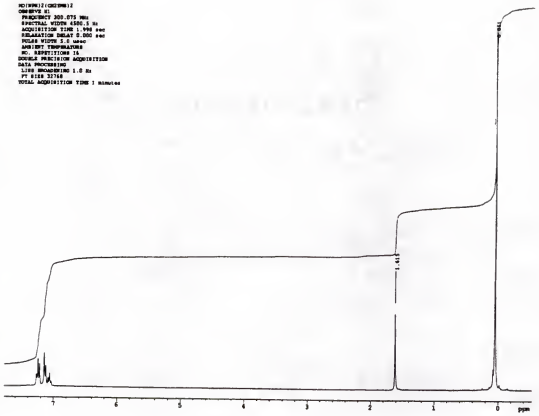

Figure A.21. Proton NMR of $Mo(NPh)_2(CH_2Si(CH_3)_3)_2$ (**11**) in C_6D_6.

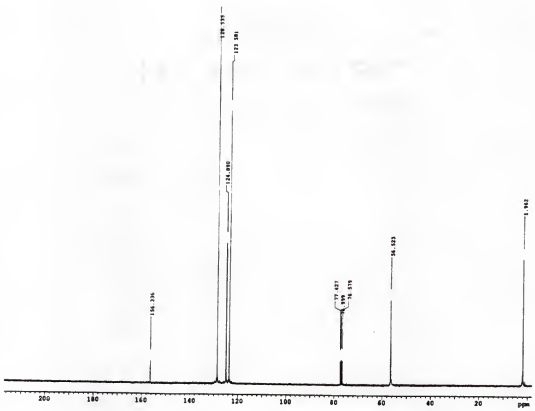

Figure A.22. Carbon-13 NMR of $Mo(NPh)_2(CH_2Si(CH_3)_3)_2$ (**11**) in $CDCl_3$.

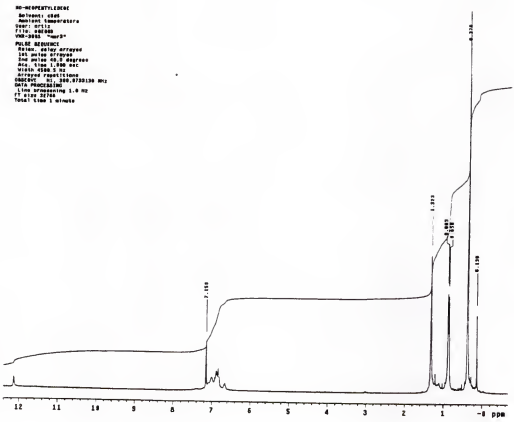

Figure A.23. Proton NMR of Mo(NPh)(C(H)C(CH$_3$)$_3$)$_2$(*o*-(Me$_3$SiN)$_2$C$_6$H$_4$)(PMe$_3$) (**13**) in C$_6$D$_6$.

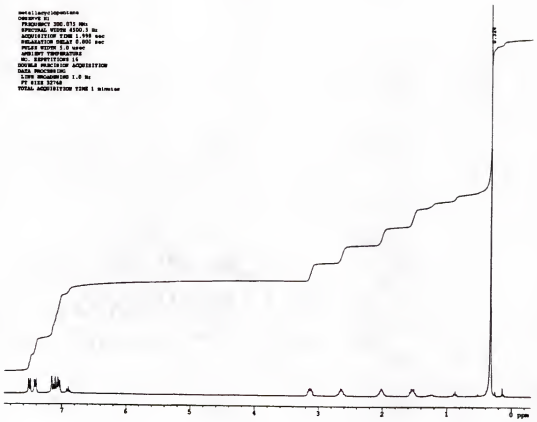

Figure A.24. Proton NMR of $Mo(CH_2CH_2CH_2CH_2)(o\text{-}(Me_3SiN)_2C_6H_4)$ (**16**) in C_6D_6.

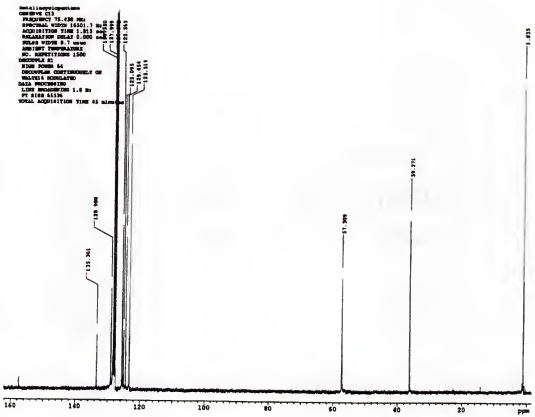

Figure A.25. Carbon-13 NMR of $Mo(CH_2CH_2CH_2CH_2)(o\text{-}(Me_3SiN)_2C_6H_4)$ (**16**) in C_6D_6.

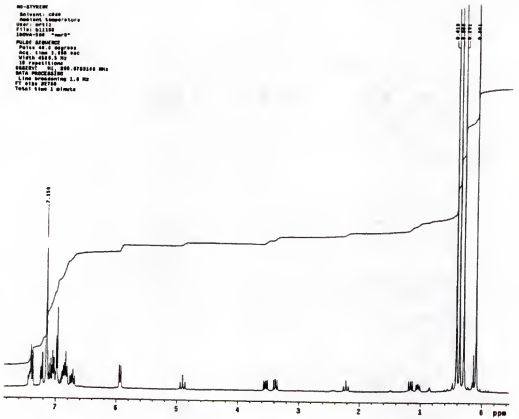

Figure A.26. Proton NMR of Mo(η^2-styrene)(*o*-$(Me_3SiN)_2C_6H_4$) (**19**) in C_6D_6.

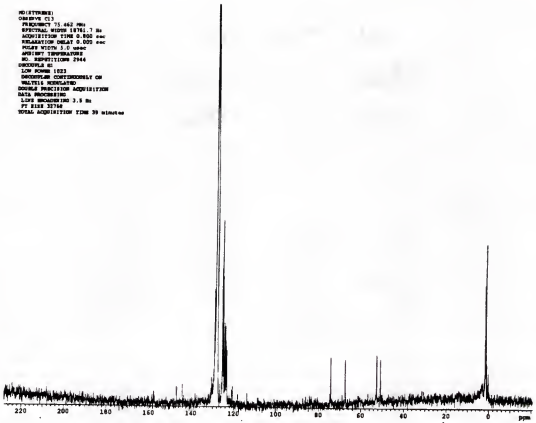

Figure A.27. Carbon-13 NMR of Mo(η^2-styrene)(*o*-$(Me_3SiN)_2C_6H_4$) (**19**) in C_6D_6.

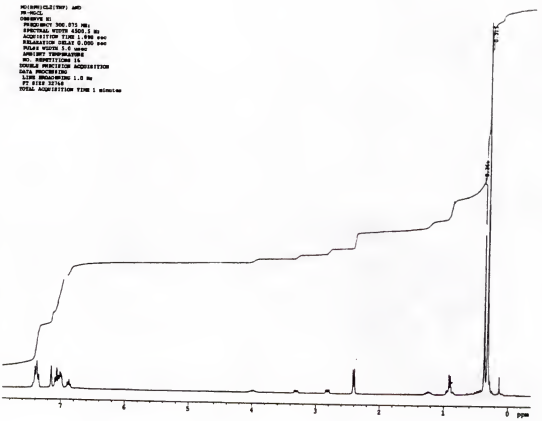

Figure A.28. Proton NMR of Mo(η^2-propene)(*o*-$(Me_3SiN)_2C_6H_4$) (**20**) in C_6D_6.

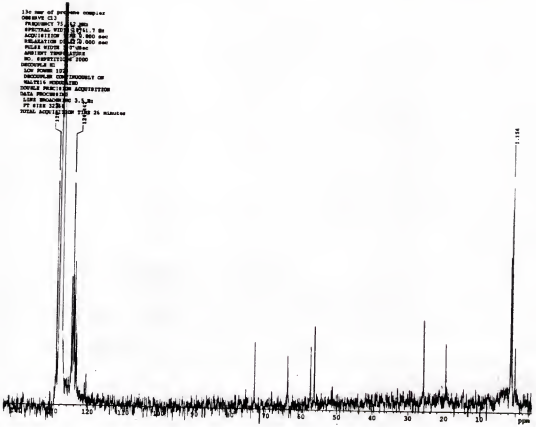

Figure A.29. Carbon-13 NMR of Mo(η^2-propene)(*o*-$(Me_3SiN)_2C_6H_4$) (**20**) in C_6D_6.

Figure A.30. Proton NMR of Mo(η^2-isobutene)(*o*-$(Me_3SiN)_2C_6H_4$) (**21**) in C_6D_6.

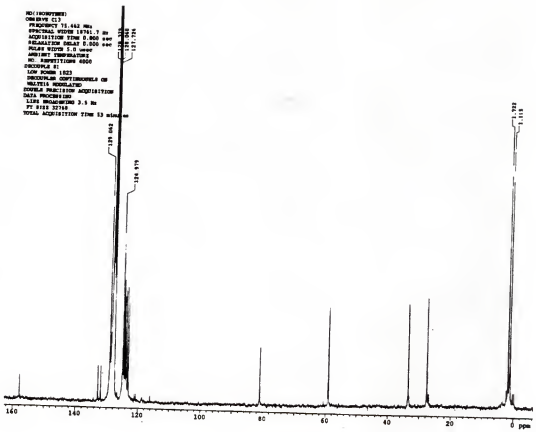

Figure A.31. Carbon-13 NMR of Mo(η^2-isobutene)(*o*-(Me_3SiN)$_2C_6H_4$) (**21**) in C_6D_6.

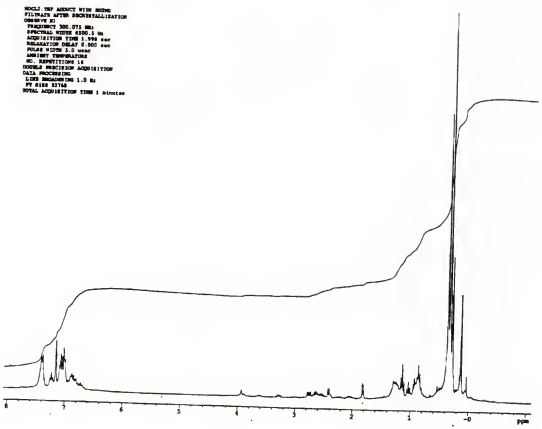

Figure A.32. Proton NMR of Mo(η^2-butene)(*o*-$(Me_3SiN)_2C_6H_4$) (**22**) in C_6D_6.

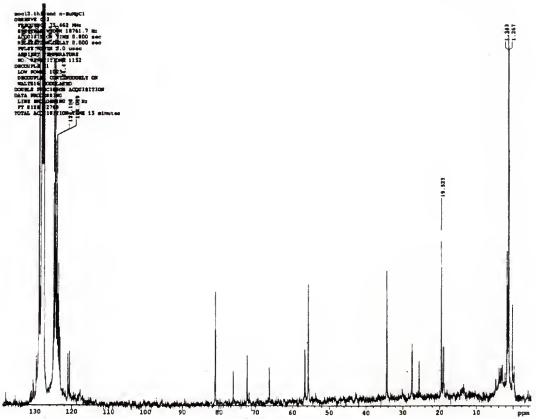

Figure A.33. Carbon-13 NMR of Mo(η^2-butene)(*o*-$(Me_3SiN)_2C_6H_4$) (**22**) in C_6D_6.

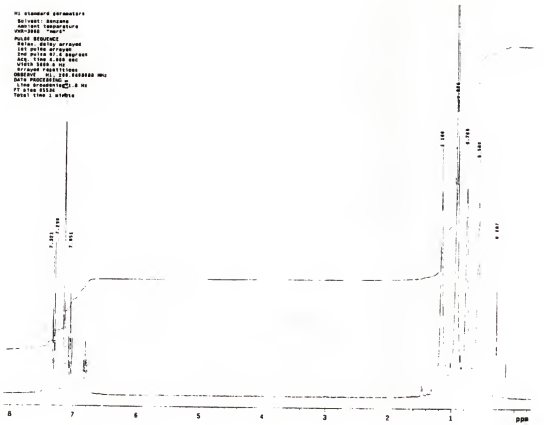

Figure A.34. Proton NMR of Mo(NPh)(*o*-$(Me_3SiN)_2C_6H_4$)$(CN(C(CH_3)_3)_3$ (**23**) in C_6D_6.

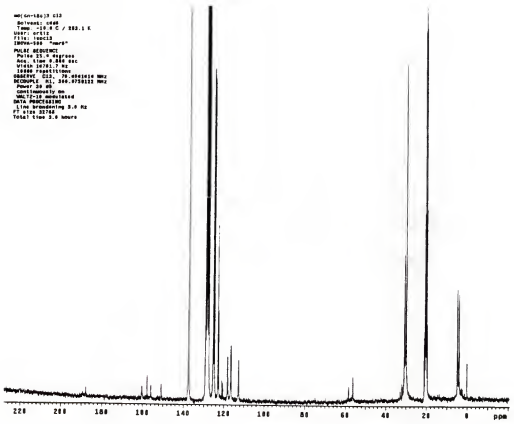

Figure A.35. Carbon-13 NMR of Mo(NPh)(*o*-$(Me_3SiN)_2C_6H_4$)$(CN(C(CH_3)_3)_3$ (**23**) in C_6D_6.

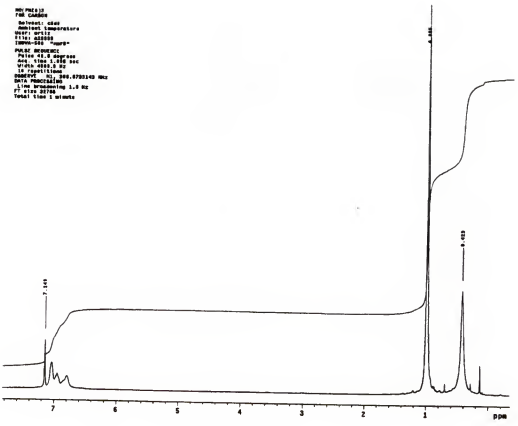

Figure A.36. Proton NMR of Mo(NPh)(*o*-$(Me_3SiN)_2C_6H_4$)$(PMe_3)_3$ (**24**) in C_6D_6.

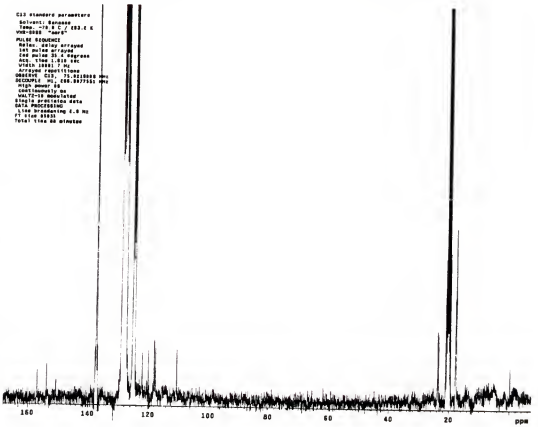

Figure A.37. Carbon-13 NMR of Mo(NPh)(*o*-$(Me_3SiN)_2C_6H_4$)$(PMe_3)_3$ (**24**) in d^8-toluene at -70° C.

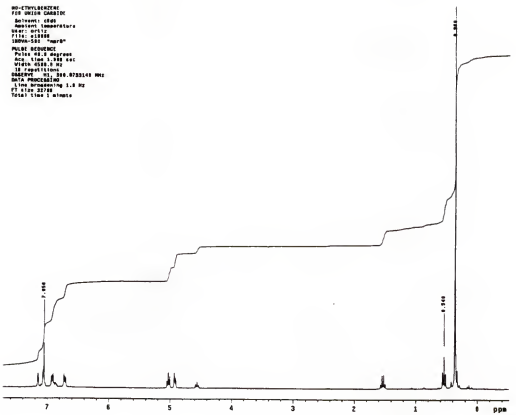

Figure A.38. Proton NMR of Mo(NPh)(η^6-ethylbenzene)(*o*-$(Me_3SiN)_2C_6H_4$) (**26**) in C_6D_6.

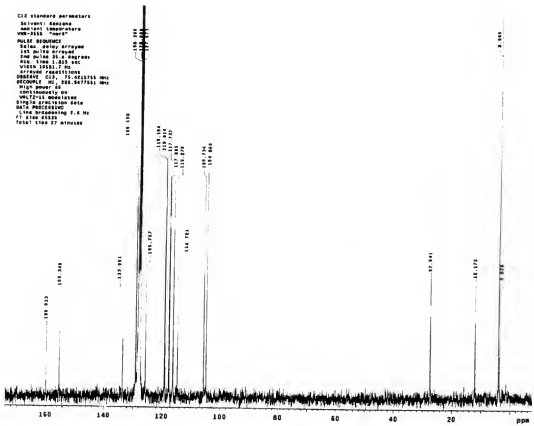

Figure A.39. Carbon-13 NMR of Mo(NPh)(η^6-ethylbenzene)(*o*-$(Me_3SiN)_2C_6H_4$) (**26**) in C_6D_6.

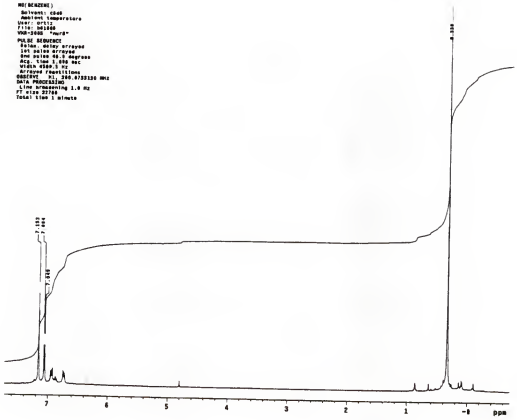

Figure A.40. Proton NMR of Mo(NPh)(η^6-benzene)(*o*-$(Me_3SiN)_2C_6H_4$) (**27**) in C_6D_6.

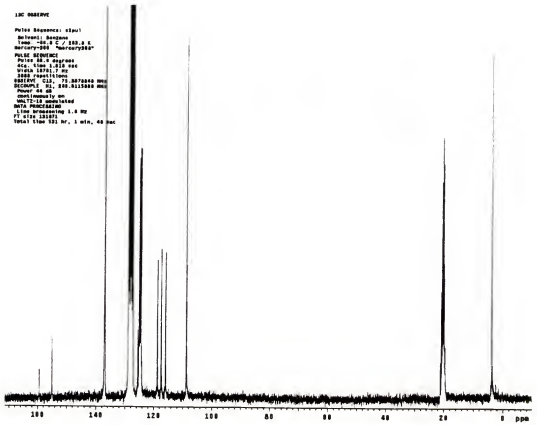

Figure A.41. Carbon-13 NMR of Mo(NPh)(η^6-benzene)(*o*-$(Me_3SiN)_2C_6H_4$) (**27**) in d^8-toluene at -20°C.

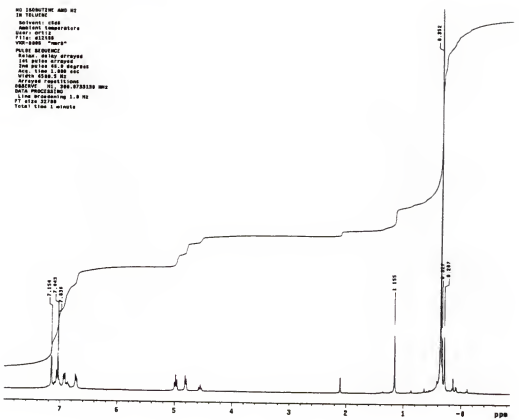

Figure A.42. Proton NMR of Mo(NPh)(η^6-toluene)(*o*-$(Me_3SiN)_2C_6H_4$) (**28**) in C_6D_6.

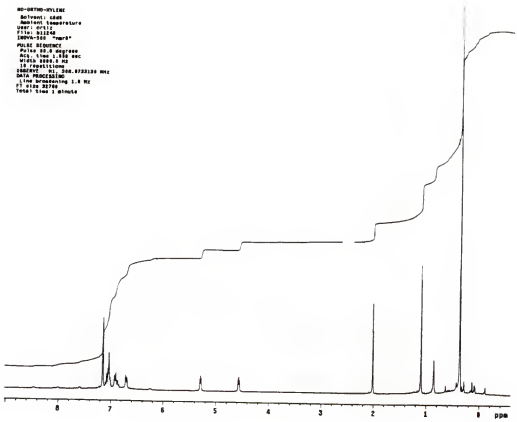

Figure A.43. Proton NMR of Mo(NPh)(η^6-*o*-xylene)(*o*-$(Me_3SiN)_2C_6H_4$) (**29**) in C_6D_6.

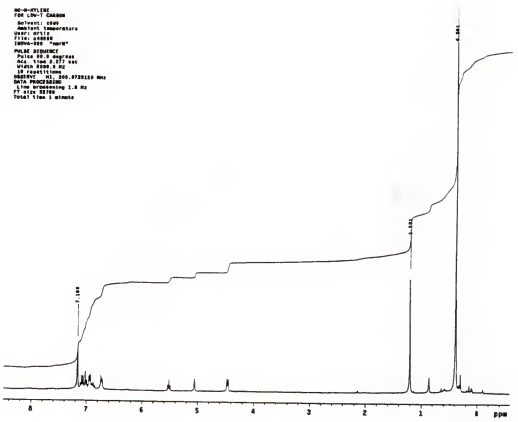

Figure A.44. Proton NMR of Mo(NPh)(η^6-*m*-xylene)(*o*-$(Me_3SiN)_2C_6H_4$) (**30**) in C_6D_6.

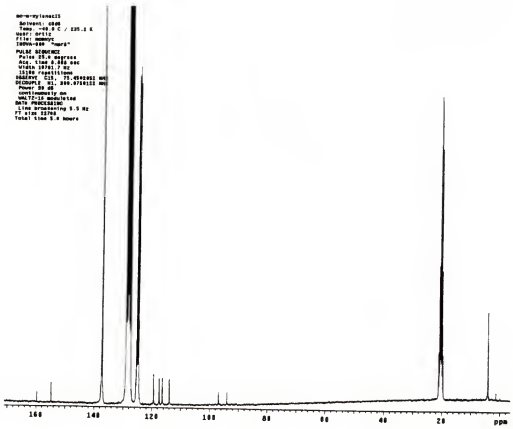

Figure A.45. Carbon-13 NMR of Mo(NPh)(η^6-*m*-xylene)(*o*-(Me_3SiN)$_2C_6H_4$) (**30**) in d^8-toluene at -40°C.

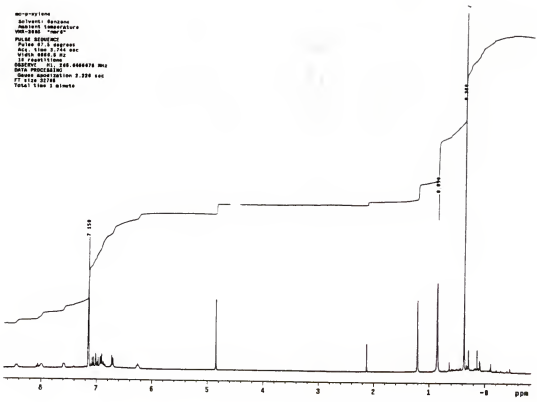

Figure A.46. Proton NMR of Mo(NPh)(η^6-*p*-xylene)(*o*-$(Me_3SiN)_2C_6H_4$) (**31**) in C_6D_6.

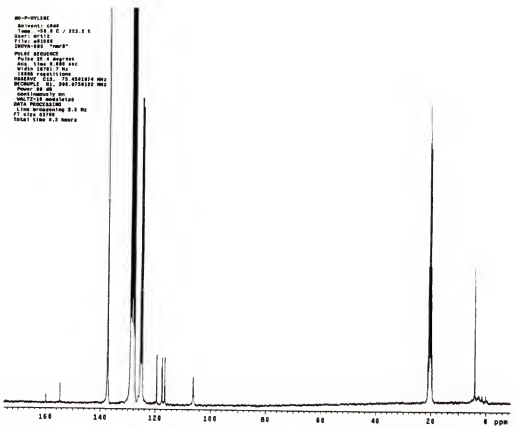

Figure A.47. Carbon-13 NMR of Mo(NPh)(η^6-*p*-xylene)(*o*-(Me_3SiN)$_2C_6H_4$) (**31**) in d^8-toluene at -50°C.

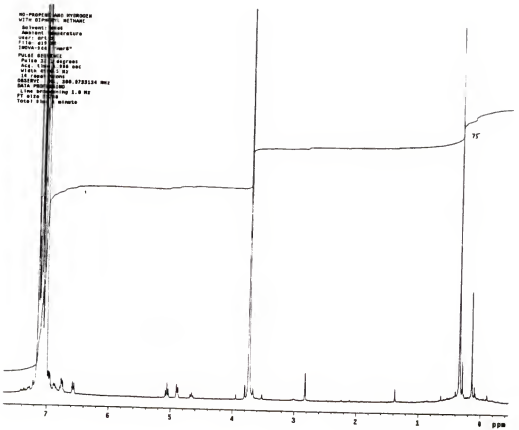

Figure A.48. Proton NMR of Mo(NPh)(η^6-diphenylmethane)(*o*-$(Me_3SiN)_2C_6H_4$) (**32**) in C_6D_6.

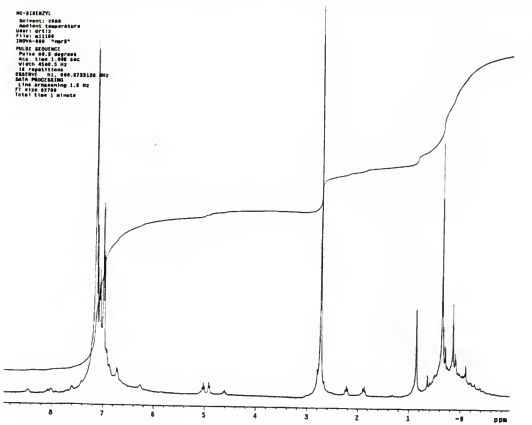

Figure A.49. Proton NMR of Mo(NPh)(η^6-bibenzyl)(*o*-$(Me_3SiN)_2C_6H_4$) (**33**) in C_6D_6.

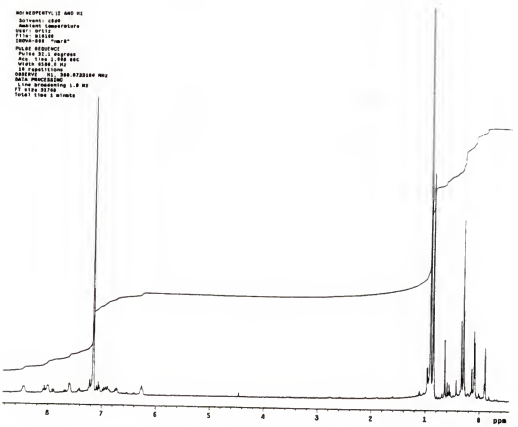

Figure A.50. Proton NMR of $[Mo(\mu\text{-}NPh)(o\text{-}(Me_3SiN)_2C_6H_4)]_n$ (**17**) in C_6D_6.

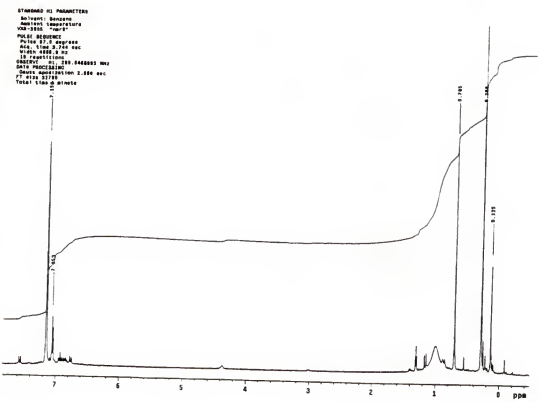

Figure A.51. Proton NMR of Mo(NPh)(*o*-(Me_3SiN)(HN)C_6H_4)(PMe_3)$_3$ (**36**) in C_6D_6.

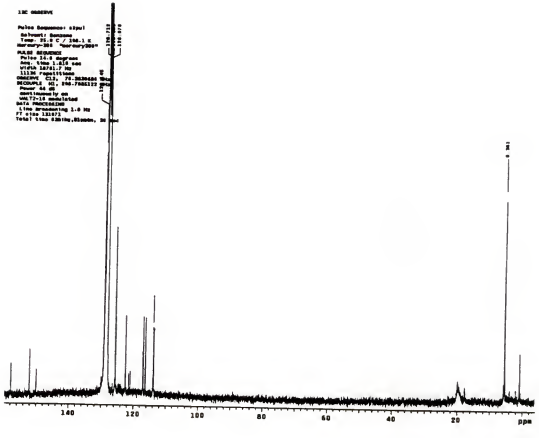

Figure A.52. Carbon[13] NMR of Mo(NPh)(*o*-(Me$_3$SiN)(HN)C$_6$H$_4$)(PMe$_3$)$_3$ (**36**) in C$_6$D$_6$.

APPENDIX B
TABLES OF CRYSTALLOGRAPHIC DATA

This appendix contains the tables of crystallographic data for the crystal structure determination experiments reported in this dissertation.

Table B.1. Crystal data and structure refinement for **3**.

Empirical formula	C25 H46 Cl2 Mo N3 O P Si2
Formula weight	658.64
Temperature	173(2) K
Wavelength	0.71073 Å
Crystal system	Monoclinic
Space group	P2(1)/c
Unit cell dimensions	a = 9.7269(2) Å α = 90°
	b = 17.7600(4) Å β = 94.237(1)°
	c = 18.9629(4) Å γ = 90°
Volume, Z	3266.88(12) $Å^3$, 4
Density (calculated)	1.339 Mg/m^3
Absorption coefficient	0.709 mm^{-1}
F(000)	1376
Crystal size	0.28 x 0.16 x 0.14 mm
Theta range for data collection	2.10 to 27.50°
Limiting indices	$-12 \le h \le 11$, $-21 \le k \le 22$, $-22 \le l \le 24$
Reflections collected	21565
Independent reflections	7435 [R(int) = 0.0308]
Absorption correction	Empirical
Max. and min. transmission	0.928 and 0.712
Refinement method	Full-matrix least-squares on F^2
Data / restraints / parameters	7435 / 0 / 461
Goodness-of-fit on F^2	1.027
Final R indices [I>2sigma(I)]	R1 = 0.0283, wR2 = 0.0676 [6045]
R indices (all data)	R1 = 0.0409, wR2 = 0.0734
Extinction coefficient	0.0010(2)
Largest diff. peak and hole	0.492 and -0.702 $e.Å^{-3}$

Table B.2. Atomic coordinates (x 10^4) and equivalent isotropic displacement parameters (A^2 x 10^3) for **3**. U(eq) is defined as one third of the trace of the orthogonalized Uij tensor.

	x	y	z	U(eq)
Mo	-76(1)	297(1)	2020(1)	20(1)
Cl1	-2353(1)	550(1)	2480(1)	29(1)
Cl2	237(1)	-797(1)	2816(1)	33(1)
P1	595(1)	926(1)	3310(1)	31(1)
Si1	-1285(1)	1875(1)	1139(1)	25(1)
Si2	3033(1)	-466(1)	1633(1)	26(1)
N1	43(2)	1341(1)	1611(1)	21(1)
N2	1936(2)	310(1)	1830(1)	22(1)
N3	-896(2)	-281(1)	1374(1)	23(1)
C1	1370(2)	1611(1)	1762(1)	22(1)
C2	2411(2)	1043(1)	1876(1)	23(1)
C3	3802(2)	1269(1)	2010(1)	29(1)
C4	4135(2)	2018(1)	2033(1)	34(1)
C5	3114(2)	2571(1)	1928(1)	34(1)
C6	1756(2)	2374(1)	1797(1)	26(1)
C7	-1742(2)	-839(1)	1074(1)	23(1)
C8	-1846(2)	-951(1)	341(1)	30(1)
C9	-2674(2)	-1520(1)	55(1)	35(1)
C10	-3390(2)	-1983(1)	483(1)	35(1)
C11	-3289(3)	-1871(1)	1209(1)	36(1)
C12	-2479(2)	-1300(1)	1508(1)	30(1)
C13	-2147(3)	2473(2)	1775(2)	37(1)
C14	-536(3)	2468(2)	449(2)	39(1)
C15	-2531(3)	1204(2)	695(2)	37(1)
C16	4026(3)	-766(2)	2463(1)	41(1)
C17	4219(3)	-178(2)	954(1)	35(1)
C18	1938(3)	-1252(1)	1276(2)	36(1)
C19	-248(3)	505(2)	4042(1)	44(1)
C20	2398(3)	881(3)	3626(2)	58(1)
C21	150(3)	1916(2)	3396(2)	47(1)
O1	4807(2)	1177(1)	4950(1)	42(1)
C22	6233(3)	1568(2)	4056(2)	65(1)
C23	6149(3)	1400(2)	4822(2)	58(1)
C24	4641(3)	965(2)	5660(1)	56(1)
C25	3177(4)	782(2)	5740(2)	77(1)

Table B.3. Selected bond lengths [Å] and angles [deg] for **3**.

Mo-N3	1.745(2)
Mo-N2	2.017(2)
Mo-N1	2.018(2)
Mo-Cl2	2.4640(5)
Mo-Cl1	2.4802(5)
Mo-P1	2.7241(6)
P1-C20	1.812(3)
P1-C21	1.821(3)
P1-C19	1.823(3)
Si1-N1	1.788(2)
Si1-C13	1.853(3)
Si1-C15	1.856(2)
Si1-C14	1.868(3)
Si2-N2	1.799(2)
Si2-C18	1.853(3)
Si2-C16	1.863(3)
Si2-C17	1.863(3)
N1-C1	1.386(2)
N2-C2	1.383(3)
N3-C7	1.384(2)
C1-C6	1.407(3)
C1-C2	1.434(3)
N3-Mo-N2	106.25(7)
N3-Mo-N1	107.85(7)
N2-Mo-N1	80.56(6)
N3-Mo-Cl2	89.77(5)
N2-Mo-Cl2	92.36(5)
N1-Mo-Cl2	162.21(5)
N3-Mo-Cl1	88.87(6)
N2-Mo-Cl1	164.69(5)
N1-Mo-Cl1	92.69(5)
Cl2-Mo-Cl1	90.06(2)
N3-Mo-P1	159.80(6)
N2-Mo-P1	89.12(5)
N1-Mo-P1	87.22(5)
Cl2-Mo-P1	76.31(2)
Cl1-Mo-P1	76.76(2)
C20-P1-C21	104.1(2)
C20-P1-C19	102.1(2)
C21-P1-C19	101.82(14)
C20-P1-Mo	116.14(11)
C21-P1-Mo	115.68(10)
C19-P1-Mo	115.05(10)
N1-Si1-C13	108.80(10)
N1-Si1-C15	108.08(10)
C13-Si1-C15	110.57(13)
N1-Si1-C14	110.14(10)
C13-Si1-C14	110.57(13)
C15-Si1-C14	108.66(13)
N2-Si2-C18	108.60(10)

Table B.3—continued.

N2-Si2-C16	108.80(11)
C18-Si2-C16	110.02(14)
N2-Si2-C17	109.85(10)
C18-Si2-C17	108.82(13)
C16-Si2-C17	110.72(13)
C1-N1-Si1	123.21(13)
C1-N1-Mo	108.49(12)
Si1-N1-Mo	128.29(8)
C2-N2-Si2	122.33(13)
C2-N2-Mo	108.86(12)
Si2-N2-Mo	128.81(9)
C7-N3-Mo	159.6(2)
N1-C1-C6	125.7(2)
N1-C1-C2	115.1(2)
C6-C1-C2	119.2(2)
N2-C2-C3	126.0(2)
N2-C2-C1	115.1(2)

Symmetry transformations used to generate equivalent atoms:

Table B.4. Anisotropic displacement parameters ($A^2 \times 10^3$) for **3**. The anisotropic displacement factor exponent takes the form: $-2\pi^2 [h^2 a^{*2} U11 + ... + 2 h k a^* b^* U12]$

	U11	U22	U33	U23	U13	U12
Mo	19(1)	20(1)	20(1)	1(1)	2(1)	-2(1)
Cl1	22(1)	36(1)	31(1)	0(1)	8(1)	-2(1)
Cl2	38(1)	28(1)	33(1)	10(1)	3(1)	1(1)
P1	28(1)	40(1)	24(1)	-1(1)	4(1)	-5(1)
Si1	22(1)	22(1)	30(1)	3(1)	2(1)	1(1)
Si2	24(1)	28(1)	27(1)	2(1)	2(1)	5(1)
N1	18(1)	22(1)	22(1)	-1(1)	4(1)	-1(1)
N2	20(1)	26(1)	22(1)	1(1)	2(1)	0(1)
N3	22(1)	22(1)	23(1)	1(1)	3(1)	0(1)
C1	23(1)	26(1)	17(1)	-2(1)	4(1)	-2(1)
C2	21(1)	30(1)	18(1)	-2(1)	6(1)	-2(1)
C3	21(1)	39(1)	28(1)	-4(1)	2(1)	-2(1)
C4	24(1)	43(1)	35(1)	-7(1)	5(1)	-11(1)
C5	38(1)	32(1)	33(1)	-7(1)	9(1)	-15(1)
C6	30(1)	25(1)	26(1)	-2(1)	7(1)	-3(1)
C7	23(1)	19(1)	28(1)	-2(1)	0(1)	1(1)
C8	30(1)	32(1)	29(1)	1(1)	5(1)	-4(1)
C9	40(1)	38(1)	26(1)	-8(1)	1(1)	-5(1)
C10	34(1)	29(1)	42(1)	-9(1)	-4(1)	-8(1)
C11	39(1)	33(1)	37(1)	2(1)	3(1)	-12(1)
C12	31(1)	31(1)	26(1)	1(1)	2(1)	-7(1)
C13	27(1)	34(1)	50(2)	-4(1)	8(1)	3(1)
C14	38(1)	38(2)	41(1)	14(1)	3(1)	3(1)
C15	37(1)	36(1)	37(1)	4(1)	-12(1)	-4(1)
C16	37(1)	47(2)	37(1)	9(1)	-2(1)	9(1)
C17	30(1)	40(2)	37(1)	-1(1)	10(1)	4(1)
C18	38(1)	29(1)	42(1)	-6(1)	7(1)	3(1)
C19	54(2)	52(2)	27(1)	3(1)	8(1)	-8(1)
C20	36(2)	106(3)	30(1)	-8(2)	-8(1)	-7(2)
C21	64(2)	43(2)	35(1)	-10(1)	16(1)	-12(1)
O1	39(1)	51(1)	36(1)	2(1)	-4(1)	-3(1)
C22	48(2)	74(2)	75(2)	1(2)	23(2)	11(2)
C23	35(1)	77(2)	62(2)	-11(2)	0(1)	5(1)
C24	71(2)	61(2)	34(1)	3(1)	-7(1)	1(2)
C25	102(3)	92(3)	39(2)	2(2)	12(2)	-48(2)

Table B.5. Hydrogen coordinates (x 10^4) and isotropic displacement parameters (A^2 x 10^3) for **3**.

	x	y	z	U(eq)
H3	4500(2)	888(13)	2102(11)	25(6)
H4	5070(3)	2161(15)	2146(14)	50(8)
H5	3390(2)	3074(12)	1952(11)	23(5)
H6	1140(2)	2727(12)	1745(11)	21(6)
H8	-1370(3)	-610(15)	73(14)	42(7)
H9	-2730(2)	-1574(14)	-415(14)	39(7)
H10	-3910(3)	-2350(15)	304(14)	44(7)
H11	-3770(3)	-2209(15)	1504(14)	48(8)
H12	-2420(2)	-1218(13)	1996(13)	30(6)
H13A	-1540(3)	2834(16)	2003(15)	54(8)
H13B	-2920(3)	2736(17)	1540(16)	61(9)
H13C	-2480(3)	2173(19)	2153(17)	71(10)
H14A	-200(3)	2893(19)	628(17)	65(10)
H14B	110(4)	2230(2)	290(2)	96(14)
H14C	-1250(3)	2646(17)	91(16)	59(8)
H15A	-3170(3)	1467(16)	415(15)	53(8)
H15B	-2090(3)	865(16)	357(14)	47(8)
H15C	-2940(3)	909(17)	1013(17)	62(9)
H16A	4620(3)	-409(17)	2620(17)	59(9)
H16B	4530(3)	-1249(18)	2349(16)	67(9)
H16C	4940(4)	120(2)	1119(18)	78(11)
H17B	4620(3)	-613(19)	791(17)	69(10)
H17C	3790(4)	70(2)	589(19)	79(11)
H18A	1370(3)	-1097(14)	860(14)	40(7)
H18B	1420(3)	-1451(16)	1600(15)	49(8)
H18C	2500(3)	-1639(16)	1129(15)	52(8)
H19A	-30(3)	750(16)	4482(16)	52(8)
H19B	50(3)	47(19)	4115(16)	58(9)
H19C	-1170(4)	463(17)	3931(17)	64(10)
H20A	2600(3)	327(15)	3667(15)	42(8)
H20B	2540(3)	1104(18)	4103(18)	68(9)
H20C	2990(4)	1200(2)	3340(2)	98(13)
H21A	430(3)	2074(16)	3872(16)	53(8)
H21B	760(4)	2206(19)	3077(18)	81(11)
H21C	-910(4)	1935(19)	3252(18)	81(11)
H22A	7155	1720	3974	97
H22B	5604	1966	3918	97
H22C	5996	1125	3783	97
H23A	6793	1001	4965	70
H23B	6400	1844	5100	70
H24A	4930	1375	5975	67
H24B	5213	530	5784	67
H25A	3065	638	6220	116
H25B	2899	373	5430	116
H25C	2617	1215	5621	116

Table B.6. Crystal data and structure refinement for **19**.

Empirical formula	C26 H35 Mo N3 Si2	
Formula weight	541.69	
Temperature	173(2) K	
Wavelength	0.71073 Å	
Crystal system	Monoclinic	
Space group	P2(1)/c	
Unit cell dimensions	a = 12.49960(10) Å	α= 90°.
	b = 11.13000(10) Å	β= 91.25°.
	c = 19.1658(2) Å	γ = 90°.
Volume	2665.72(4) $Å^3$	
Z	4	
Density (calculated)	1.350 Mg/m^3	
Absorption coefficient	0.600 mm^{-1}	
F(000)	1128	
Crystal size	0.22 x 0.17 x 0.057 mm^3	
Theta range for data collection	1.63 to 27.50°.	
Index ranges	$-11 \le h \le 16$, $-13 \le k \le 14$, $-24 \le l \le 23$	
Reflections collected	16993	
Independent reflections	6091 [R(int) = 0.0261]	
Completeness to theta = 27.50°	99.4 %	
Absorption correction	Empirical	
Max. and min. transmission	0.949 and 0.824	
Refinement method	Full-matrix least-squares on F^2	
Data / restraints / parameters	6091 / 0 / 290	
Goodness-of-fit on F^2	1.050	
Final R indices [I>2sigma(I)]	R1 = 0.0288, wR2 = 0.0684 [5129]	
R indices (all data)	R1 = 0.0396, wR2 = 0.0742	
Extinction coefficient	0.00006(16)	
Largest diff. peak and hole	0.830 and -0.506 $e.Å^{-3}$	

Table B.7. Atomic coordinates (x 10^4) and equivalent isotropic displacement parameters ($Å^2$x 10^3) for **19**. U(eq) is defined as one third of the trace of the orthogonalized U^{ij} tensor.

	x	y	z	U(eq)
Mo	7723(1)	1193(1)	1067(1)	18(1)
N1	8262(2)	-135(2)	754(1)	26(1)
N2	8620(1)	2538(2)	1464(1)	20(1)
N3	7067(1)	2468(1)	443(1)	19(1)
Si1	6661(1)	2568(1)	-436(1)	23(1)
Si2	9862(1)	2570(1)	1911(1)	23(1)
C1	7199(2)	500(2)	2046(1)	32(1)
C2	6286(2)	502(2)	1563(1)	24(1)
C3	5358(2)	1318(2)	1637(1)	24(1)
C4	4524(2)	1279(2)	1138(1)	30(1)
C5	3645(2)	2037(3)	1182(2)	40(1)
C6	3579(2)	2845(3)	1727(2)	44(1)
C7	4384(2)	2888(2)	2229(2)	42(1)
C8	5268(2)	2133(2)	2187(1)	33(1)
C9	8563(2)	-1316(2)	610(1)	21(1)
C10	7850(2)	-2250(2)	745(1)	32(1)
C11	8137(2)	-3430(2)	619(1)	36(1)
C12	9120(2)	-3693(2)	352(1)	32(1)
C13	9833(2)	-2776(2)	214(1)	31(1)
C14	9562(2)	-1592(2)	347(1)	26(1)
C15	6963(2)	3334(2)	960(1)	18(1)
C16	6096(2)	4141(2)	1003(1)	23(1)
C17	6027(2)	4947(2)	1544(1)	28(1)
C18	6813(2)	4968(2)	2075(1)	30(1)
C19	7661(2)	4187(2)	2062(1)	26(1)
C20	7782(2)	3357(2)	1509(1)	20(1)
C21	5188(2)	2354(2)	-572(1)	33(1)
C22	7054(2)	4080(2)	-768(1)	39(1)
C23	7371(2)	1350(3)	-898(1)	38(1)
C24	10628(2)	1248(2)	1603(1)	33(1)

C25	9704(2)	2437(2)	2875(1)	39(1)
C26	10524(2)	4014(2)	1687(2)	38(1)

Table B.8. Selected bond lengths [Å] and angles [°] for **19**.

Mo-N1	1.7361(18)
Mo-N2	2.0099(16)
Mo-N3	2.0181(16)
Mo-C1	2.146(2)
Mo-C2	2.190(2)
Mo-C20	2.555(2)
Mo-C15	2.572(2)
N1-C9	1.396(3)
N2-C20	1.393(3)
N2-Si2	1.7579(17)
N3-C15	1.391(3)
N3-Si1	1.7524(17)
Si1-C23	1.856(3)
Si1-C22	1.868(3)
Si1-C21	1.869(2)
Si2-C24	1.859(2)
Si2-C26	1.862(3)
Si2-C25	1.868(3)
C1-C2	1.455(3)
C1-H1A	0.9900
C1-H1B	0.9900
C2-C3	1.482(3)
C2-H2A	1.0000
N1-Mo-N2	123.19(8)
N1-Mo-N3	123.36(8)
N2-Mo-N3	85.22(7)
N1-Mo-C1	97.15(9)
N2-Mo-C1	96.56(8)
N3-Mo-C1	130.03(8)
N1-Mo-C2	100.33(8)
N2-Mo-C2	123.54(8)
N3-Mo-C2	100.22(7)

Table B.8—continued.

C1-Mo-C2	39.18(8)
N1-Mo-C20	155.34(8)
N2-Mo-C20	32.87(6)
N3-Mo-C20	62.73(6)
C1-Mo-C20	93.17(8)
C2-Mo-C20	101.80(7)
N1-Mo-C15	155.06(8)
N2-Mo-C15	62.74(6)
N3-Mo-C15	32.52(6)
C1-Mo-C15	106.44(8)
C2-Mo-C15	93.12(7)
C20-Mo-C15	32.90(6)
C9-N1-Mo	167.82(17)
C20-N2-Si2	127.85(14)
C20-N2-Mo	95.60(12)
Si2-N2-Mo	132.81(9)
C15-N3-Si1	127.71(14)
C15-N3-Mo	96.23(12)
Si1-N3-Mo	136.00(9)
N3-Si1-C23	106.33(10)
N3-Si1-C22	108.21(10)
C23-Si1-C22	111.31(13)
N3-Si1-C21	112.89(10)
C23-Si1-C21	108.65(12)
C22-Si1-C21	109.45(12)
N2-Si2-C24	106.51(10)
N2-Si2-C26	107.32(10)
C24-Si2-C26	112.02(12)
N2-Si2-C25	111.65(11)
C24-Si2-C25	108.56(12)
C26-Si2-C25	110.73(13)
C2-C1-Mo	72.06(12)
C2-C1-H1A	116.4
Mo-C1-H1A	116.4

Table B.8—continued.

C2-C1-H1B	116.4
Mo-C1-H1B	116.4
H1A-C1-H1B	113.4
C1-C2-C3	123.1(2)
C1-C2-Mo	68.76(12)
C3-C2-Mo	118.51(14)
C1-C2-H2A	113.1
C3-C2-H2A	113.1
Mo-C2-H2A	113.1

Symmetry transformations used to generate equivalent atoms:

Table B.9. Anisotropic displacement parameters ($Å^2 x\ 10^3$)for **19**. The anisotropic displacement factor exponent takes the form: $-2p^2[\ h^2a^{*2}U^{11} + ... + 2\ h\ k\ a^*\ b^*\ U^{12}\ ]$

	U^{11}	U^{22}	U^{33}	U^{23}	U^{13}	U^{12}
Mo	18(1)	15(1)	21(1)	-1(1)	0(1)	0(1)
N1	24(1)	21(1)	33(1)	-2(1)	2(1)	1(1)
N2	18(1)	18(1)	22(1)	-2(1)	-1(1)	1(1)
N3	20(1)	17(1)	20(1)	0(1)	-1(1)	0(1)
Si1	23(1)	26(1)	18(1)	0(1)	-2(1)	-4(1)
Si2	21(1)	23(1)	24(1)	-1(1)	-6(1)	1(1)
C1	29(1)	38(1)	26(1)	12(1)	-1(1)	-2(1)
C2	23(1)	20(1)	31(1)	4(1)	4(1)	-2(1)
C3	22(1)	22(1)	28(1)	4(1)	6(1)	-4(1)
C4	23(1)	33(1)	34(1)	1(1)	3(1)	-1(1)
C5	26(1)	45(2)	48(2)	9(1)	2(1)	5(1)
C6	35(1)	38(1)	60(2)	1□(1)	21(1)	11(1)
C7	47(2)	33(1)	46(2)	-4(1)	22(1)	1(1)
C8	37(1)	32(1)	31(1)	1(1)	7(1)	-4(1)
C9	23(1)	18(1)	22(1)	-3(1)	-2(1)	4(1)
C10	23(1)	25(1)	47(2)	-7(1)	6(1)	0(1)
C11	36(1)	22(1)	50(2)	-5(1)	7(1)	-6(1)
C12	42(1)	18(1)	37(1)	-6(1)	5(1)	6(1)
C13	32(1)	27(1)	35(1)	-2(1)	10(1)	9(1)
C14	28(1)	22(1)	29(1)	2(1)	5(1)	0(1)
C15	19(1)	16(1)	20(1)	1(1)	0(1)	-1(1)
C16	21(1)	20(1)	28(1)	2(1)	-1(1)	2(1)
C17	28(1)	24(1)	34(1)	-1(1)	3(1)	7(1)
C18	36(1)	26(1)	28(1)	-7(1)	2(1)	4(1)
C19	30(1)	25(1)	23(1)	-5(1)	-2(1)	1(1)
C20	21(1)	18(1)	21(1)	1(1)	1(1)	-1(1)
C21	28(1)	40(1)	30(1)	0(1)	-8(1)	-2(1)
C22	49(2)	41(1)	28(1)	1□(1)	-2(1)	-13(1)
C23	34(1)	50(2)	29(1)	-14(1)	1(1)	0(1)
C24	28(1)	33(1)	37(1)	-2(1)	-6(1)	9(1)
C25	48(2)	41(1)	27(1)	-2(1)	-9(1)	9(1)

C26	32(1)	34(1)	48(2)	0(1)	-8(1)	-8(1)

Table B.10. Hydrogen coordinates (x 10^4) and isotropic displacement parameters ($Å^2$x 10^3) for **19**.

	x	y	z	U(eq)
H1A	7482	-298	2186	38
H1B	7175	1079	2438	38
H2A	6079	-320	1399	29
H4A	4559	723	763	36
H5A	3088	2000	837	48
H6A	2982	3368	1755	53
H7A	4336	3438	2607	50
H8A	5817	2171	2537	40
H10A	7165	-2074	925	38
H11A	7651	-4061	717	43
H12A	9311	-4503	262	39
H13A	10512	-2960	27	37
H14A	10060	-968	259	31
H16A	5549	4127	651	28
H17A	5443	5492	1557	34
H18A	6758	5527	2447	36
H19A	8179	4203	2432	31
H21A	4982	1561	-398	50
H21B	5008	2410	-1071	50
H21C	4803	2978	-318	50
H22A	7827	4192	-697	59
H22B	6669	4704	-515	59
H22C	6873	4136	-1267	59
H23A	8145	1452	-831	56
H23B	7187	1384	-1397	56
H23C	7155	570	-710	56
H24A	10717	1306	1097	49
H24B	10238	510	1711	49
H24D	11333	1232	1837	49

H25A	9354	1672	2982	58
H25D	9264	3103	3041	58
H25B	10409	2465	3108	58
H26D	10600	4066	1180	57
H26A	11233	4048	1915	57
H26B	10088	4686	1848	57

Table B.11. Crystal data and structure refinement for **23**.

Empirical formula	C33 H54 Mo N6 Si2	
Formula weight	686.94	
Temperature	173(2) K	
Wavelength	0.71073 Å	
Crystal system	Orthorhombic	
Space group	P2(1)2(1)2(1)	
Unit cell dimensions	a = 10.4614(6) Å	α= 90°.
	b = 18.5712(12) Å	β= 90°.
	c = 19.7145(12) Å	γ = 90°.
Volume	3830.1(4) $Å^3$	
Z	4	
Density (calculated)	1.191 Mg/m^3	
Absorption coefficient	0.433 mm^{-1}	
F(000)	1456	
Crystal size	.34 x .08 x .08 mm^3	
Theta range for data collection	2.07 to 27.50°.	
Index ranges	$-13 \leq h \leq 7, -24 \leq k \leq 21, -25 \leq l \leq 24$	
Reflections collected	25951	
Independent reflections	8793 [R(int) = 0.0841]	
Completeness to theta = 27.50°	100.0 %	
Absorption correction	None	
Refinement method	Full-matrix least-squares on F^2	
Data / restraints / parameters	8793 / 49 / 415	
Goodness-of-fit on F^2	0.918	
Final R indices [I>2sigma(I)]	R1 = 0.0494, wR2 = 0.0904 [5197]	
R indices (all data)	R1 = 0.1095, wR2 = 0.1046	
Absolute structure parameter	-0.03(4)	
Extinction coefficient	0.00054(19)	
Largest diff. peak and hole	0.553 and -0.461 e.$Å^{-3}$	

Table B.12. Atomic coordinates (x 10^4) and equivalent isotropic displacement parameters ($Å^2$x 10^3) for **23**. U(eq) is defined as one third of the trace of the orthogonalized U^{ij} tensor.

	x	y	z	U(eq)
Mo	-1618(1)	-6432(1)	-2180(1)	34(1)
C1	-358(5)	-5898(3)	-1475(2)	40(1)
N1	289(4)	-5632(2)	-1072(2)	48(1)
C2	-1005(4)	-7466(3)	-1962(2)	38(1)
N2	-885(4)	-8084(2)	-1835(2)	46(1)
C3	-2744(4)	-6929(3)	-2954(2)	41(1)
N3	-3249(4)	-7183(2)	-3419(2)	45(1)
N4	-2803(3)	-6583(2)	-1531(2)	35(1)
N5	-2134(3)	-5440(2)	-2692(2)	30(1)
N6	-235(3)	-6361(2)	-2969(2)	38(1)
C4	1060(4)	-5302(2)	-543(2)	61(2)
C5	2453(6)	-5330(5)	-769(5)	80(4)
C6	582(8)	-4528(3)	-477(4)	66(3)
C7	839(10)	-5730(5)	107(4)	91(4)
C5'	2267(12)	-5763(9)	-507(10)	79(6)
C6'	1700(20)	-4588(8)	-714(11)	119(9)
C7'	388(14)	-5440(9)	132(4)	48(5)
C8	-1326(5)	-8832(3)	-1832(3)	52(1)
C9	-602(6)	-9238(3)	-2380(3)	79(2)
C10	-975(7)	-9163(3)	-1162(3)	87(2)
C11	-2735(6)	-8830(4)	-1926(4)	100(3)
C12	-3750(5)	-7448(3)	-4058(3)	59(2)
C13	-4885(7)	-7928(4)	-3912(4)	112(3)
C14	-4232(6)	-6781(4)	-4450(3)	87(2)
C15	-2682(6)	-7804(5)	-4423(3)	131(4)
C16	-3597(4)	-6820(2)	-1033(2)	36(1)
C17	-3270(6)	-6762(3)	-352(2)	60(1)
C18	-4054(6)	-7032(3)	145(3)	69(2)
C19	-5214(6)	-7356(4)	-19(3)	74(2)
C20	-5544(6)	-7418(3)	-700(3)	72(2)

C21	-4766(5)	-7178(3)	-1186(3)	61(2)
C22	-1757(5)	-5475(2)	-3366(2)	32(1)
C23	-2282(5)	-5081(3)	-3902(2)	45(1)
C24	-1851(5)	-5151(3)	-4566(2)	50(1)
C25	-898(6)	-5621(3)	-4707(2)	56(2)
C26	-351(5)	-6044(3)	-4192(2)	49(2)
C27	-745(4)	-5971(2)	-3515(2)	37(1)
Si1	-3328(18)	-4918(11)	-2358(8)	32(3)
C28	-3550(30)	-4013(12)	-2756(11)	47(7)
C29	-4910(20)	-5380(20)	-2390(30)	77(12)
C30	-2960(50)	-4759(19)	-1442(9)	89(14)
Si1'	-3149(14)	-4821(7)	-2338(6)	44(2)
C28'	-3200(20)	-3921(8)	-2761(8)	51(4)
C29'	-4821(15)	-5173(14)	-2325(13)	79(6)
C30'	-2680(30)	-4659(12)	-1436(7)	62(5)
Si2	1236(1)	-6782(1)	-3035(1)	44(1)
C33	2433(5)	-6209(3)	-3496(3)	68(2)
C32	1965(4)	-6945(3)	-2186(3)	59(2)
C31	1103(5)	-7669(3)	-3485(3)	51(1)

Table B.13. Selected bond lengths [Å] and angles [°] for **23**.

Mo-N4	1.804(4)
Mo-C2	2.070(5)
Mo-N6	2.127(3)
Mo-C3	2.137(5)
Mo-C1	2.157(5)
Mo-N5	2.169(3)
C1-N1	1.154(5)
N1-C4	1.453(6)
C2-N2	1.182(6)
N2-C8	1.464(6)
C3-N3	1.159(5)
N3-C12	1.451(6)
N4-C16	1.360(5)
N5-C22	1.387(5)
N5-Si1'	1.713(4)
N5-Si1	1.713(4)
N6-C27	1.404(5)
N6-Si2	1.732(4)
N4-Mo-C2	85.47(16)
N4-Mo-N6	174.49(16)
C2-Mo-N6	89.95(15)
N4-Mo-C3	93.44(16)
C2-Mo-C3	85.31(17)
N6-Mo-C3	83.11(15)
N4-Mo-C1	91.95(17)
C2-Mo-C1	95.94(18)
N6-Mo-C1	91.57(15)
C3-Mo-C1	174.55(18)
N4-Mo-N5	106.92(14)
C2-Mo-N5	164.15(15)
N6-Mo-N5	77.08(13)
C3-Mo-N5	84.13(15)

Table B.13—continued.

C1-Mo-N5	93.53(15)
N1-C1-Mo	176.7(4)
C1-N1-C4	177.5(5)
N2-C2-Mo	168.1(4)
C2-N2-C8	152.8(5)
N3-C3-Mo	172.8(4)
C3-N3-C12	172.0(5)
C16-N4-Mo	169.4(3)
C22-N5-Si1'	126.7(5)
C22-N5-Si1	127.0(6)
Si1'-N5-Si1	8.8(11)
C22-N5-Mo	109.6(3)
Si1'-N5-Mo	122.3(5)
Si1-N5-Mo	118.9(7)
C27-N6-Si2	120.9(3)
C27-N6-Mo	109.6(3)
Si2-N6-Mo	129.1(2)
N1-C4-C5	107.8(5)
N1-C4-C7	107.4(6)
C5-C4-C7	111.9(3)
N1-C4-C6'	116.9(9)
C5-C4-C6'	62.8(9)
C7-C4-C6'	134.9(10)
N1-C4-C7'	107.4(6)
C5-C4-C7'	133.6(7)
C7-C4-C7'	27.2(6)
C6'-C4-C7'	122.7(10)
N1-C4-C5'	104.9(8)
C5-C4-C5'	37.3(7)
C7-C4-C5'	78.1(7)
C6'-C4-C5'	97.7(11)
C7'-C4-C5'	104.3(9)
N1-C4-C6	106.0(5)

Table B.14. Anisotropic displacement parameters ($Å^2 x\ 10^3$) for **23**. The anisotropic displacement factor exponent takes the form: $-2\pi^2[\ h^2 a^{*2} U^{11} + ... + 2\ h\ k\ a^*\ b^*\ U^{12}\ ]$

	U^{11}	U^{22}	U^{33}	U^{23}	U^{13}	U^{12}
Mo	43(1)	34(1)	26(1)	-1(1)	-4(1)	1(1)
C1	50(3)	36(3)	34(3)	7(2)	3(3)	3(2)
N1	55(3)	52(3)	38(3)	-1□(2)	-11(2)	-7(2)
C2	34(3)	55(3)	25(3)	1(2)	-1(2)	2(2)
N2	52(3)	37(3)	48(3)	8(2)	2(2)	3(2)
C3	39(3)	41(3)	41(3)	-4(3)	0(2)	5(2)
N3	48(3)	49(2)	37(2)	-7(2)	-6(2)	-7(2)
N4	31(2)	37(3)	37(2)	0(2)	-2(2)	8(2)
N5	38(2)	30(2)	22(2)	0(2)	-1(2)	5(2)
N6	43(2)	35(2)	34(2)	-1(2)	-5(2)	5(2)
C4	69(4)	63(4)	50(4)	-2(3)	-18(3)	-18(3)
C8	62(4)	44(3)	50(3)	0(2)	0(3)	2(3)
C9	117(5)	48(4)	72(5)	-11(3)	36(4)	-1(3)
C10	129(6)	58(4)	73(5)	16(4)	-3(4)	-12(4)
C11	71(4)	83(5)	147(7)	-4(5)	-15(4)	-16(4)
C12	62(4)	73(4)	42(3)	-19(3)	-13(3)	-1(3)
C13	134(7)	108(6)	96(6)	-11(5)	-31(5)	-62(5)
C14	96(5)	112(6)	51(4)	-2(4)	-21(4)	-1(4)
C15	95(6)	210(9)	88(6)	-99(6)	-32(5)	64(6)
C16	32(3)	42(3)	33(3)	0(2)	0(2)	6(2)
C17	68(4)	70(4)	43(3)	-6(3)	-5(3)	-3(3)
C18	75(5)	103(5)	29(3)	8(3)	4(3)	-6(4)
C19	72(5)	81(5)	69(5)	6(4)	26(4)	-7(4)
C20	60(4)	94(5)	62(4)	7(4)	9(3)	-19(3)
C21	46(4)	83(4)	54(4)	1□(3)	6(3)	0(3)
C22	44(3)	30(2)	23(2)	-3(2)	-1(2)	0(2)
C23	53(3)	46(3)	35(3)	0(2)	-1□(2)	15(2)
C24	74(4)	48(3)	28(3)	4(2)	1(3)	4(3)
C25	84(4)	62(4)	23(3)	-2(3)	4(3)	7(3)
C26	63(4)	55(4)	30(3)	-6(3)	9(3)	13(3)
C27	45(3)	36(3)	31(3)	-3(2)	-2(2)	-5(2)

Si1	36(4)	32(4)	29(5)	4(3)	6(3)	1(4)
C28	53(14)	47(12)	40(12)	-22(10)	41(13)	-1(9)
C29	21(11)	22(14)	190(30)	9(14)	-3(13)	3(7)
C30	140(30)	100(30)	27(15)	-28(15)	-4(16)	70(30)
Si1'	43(3)	38(3)	51(4)	-1(2)	4(2)	4(3)
C28'	63(9)	33(5)	56(8)	16(6)	-19(8)	-2(6)
C29'	77(10)	35(10)	126(14)	1□(9)	23(9)	5(6)
C30'	100(11)	45(9)	42(10)	-2(7)	24(8)	1□(9)
Si2	41(1)	45(1)	45(1)	-7(1)	0(1)	5(1)
C33	56(4)	58(4)	89(5)	4(3)	8(3)	0(3)
C32	43(3)	69(4)	66(4)	-5(3)	-14(3)	19(2)
C31	62(4)	41(3)	50(3)	-2(3)	1(3)	7(2)

Table B.15. Hydrogen coordinates (x 10^4) and isotropic displacement parameters ($Å^2$x 10^3) for **23**.

	x	y	z	U(eq)
H5A	2727	-5833	-807	120
H5B	2988	-5081	-435	120
H5C	2540	-5093	-1211	120
H6A	-346	-4517	-544	99
H6B	997	-4227	-821	99
H6C	789	-4344	-24	99
H7A	1163	-6221	48	137
H7B	-78	-5747	207	137
H7C	1291	-5497	483	137
H5'A	2047	-6268	-593	118
H5'B	2650	-5719	-55	118
H5'C	2879	-5598	-850	118
H6'A	2552	-4679	-905	178
H6'B	1787	-4298	-300	178
H6'C	1182	-4326	-1046	178
H7'A	515	-5943	267	72
H7'B	-528	-5343	83	72
H7'C	747	-5121	480	72
H9A	-811	-9034	-2824	119
H9B	-847	-9747	-2369	119
H9C	319	-9194	-2299	119
H10A	-1427	-8912	-797	130
H10B	-51	-9120	-1091	130
H10C	-1217	-9673	-1161	130
H11A	-3137	-8560	-1556	151
H11B	-3052	-9327	-1924	151
H11C	-2945	-8602	-2360	151
H13A	-4599	-8356	-3663	169
H13B	-5281	-8076	-4340	169

H13C	-5509	-7663	-3638	169
H14A	-3509	-6461	-4549	130
H14B	-4862	-6523	-4173	130
H14C	-4630	-6934	-4876	130
H15A	-2395	-8225	-4164	197
H15B	-1971	-7464	-4473	197
H15C	-2974	-7958	-4872	197
H17A	-2492	-6533	-229	73
H18A	-3803	-6997	607	83
H19A	-5767	-7531	326	88
H20A	-6335	-7635	-821	87
H21A	-4997	-7248	-1647	73
H23A	-2957	-4754	-3809	53
H24A	-2224	-4872	-4918	60
H25A	-595	-5665	-5160	68
H26A	294	-6383	-4304	59
H28A	-3712	-4072	-3242	70
H28B	-2770	-3726	-2692	70
H28C	-4272	-3767	-2543	70
H29A	-5133	-5483	-2866	115
H29B	-5567	-5070	-2191	115
H29C	-4866	-5834	-2138	115
H30A	-2847	-5222	-1212	133
H30B	-3673	-4497	-1231	133
H30C	-2178	-4474	-1402	133
H28D	-3451	-3981	-3237	76
H28E	-2357	-3696	-2738	76
H28F	-3828	-3614	-2531	76
H29D	-5107	-5263	-2791	119
H29E	-5385	-4817	-2112	119
H29F	-4849	-5623	-2066	119
H30D	-2625	-5121	-1196	94
H30E	-3319	-4353	-1217	94
H30F	-1844	-4420	-1423	94
H33A	2514	-5743	-3266	101
H33B	2146	-6132	-3963	101

H33D	3264	-6452	-3499	101
H32A	1389	-7244	-1913	89
H32D	2104	-6483	-1957	89
H32B	2785	-7193	-2242	89
H31D	481	-7974	-3250	77
H31A	1939	-7907	-3488	77
H31B	820	-7588	-3953	77

Table B.16. Crystal data and structure refinement for **24**.

Empirical formula	C21.60 H43.20 Mo0.80 N2.40 P2.40 Si1.60	
Formula weight	532.61	
Temperature	173(2) K	
Wavelength	0.71073 Å	
Crystal system	Monoclinic	
Space group	P2(1)/n	
Unit cell dimensions	a = 10.4675(6) Å	α= 90°.
	b = 31.0939(16) Å	β= 111.7210(10)°.
	c = 11.3851(6) Å	γ = 90°.
Volume	3442.5(3) $Å^3$	
Z	5	
Density (calculated)	1.285 Mg/m^3	
Absorption coefficient	0.610 mm^{-1}	
F(000)	1408	
Crystal size	0.17 x 0.19 x 0.30 mm^3	
Theta range for data collection	1.31 to 27.50°.	
Index ranges	$-13 \le h \le 9$, $-40 \le k \le 38$, $-14 \le l \le 14$	
Reflections collected	24110	
Independent reflections	7865 [R(int) = 0.0266]	
Completeness to theta = 27.50°	99.5 %	
Absorption correction	Empirical	
Max. and min. transmission	0.928 and 0.747	
Refinement method	Full-matrix least-squares on F^2	
Data / restraints / parameters	7865 / 0 / 326	
Goodness-of-fit on F^2	1.037	
Final R indices [I>2sigma(I)]	R1 = 0.0264, wR2 = 0.0652 [6606]	
R indices (all data)	R1 = 0.0339, wR2 = 0.0667	
Extinction coefficient	0.00075(11)	
Largest diff. peak and hole	0.361 and -0.475 $e.Å^{-3}$	

Table B.17. Atomic coordinates (x 10^4) and equivalent isotropic displacement parameters ($Å^2$x 10^3) for **24**. U(eq) is defined as one third of the trace of the orthogonalized U^{ij} tensor.

	x	y	z	U(eq)
Mo	7923(1)	8779(1)	7623(1)	17(1)
P1	8994(1)	9340(1)	6631(1)	24(1)
P2	10087(1)	8758(1)	9589(1)	24(1)
P3	6541(1)	8198(1)	8196(1)	24(1)
Si1	9646(1)	7841(1)	6987(1)	25(1)
Si2	4604(1)	9000(1)	5219(1)	27(1)
N1	7385(2)	9160(1)	8520(1)	21(1)
N2	6208(2)	8758(1)	5736(1)	22(1)
N3	8658(2)	8313(1)	6640(1)	21(1)
C1	9356(3)	9867(1)	7379(2)	48(1)
C2	10619(3)	9216(1)	6479(3)	60(1)
C3	7990(3)	9509(1)	5022(2)	65(1)
C4	10167(3)	8458(1)	11010(2)	40(1)
C5	11756(2)	8610(1)	9540(2)	40(1)
C6	10539(2)	9285(1)	10341(2)	38(1)
C7	5901(2)	7782(1)	6993(2)	37(1)
C8	4943(2)	8399(1)	8296(2)	36(1)
C9	7107(2)	7876(1)	9650(2)	38(1)
C10	7123(2)	9416(1)	9400(2)	26(1)
C11	6896(2)	9860(1)	9209(2)	32(1)
C12	6685(2)	10107(1)	10138(3)	44(1)
C13	6700(2)	9924(1)	11245(2)	50(1)
C14	6903(3)	9489(1)	11431(2)	47(1)
C15	7109(2)	9234(1)	10521(2)	35(1)
C16	6667(2)	8571(1)	4857(2)	23(1)
C17	5929(2)	8552(1)	3542(2)	30(1)
C18	6536(3)	8420(1)	2705(2)	38(1)
C19	7895(3)	8294(1)	3151(2)	43(1)
C20	8615(2)	8277(1)	4446(2)	34(1)
C21	8013(2)	8385(1)	5317(2)	24(1)

C22	4369(2)	9351(1)	6457(2)	38(1)
C23	4242(3)	9389(1)	3853(2)	45(1)
C24	3165(2)	8596(1)	4682(2)	42(1)
C25	11430(2)	7906(1)	6979(2)	38(1)
C26	8781(2)	7397(1)	5845(2)	35(1)
C27	9852(2)	7608(1)	8560(2)	34(1)

Table B.18. Selected bond lengths [Å] and angles [°] for **24**.

Mo-N1	1.7847(15)
Mo-N3	2.1405(15)
Mo-N2	2.2334(15)
Mo-P2	2.5280(5)
Mo-P3	2.5459(5)
Mo-P1	2.5532(5)
P1-C2	1.813(3)
P1-C3	1.819(2)
P1-C1	1.820(2)
P2-C5	1.828(2)
P2-C6	1.829(2)
P2-C4	1.840(2)
P3-C7	1.820(2)
P3-C8	1.829(2)
P3-C9	1.834(2)
Si1-N3	1.7536(16)
Si1-C27	1.868(2)
Si1-C25	1.881(2)
Si1-C26	1.882(2)
Si2-N2	1.7317(16)
Si2-C22	1.871(2)
Si2-C24	1.881(2)
Si2-C23	1.896(2)
N1-C10	1.385(2)
N2-C16	1.388(2)
N3-C21	1.422(2)
N1-Mo-N3	176.91(6)
N1-Mo-N2	104.96(6)
N3-Mo-N2	78.08(6)
N1-Mo-P2	83.11(5)
N3-Mo-P2	93.88(4)
N2-Mo-P2	171.38(4)

Table B.18—continued.

N1-Mo-P3	89.69(5)
N3-Mo-P3	90.10(4)
N2-Mo-P3	83.94(4)
P2-Mo-P3	99.344(17)
N1-Mo-P1	94.74(5)
N3-Mo-P1	85.99(4)
N2-Mo-P1	85.60(4)
P2-Mo-P1	90.773(17)
P3-Mo-P1	169.385(17)
C2-P1-C3	100.28(15)
C2-P1-C1	101.36(13)
C3-P1-C1	98.86(13)
C2-P1-Mo	118.47(9)
C3-P1-Mo	117.25(9)
C1-P1-Mo	117.24(8)
C5-P2-C6	98.92(11)
C5-P2-C4	99.61(11)
C6-P2-C4	96.99(10)
C5-P2-Mo	122.20(8)
C6-P2-Mo	112.50(7)
C4-P2-Mo	121.72(8)
C7-P3-C8	101.49(11)
C7-P3-C9	101.44(11)
C8-P3-C9	97.33(10)
C7-P3-Mo	113.35(7)
C8-P3-Mo	113.13(7)
C9-P3-Mo	126.42(8)
N3-Si1-C27	112.89(8)
N3-Si1-C25	114.36(9)
C27-Si1-C25	106.45(10)
N3-Si1-C26	111.45(9)
C27-Si1-C26	103.47(10)
C25-Si1-C26	107.48(10)
N2-Si2-C22	112.27(9)

Table B.18—continued.

N2-Si2-C24	112.29(10)
C22-Si2-C24	108.81(11)
N2-Si2-C22 2955	115.56(10)
C22-Si2-C22	101.67(11)
C24-Si2-C22	105.47(11)
C10-N1-Mo	169.85(14)
C16-N2-Si2	119.14(12)
C16-N2-Mo	109.67(12)
Si2-N2-Mo	130.54(8)
C21-N2-Si1	112.22(12)
C21-N2-Mo	108.97(11)
Si1-N2-Mo	138.15(8)

Symmetry transformations used to generate equivalent atoms:

Table B.19. Anisotropic displacement parameters ($Å^2 x\ 10^3$)for **24**. The anisotropic displacement factor exponent takes the form: $-2\pi^2[\ h^2 a^{*2} U^{11} + ... + 2\ h\ k\ a^*\ b^*\ U^{12}\ ]$

	U^{11}	U^{22}	U^{33}	U^{23}	U^{13}	U^{12}
Mo	20(1)	18(1)	15(1)	-1(1)	7(1)	-1(1)
P1	27(1)	22(1)	25(1)	1(1)	11(1)	-4(1)
P2	25(1)	23(1)	20(1)	-2(1)	4(1)	-1(1)
P3	28(1)	25(1)	20(1)	0(1)	10(1)	-6(1)
Si1	23(1)	23(1)	27(1)	-6(1)	7(1)	1(1)
Si2	23(1)	31(1)	23(1)	1(1)	4(1)	2(1)
N1	24(1)	21(1)	19(1)	-2(1)	9(1)	-1(1)
N2	23(1)	24(1)	16(1)	0(1)	5(1)	-1(1)
N3	25(1)	20(1)	20(1)	-1(1)	8(1)	1(1)
C1	71(2)	26(1)	52(2)	-4(1)	29(1)	-11(1)
C2	61(2)	44(1)	104(2)	12(2)	61(2)	4(1)
C3	78(2)	65(2)	34(1)	20(1)	-1(1)	-38(2)
C4	46(1)	44(1)	23(1)	4(1)	4(1)	-3(1)
C5	27(1)	47(1)	40(1)	-7(1)	6(1)	2(1)
C6	35(1)	31(1)	37(1)	-11(1)	0(1)	-4(1)
C7	44(1)	31(1)	35(1)	-7(1)	14(1)	-14(1)
C8	31(1)	44(1)	39(1)	3(1)	18(1)	-6(1)
C9	45(1)	42(1)	31(1)	11(1)	17(1)	-2(1)
C10	23(1)	30(1)	24(1)	-8(1)	9(1)	-2(1)
C11	28(1)	29(1)	41(1)	-1□(1)	14(1)	-2(1)
C12	31(1)	36(1)	67(2)	-26(1)	20(1)	-4(1)
C13	35(1)	69(2)	50(2)	-36(1)	22(1)	-9(1)
C14	45(1)	71(2)	29(1)	-17(1)	20(1)	-6(1)
C15	39(1)	41(1)	27(1)	-4(1)	16(1)	0(1)
C16	30(1)	21(1)	18(1)	-1(1)	9(1)	-6(1)
C17	39(1)	29(1)	20(1)	0(1)	6(1)	-5(1)
C18	57(2)	38(1)	18(1)	-2(1)	13(1)	-11(1)
C19	64(2)	46(1)	29(1)	-5(1)	31(1)	-4(1)
C20	41(1)	38(1)	31(1)	-1(1)	21(1)	4(1)
C21	32(1)	21(1)	21(1)	-3(1)	12(1)	-3(1)
C22	31(1)	40(1)	40(1)	-2(1)	1□(1)	9(1)

C23	46(1)	44(1)	38(1)	12(1)	7(1)	11(1)
C24	29(1)	56(2)	36(1)	-3(1)	4(1)	-9(1)
C25	28(1)	41(1)	44(1)	-13(1)	14(1)	2(1)
C26	35(1)	27(1)	38(1)	-10(1)	7(1)	2(1)
C27	36(1)	28(1)	31(1)	-2(1)	5(1)	4(1)

Table B.20. Hydrogen coordinates (x 10^4) and isotropic displacement parameters ($Å^2$x 10^3) for **24**.

	x	y	z	U(eq)
H1A	9754	10049	6923	72
H1B	9988	9837	8237	72
H1C	8516	9994	7372	72
H2A	10898	9454	6094	91
H2B	10514	8964	5963	91
H2C	11305	9163	7302	91
H3A	8498	9719	4756	98
H3B	7138	9632	4993	98
H3C	7805	9265	4469	98
H4A	11067	8488	11652	60
H4B	9981	8160	10802	60
H4C	9494	8571	11315	60
H5A	12443	8621	10379	60
H5B	11994	8807	9005	60
H5C	11709	8323	9211	60
H6A	11364	9261	11081	57
H6B	9803	9387	10579	57
H6C	10687	9483	9759	57
H7A	5391	7574	7261	55
H7B	6662	7644	6870	55
H7C	5313	7911	6213	55
H8A	4467	8167	8514	55
H8B	4372	8517	7494	55
H8C	5150	8619	8932	55
H9A	6388	7681	9627	58
H9B	7312	8063	10367	58
H9C	7915	7717	9716	58
H11A	6887	9987	8467	39
H12A	6530	10401	10010	53

H13A	6574	10094	11865	59
H14A	6903	9365	12174	56
H15A	7238	8940	10655	42
H17A	5006	8631	3224	36
H18A	6025	8417	1840	45
H19A	8322	8222	2592	51
H20A	9531	8190	4746	41
H22A	4529	9186	7211	57
H22B	3448	9462	6154	57
H22C	5010	9586	6642	57
H23A	4947	9605	4071	68
H23B	3365	9524	3679	68
H23C	4229	9236	3117	68
H24A	3292	8388	5339	64
H24B	3167	8453	3935	64
H24C	2303	8740	4498	64
H25A	11899	8131	7554	57
H25B	11373	7979	6142	57
H25C	11927	7641	7237	57
H26A	7865	7356	5828	53
H26B	9295	7135	6111	53
H26C	8741	7473	5015	53
H27A	10291	7815	9211	51
H27B	10407	7353	8705	51
H27C	8964	7537	8571	51

Table B21. Crystal data and structure refinement for **30**.

Empirical formula	C26 H37 Mo N3 Si2	
Formula weight	543.71	
Temperature	173(2) K	
Wavelength	0.71073 Å	
Crystal system	Triclinic	
Space group	P-1	
Unit cell dimensions	a = 9.2793(6) Å	α= 87.784(1)°
	b = 10.5045(7) Å	β= 76.796(1)°
	c = 15.466(1) Å	γ = 64.068(1)°
Volume	1316.7(2) $Å^3$	
Z	2	
Density (calculated)	1.371 Mg/m^3	
Absorption coefficient	0.608 mm^{-1}	
F(000)	568	
Crystal size	0.25 x 0.10 x 0.09 mm^3	
Theta range for data collection	1.36 to 27.50°.	
Index ranges	$-11 \le h \le 12, -13 \le k \le 13, -17 \le l \le 20$	
Reflections collected	9045	
Independent reflections	5910 [R(int) = 0.0403]	
Completeness to theta = 27.50°	97.8 %	
Absorption correction	Integration	
Max. and min. transmission	0.9518 and 0.8398	
Refinement method	Full-matrix least-squares on F^2	
Data / restraints / parameters	5910 / 0 / 297	
Goodness-of-fit on F^2	0.968	
Final R indices [I>2sigma(I)]	R1 = 0.0453, wR2 = 0.0917 [4124]	
R indices (all data)	R1 = 0.0740, wR2 = 0.0974	
Largest diff. peak and hole	0.629 and -0.974 $e.Å^{-3}$	

Table B22. Atomic coordinates (x 10^4) and equivalent isotropic displacement parameters ($Å^2$x 10^3)for **30**. U(eq) is defined as one third of the trace of the orthogonalized U^{ij} tensor.

	x	y	z	U(eq)
Mo	10871(1)	3359(1)	-2400(1)	19(1)
Si1	11565(1)	425(1)	-3610(1)	23(1)
Si2	7130(1)	6005(1)	-1507(1)	26(1)
N1	11011(4)	2435(3)	-1425(2)	20(1)
N2	10342(4)	2218(3)	-3239(2)	19(1)
N3	8369(4)	4583(3)	-2295(2)	20(1)
C1	12167(5)	4004(4)	-3858(2)	25(1)
C1'	12075(5)	3767(5)	-4796(3)	34(1)
C2	13300(5)	2861(4)	-3451(2)	24(1)
C3	13635(5)	3172(4)	-2654(3)	26(1)
C3'	15106(5)	2109(5)	-2337(3)	32(1)
C4	12537(5)	4429(4)	-2153(3)	29(1)
C5	11140(5)	5424(4)	-2443(3)	29(1)
C6	11115(5)	5266(4)	-3360(3)	27(1)
C7	11152(5)	1690(4)	-663(2)	23(1)
C8	9753(5)	1974(4)	36(3)	29(1)
C9	9951(6)	1206(5)	787(3)	39(1)
C10	11482(6)	199(5)	866(3)	41(1)
C11	12830(6)	-75(4)	190(3)	34(1)
C12	12683(5)	664(4)	-577(3)	29(1)
C13	10292(5)	-589(4)	-3430(3)	32(1)
C14	12669(5)	169(5)	-4807(3)	35(1)
C15	13184(5)	-464(4)	-2969(3)	36(1)
C16	8849(4)	2969(4)	-3486(2)	19(1)
C17	8354(5)	2597(4)	-4183(2)	25(1)
C18	6836(5)	3447(4)	-4364(3)	27(1)
C19	5757(5)	4697(4)	-3853(3)	28(1)
C20	6235(5)	5096(4)	-3158(2)	25(1)
C21	7768(4)	4248(4)	-2966(2)	19(1)
C22	8044(5)	5853(4)	-526(3)	36(1)

C23	5045(5)	6062(5)	-1042(3)	43(1)
C24	6838(5)	7732(4)	-2009(3)	38(1)

Table B23. Selected bond lengths [Å] and angles [°] for **30**.

Mo-N1	1.761(3)
Mo-N2	2.070(3)
Mo-N3	2.075(3)
Mo-C5	2.287(4)
Mo-C2	2.315(4)
Mo-C4	2.371(4)
Mo-C3	2.424(4)
Mo-C6	2.506(4)
Mo-C1	2.518(3)
Si1-N2	1.756(3)
Si1-C14	1.865(4)
Si1-C15	1.869(4)
Si1-C13	1.881(4)
Si2-N3	1.743(3)
Si2-C22	1.870(4)
Si2-C24	1.877(4)
Si2-C23	1.879(4)
N1-C7	1.388(4)
N2-C16	1.397(4)
N3-C21	1.406(4)
C1-C6	1.381(5)
C1-C2	1.443(5)
C1-C1'	1.510(5)
C2-C3	1.420(5)
C3-C4	1.387(6)
C3-C3'	1.510(5)
C4-C5	1.420(5)
C5-C6	1.441(5)
N1-Mo-N2	105.07(12)
N1-Mo-N3	105.41(12)
N2-Mo-N3	77.55(11)
N1-Mo-C5	118.82(14)
N2-Mo-C5	136.00(12)

Table B.23—continued.

N3-Mo-C5	87.69(13)
N1-Mo-C2	117.47(13)
N2-Mo-C2	87.90(12)
N3-Mo-C2	136.99(12)
C5-Mo-C2	75.15(14)
N1-Mo-C4	94.25(13)
N2-Mo-C4	149.48(13)
N3-Mo-C4	120.17(13)
C5-Mo-C4	35.45(13)
C2-Mo-C4	62.03(14)
N1-Mo-C3	93.94(13)
N2-Mo-C3	119.94(13)
N3-Mo-C3	149.82(12)
C5-Mo-C3	62.50(14)
C2-Mo-C3	34.79(12)
C4-Mo-C3	33.61(13)
N1-Mo-C6	152.91(13)
N2-Mo-C6	101.87(12)
N3-Mo-C6	82.98(12)
C5-Mo-C6	34.60(13)
C2-Mo-C6	60.52(13)
C4-Mo-C6	60.11(13)
C3-Mo-C6	69.88(12)
N1-Mo-C1	151.65(13)
N2-Mo-C1	82.13(12)
N3-Mo-C1	102.92(12)
C5-Mo-C1	60.95(14)
C2-Mo-C1	34.42(12)
C4-Mo-C1	70.14(13)
C3-Mo-C1	59.80(12)
C6-Mo-C1	31.90(12)
N2-Si1-C14	113.04(17)
N2-Si1-C15	111.49(17)
C14-Si1-C15	106.4(2)

Table B.23—continued.

N2-Si1-C13	110.98(17)
C14-Si1-C13	108.95(18)
C15-Si1-C13	105.57(19)
N3-Si2-C22	111.38(17)
N3-Si2-C24	110.70(18)
C22-Si2-C24	109.0(2)
N3-Si2-C23	111.70(17)
C22-Si2-C23	105.4(2)
C24-Si2-C23	108.5(2)
C7-N1-Mo	178.9(3)
C16-N2-Si1	119.6(2)
C16-N2-Mo	114.9(2)
Si1-N2-Mo	125.38(15)
C21-N3-Si2	121.9(2)
C21-N3-Mo	114.1(2)
Si2-N3-Mo	123.70(15)
C6-C1-C2	119.1(4)
C6-C1-C1'	121.3(4)
C2-C1-C1'	119.5(4)
C6-C1-Mo	73.6(2)
C2-C1-Mo	65.04(19)
C1'-C1-Mo	130.6(2)
C3-C2-C1	118.8(4)
C3-C2-Mo	76.8(2)
C1-C2-Mo	80.5(2)
C4-C3-C2	118.6(4)
C4-C3-C3'	121.0(4)
C2-C3-C3'	120.2(4)
C4-C3-Mo	71.1(2)
C2-C3-Mo	68.4(2)
C3'-C3-Mo	129.6(2)
C3-C4-C5	121.3(4)
C3-C4-Mo	75.3(2)
C5-C4-Mo	69.0(2)

Table B.23—continued.

C4-C5-C6	117.5(4)
C4-C5-Mo	75.5(2)
C6-C5-Mo	81.1(2)
C1-C6-C5	120.1(4)
C1-C6-Mo	74.5(2)
C5-C6-Mo	64.34(19)
N1-C7-C12	120.2(3)
N1-C7-C8	120.5(4)

Symmetry transformations used to generate equivalent atoms:

Table B24. Anisotropic displacement parameters ($Å^2 x\ 10^3$) for **30**. The anisotropic displacement factor exponent takes the form: $-2\pi^2[\ h^2\ a^{*2}U^{11} + ...\ + 2\ h\ k\ a^*\ b^*\ U^{12}\ ]$

	U^{11}	U^{22}	U^{33}	U^{23}	U^{13}	U^{12}
Mo	15(1)	23(1)	20(1)	2(1)	-4(1)	-8(1)
Si1	20(1)	23(1)	25(1)	-1(1)	-5(1)	-8(1)
Si2	19(1)	24(1)	28(1)	-3(1)	-4(1)	-5(1)
N1	16(2)	21(2)	21(2)	1(1)	-4(1)	-5(1)
N2	14(2)	25(2)	18(2)	3(1)	-4(1)	-9(1)
N3	14(2)	21(2)	21(2)	-1(1)	-2(1)	-6(1)
C1	20(2)	34(2)	24(2)	10(2)	-3(2)	-16(2)
C1'	32(3)	43(3)	28(2)	14(2)	-9(2)	-19(2)
C2	20(2)	31(2)	25(2)	9(2)	-4(2)	-15(2)
C3	17(2)	35(2)	30(2)	13(2)	-7(2)	-15(2)
C3'	24(2)	42(3)	35(2)	10(2)	-14(2)	-17(2)
C4	24(2)	37(2)	34(2)	4(2)	-10(2)	-19(2)
C5	26(2)	30(2)	38(2)	3(2)	-7(2)	-19(2)
C6	22(2)	26(2)	38(2)	11(2)	-10(2)	-14(2)
C7	23(2)	26(2)	19(2)	-2(2)	-3(2)	-12(2)
C8	24(2)	31(2)	30(2)	-1(2)	1(2)	-12(2)
C9	49(3)	42(3)	27(2)	1(2)	4(2)	-27(3)
C10	59(3)	43(3)	22(2)	10(2)	-10(2)	-25(3)
C11	40(3)	37(3)	31(2)	11(2)	-17(2)	-18(2)
C12	26(2)	34(2)	28(2)	3(2)	-7(2)	-14(2)
C13	40(3)	31(2)	28(2)	0(2)	-4(2)	-20(2)
C14	30(2)	39(3)	33(2)	-4(2)	0(2)	-16(2)
C15	38(3)	24(2)	47(3)	1(2)	-17(2)	-10(2)
C16	15(2)	24(2)	19(2)	8(2)	-3(2)	-11(2)
C17	24(2)	26(2)	25(2)	2(2)	-4(2)	-12(2)
C18	30(2)	35(2)	25(2)	8(2)	-12(2)	-21(2)
C19	19(2)	39(2)	34(2)	16(2)	-14(2)	-17(2)
C20	22(2)	26(2)	27(2)	9(2)	-5(2)	-12(2)
C21	18(2)	23(2)	18(2)	6(2)	-3(2)	-12(2)
C22	34(3)	36(3)	31(2)	-10(2)	-9(2)	-8(2)
C23	27(3)	53(3)	39(3)	-7(2)	4(2)	-13(2)

C24	30(3)	27(2)	51(3)	-1(2)	-12(2)	-7(2)

Table B25. Hydrogen coordinates (x 10^4) and isotropic displacement parameters ($Å^2$x 10^3)for **30**.

	x	y	z	U(eq)
H1'1	11387	3274	-4787	50
H1'2	13187	3189	-5157	50
H1'3	11591	4684	-5053	50
H2A	13960	1899	-3771	29
H3'1	16074	2268	-2601	48
H3'2	15321	1146	-2517	48
H3'3	14876	2223	-1686	48
H4A	12617	4554	-1531	35
H5A	10297	6284	-2054	35
H6A	10131	5942	-3573	32
H8A	8696	2676	-6	35
H9A	9013	1377	1256	47
H10A	11593	-301	1391	49
H11A	13881	-777	242	41
H12A	13634	467	-1044	35
H13A	9821	-562	-2792	48
H13B	10991	-1577	-3663	48
H13C	9400	-158	-3742	48
H14A	11865	612	-5172	52
H14B	13294	-848	-4983	52
H14C	13426	608	-4894	52
H15A	13963	-46	-3089	54
H15B	13774	-1480	-3152	54
H15C	12663	-333	-2332	54
H17A	9071	1743	-4542	29
H18A	6531	3170	-4845	32
H19A	4711	5271	-3973	33
H20A	5511	5957	-2809	30
H22A	8266	4927	-283	54
H22B	7267	6609	-68	54

H22C	9076	5943	-712	54
H23A	4288	6632	-1408	64
H23B	4619	6488	-430	64
H23C	5141	5095	-1046	64
H24A	7854	7843	-2088	57
H24B	5931	8517	-1612	57
H24C	6575	7737	-2588	57

Table B.26. Crystal data and structure refinement for **31**.

Empirical formula	C26 H37 Mo N3 Si2	
Formula weight	543.71	
Temperature	173(2) K	
Wavelength	0.71073 Å	
Crystal system	Monoclinic	
Space group	P2(1)/n	
Unit cell dimensions	a = 9.7367(4) Å	α= 90°.
	b = 14.3272(6) Å	β= 95.080(1)°.
	c = 19.5480(8) Å	γ = 90°.
Volume	2716.2(2) $Å^3$	
Z	4	
Density (calculated)	1.330 Mg/m^3	
Absorption coefficient	0.589 mm^{-1}	
F(000)	1136	
Crystal size	0.16 x 0.17 x 0.23 mm^3	
Theta range for data collection	1.76 to 27.50°.	
Index ranges	$-11 \le h \le 12$, $-17 \le k \le 18$, $-14 \le l \le 25$	
Reflections collected	19388	
Independent reflections	6234 [R(int) = 0.0248]	
Completeness to theta = 27.50°	99.7 %	
Absorption correction	Integration	
Max. and min. transmission	0.9651 and 0.8641	
Refinement method	Full-matrix least-squares on F^2	
Data / restraints / parameters	6234 / 0 / 298	
Goodness-of-fit on F^2	1.018	
Final R indices [I>2sigma(I)]	R1 = 0.0237, wR2 = 0.0590 [5112]	
R indices (all data)	R1 = 0.0345, wR2 = 0.0621	
Extinction coefficient	0.00131(18)	
Largest diff. peak and hole	0.336 and -0.337 $e.Å^{-3}$	

Table B.27. Atomic coordinates (x 10^4) and equivalent isotropic displacement parameters ($Å^2$x 10^3) for **31**. U(eq) is defined as one third of the trace of the orthogonalized U^{ij} tensor.

	x	y	z	U(eq)
Mo	4569(1)	1611(1)	1996(1)	20(1)
Si1	6450(1)	2018(1)	661(1)	27(1)
Si2	5226(1)	2547(1)	3570(1)	28(1)
N1	3598(1)	2614(1)	1728(1)	23(1)
N2	6342(1)	1899(1)	1546(1)	22(1)
N3	5835(1)	2108(1)	2819(1)	22(1)
C1	2919(2)	505(1)	1512(1)	32(1)
C1'	1775(2)	750(2)	972(1)	41(1)
C2	2724(2)	583(1)	2207(1)	33(1)
C3	3824(2)	463(1)	2718(1)	34(1)
C4	5069(2)	2(1)	2537(1)	37(1)
C4'	6131(2)	-300(2)	3095(1)	52(1)
C5	5256(2)	-83(1)	1859(1)	36(1)
C6	4273(2)	288(1)	1334(1)	33(1)
C7	3658(2)	3541(1)	1524(1)	25(1)
C8	2709(2)	3904(1)	1019(1)	34(1)
C9	2871(2)	4806(2)	782(1)	44(1)
C10	3939(2)	5362(2)	1058(1)	44(1)
C11	4864(2)	5014(1)	1574(1)	41(1)
C12	4739(2)	4111(1)	1801(1)	33(1)
C13	4735(2)	2055(2)	153(1)	42(1)
C14	7408(2)	1008(2)	325(1)	41(1)
C15	7300(2)	3143(2)	459(1)	40(1)
C16	7504(2)	2067(1)	2007(1)	22(1)
C17	8869(2)	2130(1)	1839(1)	27(1)
C18	9932(2)	2348(1)	2337(1)	29(1)
C19	9648(2)	2469(1)	3013(1)	28(1)
C20	8317(2)	2376(1)	3194(1)	26(1)
C21	7225(2)	2188(1)	2698(1)	21(1)
C22	3318(2)	2715(2)	3452(1)	38(1)

C23	5628(2)	1750(2)	4322(1)	49(1)
C24	5970(2)	3727(2)	3797(1)	47(1)

Table B.28. Selected bond lengths [Å] and angles [°] for **31**.

Mo-N1	1.7748(14)
Mo-N2	2.0470(14)
Mo-N3	2.0644(14)
Mo-C6	2.2987(18)
Mo-C3	2.3253(19)
Mo-C2	2.3870(18)
Mo-C1	2.3912(17)
Mo-C5	2.5368(19)
Mo-C4	2.5636(19)
Si1-N2	1.7518(15)
Si1-C13	1.866(2)
Si1-C15	1.870(2)
Si1-C14	1.871(2)
Si2-N3	1.7482(15)
Si2-C22	1.8676(19)
Si2-C23	1.875(2)
Si2-C24	1.877(2)
N1-C7	1.388(2)
N2-C16	1.403(2)
N3-C21	1.399(2)
C1-C2	1.392(3)
C1-C6	1.428(3)
C1-C1'	1.506(3)
C1'-H1'A	0.9800
C1'-H1'B	0.9800
C1'-H1'C	0.9800
C2-C3	1.410(3)
C2-H2A	0.9500
C3-C4	1.451(3)
C3-H3A	0.9500
C4-C5	1.359(3)
C4-C4'	1.499(3)
C4'-H4'A	0.9800

Table B.28—continued.

C4'-H4'B	0.9800
C4'-H4'C	0.9800
C5-C6	1.441(3)
C5-H5A	0.9500
C6-H6A	0.9500
N1-Mo-N2	99.05(6)
N1-Mo-N3	102.48(6)
N2-Mo-N3	78.32(6)
N1-Mo-C6	117.71(7)
N2-Mo-C6	89.61(6)
N3-Mo-C6	139.43(6)
N1-Mo-C3	124.44(7)
N2-Mo-C3	136.37(6)
N3-Mo-C3	88.13(6)
C6-Mo-C3	74.24(8)
N1-Mo-C2	99.28(7)
N2-Mo-C2	151.01(6)
N3-Mo-C2	118.98(6)
C6-Mo-C2	61.94(7)
C3-Mo-C2	34.78(7)
N1-Mo-C1	95.62(6)
N2-Mo-C1	121.77(6)
N3-Mo-C1	150.53(6)
C6-Mo-C1	35.38(6)
C3-Mo-C1	62.41(7)
C2-Mo-C1	33.88(7)
N1-Mo-C5	151.92(7)
N2-Mo-C5	84.71(6)
N3-Mo-C5	105.52(6)
C6-Mo-C5	34.23(7)
C3-Mo-C5	59.14(7)
C2-Mo-C5	68.75(6)
C1-Mo-C5	59.93(6)

Table B.28—continued.

N1-Mo-C4	157.92(7)
N2-Mo-C4	102.85(6)
N3-Mo-C4	84.86(6)
C6-Mo-C4	60.06(7)
C3-Mo-C4	34.08(7)
C2-Mo-C4	59.49(6)
C1-Mo-C4	70.37(7)
C5-Mo-C4	30.90(7)
N2-Si1-C13	113.52(9)
N2-Si1-C15	111.03(9)
C13-Si1-C15	104.76(10)
N2-Si1-C14	110.27(9)
C13-Si1-C14	106.60(10)
C15-Si1-C14	110.44(11)
N3-Si2-C22	110.49(8)
N3-Si2-C23	112.09(9)
C22-Si2-C23	108.17(10)
N3-Si2-C24	111.77(9)
C22-Si2-C24	105.80(10)
C23-Si2-C24	108.25(12)
C7-N1-Mo	145.50(12)
C16-N2-Si1	120.11(12)
C16-N2-Mo	114.94(11)
Si1-N2-Mo	124.81(8)
C21-N3-Si2	121.14(11)
C21-N3-Mo	114.58(11)
Si2-N3-Mo	123.74(8)
C2-C1-C6	117.60(17)
C2-C1-C1'	120.61(17)
C6-C1-C1'	121.43(19)
C2-C1-Mo	72.89(10)
C6-C1-Mo	68.77(10)
C1'-C1-Mo	123.50(13)
C1-C2-C3	121.48(18)

Table B.28—continued.

C1-C2-Mo	73.22(10)
C3-C2-Mo	70.22(10)
C1-C2-H2A	119.3
C3-C2-H2A	119.3
Mo-C2-H2A	129.9
C2-C3-C4	118.71(19)
C2-C3-Mo	75.00(11)
C4-C3-Mo	81.99(12)
C2-C3-H3A	120.6
C4-C3-H3A	120.6
Mo-C3-H3A	113.0
C5-C4-C3	117.80(18)
C5-C4-C4'	122.7(2)
C3-C4-C4'	119.4(2)
C5-C4-Mo	73.46(11)
C3-C4-Mo	63.93(10)
C4'-C4-Mo	130.77(14)
C4-C5-C6	121.56(18)
C4-C5-Mo	75.64(11)
C6-C5-Mo	63.80(10)
C4-C5-H5A	119.2
C6-C5-H5A	119.2
Mo-C5-H5A	134.9
C1-C6-C5	118.44(19)
C1-C6-Mo	75.85(10)
C5-C6-Mo	81.97(11)
C1-C6-H6A	120.8
C5-C6-H6A	120.8
Mo-C6-H6A	112.0
N1-C7-C8	121.22(16)

Symmetry transformations used to generate equivalent atoms:

Table B.29. Anisotropic displacement parameters ($Å^2 x\ 10^3$) for **31**. The anisotropic displacement factor exponent takes the form: $-2\pi^2[\ h^2 a^{*2} U^{11} + ... + 2\ h\ k\ a^*\ b^*\ U^{12}\ ]$

	U^{11}	U^{22}	U^{33}	U^{23}	U^{13}	U^{12}
Mo	18(1)	18(1)	24(1)	-1(1)	0(1)	0(1)
Si1	30(1)	29(1)	21(1)	-3(1)	2(1)	1(1)
Si2	22(1)	41(1)	22(1)	-5(1)	2(1)	0(1)
N1	21(1)	24(1)	24(1)	-1(1)	-1(1)	1(1)
N2	20(1)	24(1)	22(1)	-2(1)	0(1)	0(1)
N3	18(1)	26(1)	21(1)	0(1)	0(1)	0(1)
C1	25(1)	23(1)	47(1)	-10(1)	0(1)	-6(1)
C1'	27(1)	46(1)	49(1)	-16(1)	-4(1)	-3(1)
C2	25(1)	24(1)	51(1)	-1(1)	7(1)	-7(1)
C3	33(1)	28(1)	42(1)	7(1)	6(1)	-5(1)
C4	35(1)	20(1)	55(1)	8(1)	-2(1)	-2(1)
C4'	49(1)	36(1)	68(2)	15(1)	-8(1)	9(1)
C5	29(1)	19(1)	60(1)	-5(1)	3(1)	2(1)
C6	28(1)	25(1)	44(1)	-11(1)	2(1)	-1(1)
C7	28(1)	23(1)	25(1)	-2(1)	5(1)	5(1)
C8	37(1)	30(1)	32(1)	-2(1)	-6(1)	6(1)
C9	59(1)	38(1)	35(1)	8(1)	-3(1)	14(1)
C10	63(2)	26(1)	45(1)	6(1)	8(1)	3(1)
C11	43(1)	28(1)	51(1)	1(1)	3(1)	-4(1)
C12	33(1)	27(1)	36(1)	1(1)	-1(1)	0(1)
C13	40(1)	58(1)	27(1)	-2(1)	-4(1)	2(1)
C14	49(1)	40(1)	36(1)	-8(1)	8(1)	7(1)
C15	51(1)	38(1)	31(1)	6(1)	3(1)	-5(1)
C16	21(1)	20(1)	24(1)	0(1)	-1(1)	1(1)
C17	24(1)	27(1)	29(1)	0(1)	5(1)	2(1)
C18	18(1)	28(1)	40(1)	1(1)	3(1)	1(1)
C19	21(1)	28(1)	35(1)	-1(1)	-5(1)	1(1)
C20	24(1)	27(1)	26(1)	-1(1)	-2(1)	3(1)
C21	19(1)	19(1)	25(1)	1(1)	0(1)	1(1)
C22	25(1)	57(1)	32(1)	-9(1)	5(1)	5(1)
C23	41(1)	77(2)	28(1)	9(1)	2(1)	1(1)

C24	40(1)	52(1)	49(1)	-24(1)	3(1)	-2(1)

Table B.30. Hydrogen coordinates (x 10^4) and isotropic displacement parameters ($Å^2$x 10^3) for **31**.

	x	y	z	U(eq)
H1'A	1364	176	773	61
H1'B	2149	1121	610	61
H1'C	1069	1113	1182	61
H2A	1831	719	2339	39
H3A	3752	679	3173	41
H4'A	5684	-654	3442	78
H4'B	6584	252	3308	78
H4'C	6819	-694	2898	78
H5A	6054	-394	1728	43
H6A	4521	385	880	39
H8A	1952	3535	838	41
H9A	2240	5044	426	53
H10A	4038	5981	895	53
H11A	5587	5400	1772	49
H12A	5389	3872	2148	39
H13A	4153	2525	349	63
H13B	4293	1442	168	63
H13C	4860	2218	-325	63
H14A	6977	423	454	62
H14B	8369	1023	522	62
H14C	7379	1049	-176	62
H15A	6737	3666	596	60
H15B	7393	3178	-36	60
H15C	8215	3175	710	60
H17A	9072	2023	1380	32
H18A	10849	2413	2213	34
H19A	10373	2616	3354	34
H20A	8139	2441	3662	31
H22A	2867	2111	3359	57

H22B	3086	3137	3064	57
H22C	2998	2986	3870	57
H23A	5124	1163	4243	73
H23B	5350	2048	4739	73
H23C	6621	1623	4376	73
H24A	5796	4149	3404	71
H24B	6966	3670	3914	71
H24C	5536	3978	4192	71

Table B.31. Crystal data and structure refinement for **36**.

Empirical formula	C27.50 H50 Mo N3 P3 Si	
Formula weight	639.64	
Temperature	173(2) K	
Wavelength	0.71073 Å	
Crystal system	Monoclinic	
Space group	P2(1)/n	
Unit cell dimensions	a = 10.585(1) Å	α= 90°.
	b = 14.259(2) Å	β= 91.728(2)°.
	c = 21.665(2) Å	γ = 90°.
Volume	3268.3(6) $Å^3$	
Z	4	
Density (calculated)	1.300 Mg/m^3	
Absorption coefficient	0.605 mm^{-1}	
F(000)	1348	
Crystal size	0.25 x 0.23 x 0.09 mm^3	
Theta range for data collection	1.71 to 27.50°.	
Index ranges	$-13 \le h \le 13$, $-12 \le k \le 18$, $-28 \le l \le 26$	
Reflections collected	23240	
Independent reflections	7495 [R(int) = 0.0369]	
Completeness to theta = 27.50°	99.9 %	
Absorption correction	Integration	
Max. and min. transmission	0.944 and 0.878	
Refinement method	Full-matrix least-squares on F^2	
Data / restraints / parameters	7495 / 0 / 343	
Goodness-of-fit on F^2	0.958	
Final R indices [I>2sigma(I)]	R1 = 0.0276, wR2 = 0.0662 [5856]	
R indices (all data)	R1 = 0.0400, wR2 = 0.0699	
Extinction coefficient	0.00056(13)	
Largest diff. peak and hole	0.529 and -0.595 $e.Å^{-3}$	

Table B.32. Atomic coordinates (x 10^4) and equivalent isotropic displacement parameters ($Å^2$x 10^3) for **36**. U(eq) is defined as one third of the trace of the orthogonalized U^{ij} tensor.

	x	y	z	U(eq)
Mo	4627(1)	7466(1)	1532(1)	20(1)
N1	6166(1)	7171(1)	1262(1)	24(1)
N2	4736(2)	7666(1)	2548(1)	23(1)
N3	2757(2)	7654(1)	1785(1)	25(1)
P1	4240(1)	5752(1)	1738(1)	25(1)
P2	3794(1)	7390(1)	461(1)	28(1)
P3	4732(1)	9242(1)	1468(1)	28(1)
C1	7258(2)	6796(1)	1026(1)	28(1)
C2	7383(2)	6639(2)	393(1)	40(1)
C3	8482(2)	6254(2)	168(1)	47(1)
C4	9470(2)	6011(2)	566(1)	47(1)
C5	9356(2)	6167(2)	1191(1)	49(1)
C6	8264(2)	6546(2)	1422(1)	40(1)
C7	3565(2)	7602(1)	2817(1)	24(1)
C8	3339(2)	7514(1)	3452(1)	32(1)
C9	2115(2)	7467(1)	3669(1)	36(1)
C10	1078(2)	7503(1)	3267(1)	37(1)
C11	1266(2)	7574(1)	2635(1)	31(1)
C12	2485(2)	7615(1)	2407(1)	24(1)
Si	6129(1)	7846(1)	2967(1)	30(1)
C13	7369(2)	8418(1)	2491(1)	37(1)
C14	6875(2)	6737(2)	3267(1)	53(1)
C15	5950(2)	8641(2)	3657(1)	50(1)
C16	5332(2)	4940(1)	1388(1)	44(1)
C17	2699(2)	5278(2)	1505(1)	49(1)
C18	4307(3)	5348(2)	2538(1)	47(1)
C19	4571(2)	8157(2)	-93(1)	42(1)
C20	3859(2)	6285(2)	27(1)	45(1)
C21	2143(2)	7704(2)	312(1)	45(1)
C22	6094(2)	9778(2)	1113(1)	47(1)

C23	4649(2)	9861(1)	2205(1)	45(1)
C24	3405(2)	9829(2)	1070(1)	45(1)
C25	349(4)	10370(4)	548(3)	115(2)
C26	-339(8)	9456(8)	499(3)	220(5)
C27	-689(5)	9111(5)	-44(3)	145(2)
C28	-405(7)	9242(8)	939(4)	125(5)

Table B.33. Bond lengths [Å] and angles [°] for **36**.

Mo-N1	1.7971(15)
Mo-N3	2.0872(16)
Mo-N2	2.2176(15)
Mo-P2	2.4612(6)
Mo-P1	2.5204(5)
Mo-P3	2.5385(6)
N1-C1	1.385(2)
N2-C7	1.389(2)
N2-Si	1.7278(17)
N3-C12	1.388(2)
N3-H3	0.86(2)
P1-C16	1.818(2)
P1-C17	1.822(2)
P1-C18	1.827(2)
P2-C21	1.823(2)
P2-C19	1.836(2)
P2-C20	1.837(2)
P3-C22	1.822(2)
P3-C24	1.828(2)
P3-C23	1.829(2)
N1-Mo-N3	172.52(6)
N1-Mo-N2	109.48(6)
N3-Mo-N2	75.17(6)
N1-Mo-P2	89.10(5)
N3-Mo-P2	86.43(5)
N2-Mo-P2	161.41(4)
N1-Mo-P1	89.09(5)
N3-Mo-P1	85.24(4)
N2-Mo-P1	87.32(4)
P2-Mo-P1	93.891(17)
N1-Mo-P3	100.06(5)
N3-Mo-P3	85.97(4)

Table B.33—continued.

N2-Mo-P3	85.74(4)
P2-Mo-P3	90.405(17)
P1-Mo-P3	169.961(16)
C1-N1-Mo	170.14(14)
C7-N2-Si	123.11(13)
C7-N2-Mo	112.89(12)
Si-N2-Mo	123.97(8)
C12-N3-Mo	118.47(13)
C12-N3-H3	112.9(14)
Mo-N3-H3	127.3(14)
C16-P1-C17	102.95(12)
C16-P1-C18	100.80(11)
C17-P1-C18	98.87(11)
C16-P1-Mo	115.80(7)
C17-P1-Mo	117.40(8)
C18-P1-Mo	118.13(7)
C21-P2-C19	100.60(11)
C21-P2-C20	99.86(11)
C19-P2-C20	98.77(10)
C21-P2-Mo	118.03(8)
C19-P2-Mo	115.78(8)
C20-P2-Mo	120.18(8)
C22-P3-C24	102.47(11)
C22-P3-C23	103.00(11)
C24-P3-C23	97.71(11)
C22-P3-Mo	118.53(8)
C24-P3-Mo	116.66(8)
C23-P3-Mo	115.48(7)
N1-C1-C6	120.15(18)
N1-C1-C2	121.86(19)

Symmetry transformations used to generate equivalent atoms:
#1 -x,-y+2,-z

Table B.34. Anisotropic displacement parameters ($Å^2 x\ 10^3$) for **36**. The anisotropic displacement factor exponent takes the form: $-2\pi^2[\ h^2\ a^{*2}U^{11} + ... + 2\ h\ k\ a^*\ b^*\ U^{12}\ ]$

	U^{11}	U^{22}	U^{33}	U^{23}	U^{13}	U^{12}
Mo	20(1)	21(1)	18(1)	1(1)	3(1)	2(1)
N1	23(1)	26(1)	24(1)	3(1)	3(1)	1(1)
N2	25(1)	26(1)	20(1)	1(1)	2(1)	2(1)
N3	22(1)	31(1)	21(1)	-1(1)	1(1)	4(1)
P1	26(1)	22(1)	27(1)	1(1)	3(1)	1(1)
P2	30(1)	32(1)	20(1)	-1(1)	0(1)	4(1)
P3	35(1)	22(1)	28(1)	2(1)	0(1)	1(1)
C1	23(1)	25(1)	35(1)	2(1)	8(1)	1(1)
C2	36(1)	51(1)	34(1)	4(1)	9(1)	10(1)
C3	45(1)	54(1)	42(1)	-2(1)	22(1)	6(1)
C4	31(1)	41(1)	70(2)	-7(1)	22(1)	5(1)
C5	26(1)	57(2)	65(2)	-3(1)	0(1)	11(1)
C6	29(1)	49(1)	41(1)	-3(1)	3(1)	8(1)
C7	29(1)	20(1)	23(1)	-1(1)	6(1)	2(1)
C8	42(1)	30(1)	24(1)	0(1)	6(1)	1(1)
C9	49(1)	32(1)	28(1)	-2(1)	17(1)	-2(1)
C10	37(1)	32(1)	42(1)	-3(1)	20(1)	-3(1)
C11	27(1)	27(1)	38(1)	-2(1)	9(1)	1(1)
C12	27(1)	21(1)	25(1)	-1(1)	6(1)	3(1)
Si	29(1)	35(1)	27(1)	4(1)	-5(1)	0(1)
C13	31(1)	41(1)	38(1)	-1(1)	-3(1)	-5(1)
C14	40(1)	50(2)	69(2)	20(1)	-16(1)	3(1)
C15	54(2)	63(2)	32(1)	-10(1)	-5(1)	-11(1)
C16	50(1)	25(1)	58(2)	1(1)	19(1)	6(1)
C17	37(1)	45(1)	66(2)	13(1)	-6(1)	-13(1)
C18	74(2)	31(1)	35(1)	9(1)	3(1)	-5(1)
C19	56(2)	47(1)	24(1)	8(1)	8(1)	7(1)
C20	63(2)	43(1)	31(1)	-11(1)	0(1)	5(1)
C21	35(1)	63(2)	36(1)	-9(1)	-9(1)	8(1)
C22	51(1)	41(1)	48(1)	14(1)	0(1)	-15(1)
C23	68(2)	29(1)	40(1)	-6(1)	-3(1)	11(1)

C24	49(1)	31(1)	52(1)	0(1)	-13(1)	12(1)
C25	74(3)	110(4)	158(5)	-72(4)	-51(3)	53(3)
C26	174(7)	364(13)	118(5)	-81(7)	-48(5)	220(9)
C27	107(4)	190(6)	133(5)	-56(5)	-57(4)	103(4)
C28	40(4)	205(11)	129(8)	-118(8)	-16(5)	34(5)

Table B.35. Hydrogen coordinates (x 10^4) and isotropic displacement parameters ($Å^2$x 10^3) for **36**.

	x	y	z	U(eq)
H3	2090(20)	7641(13)	1548(10)	28(6)
H2A	6707	6798	114	48
H3A	8554	6157	-263	56
H4A	10218	5740	412	56
H5A	10039	6010	1467	59
H6A	8200	6638	1854	48
H8A	4036	7485	3738	38
H9A	1991	7410	4100	43
H10A	247	7478	3419	44
H11A	557	7595	2356	37
H13A	7305	8180	2067	55
H13B	8209	8275	2669	55
H13C	7240	9099	2489	55
H14A	6289	6416	3538	80
H14B	7657	6887	3499	80
H14C	7068	6326	2919	80
H15A	5247	9075	3577	75
H15B	6732	8998	3729	75
H15C	5780	8262	4023	75
H16A	5067	4294	1470	66
H16B	6185	5041	1565	66
H16C	5335	5046	941	66
H17A	2564	5355	1059	74
H17B	2037	5613	1722	74
H17C	2667	4610	1610	74
H18A	4109	4677	2551	70
H18B	3691	5696	2777	70
H18C	5158	5453	2716	70
H19A	4293	7988	-514	63

H19B	5489	8082	-49	63
H19C	4345	8811	-12	63
H20A	3315	5819	218	68
H20B	4732	6053	32	68
H20C	3567	6393	-401	68
H21A	1990	8337	469	67
H21B	1598	7257	521	67
H21C	1954	7686	-133	67
H22A	6150	9556	687	70
H22B	6866	9603	1347	70
H22C	6000	10461	1115	70
H23A	5425	9746	2451	68
H23B	3920	9634	2429	68
H23C	4557	10535	2128	68
H24A	3511	10510	1104	67
H24B	2614	9643	1259	67
H24C	3379	9648	633	67
H25A	561	10605	949	138
H26A	-526	9119	863	264
H27A	-1147	8540	-85	174
H28A	-909	9695	1167	188
H28B	444	9199	1131	188
H28C	-812	8626	948	188

LIST OF REFERENCES

1. Crabtree, R. H. *The Organometallic Chemistry of the Transition Metals*; John Wiley & Sons: New York, 1994.

2. Hueey, J. E.; Keiter, E. A.; Keiter, R. L. *Inorganic Chemistry: Principles of Structure and Reactivity*; Harper Collins College: New York, 1993.

3. Cotton, F. A.; Wilkinson, G. *Advanced Inorganic Chemistry*; John Wiley & Sons: New York, 1988.

4. Collman, J. P.; Hegedus, L. S.; Norton, J. R; Finke, R. G. *Principles and Applications of Organotransition Metal Chemistry*; University Science Books: Mill Valley, 1987.

5. Yamamoto, A. *Organotransition Metal Chemistry*; Wiley-Interscience: New York, 1986.

6. Puddephatt, R. J. In *The Chemistry of the Metal-Carbon Bond*; Hartley, F. R.; Patai, S., Eds.; John Wiley & Sons: New York, 1982.

7. Kondakov, D.; Negishi, E. *J. Chem. Soc., Chem. Comm.* **1996**, 963.

8. Soleil, F.; Choukroun, R. *J. Am. Chem. Soc.* **1997**, *119*, 2938.

9. Millard, D. B.; Waymouth, R. M. *Organometallics* **1997**, *16*, 1153.

10. Takahashi, T.; Kotora, M.; Fischer, R.; Nishihara, Y.; Nakajima, K. *J. Am. Chem. Soc.* **1995**, *117*, 11039.

11. Knight, K. S.; Wang, D.; Waymouth, R. M.; Ziller, J. *J. Am. Chem. Soc.* **1994**, *116*, 1845.

12. Nugent, W. A.; Taber, D. F. *J. Am. Chem. Soc.* **1989**, *111*, 6435.

13. Taber, D. F.; Louey, J. P.; Wang, Y.; Nugent, W. A.; Dixon, D. A.; Harlow, R. L. *J. Am. Chem. Soc.* **1994**, *116*, 9457.

14. Negishi, E.; Holmes, S. J.; Tour, J. M.; Miller, J. A.; Cederbaum, F. E.; Swanson, D. R.; Takahashi, T. *J. Am. Chem. Soc.* **1989**, *111*, 3336.

15. Buchwald, S. L.; Nielsen, R. B. *Chem. Rev.* **1988**, *88*, 1047.

16. Ivin, K. J. *Olefin Metathesis*; Academic Press: London, 1983.

17. Grubbs, R. H. In *Comprehensive Organometallic Chemistry*; Wilkinson, G., Stone, F. G. A., Abel, E. W., Eds.; Pergamon: New York, 1982; Vol. 8.

18. Schrock, R. R.; De Pue, R. T.; Feldman, J.; Yap, K. B.; Yang, D. C.; Davis, W. M.; Park, L.; DiMare, M.; Schoefield, M.; Anhaus, J.; Walborsky, E.; Evitt, E.; Krüger, C.; Betz, P. *Organometallics* **1990**, *9*, 2262.

19. Schrock, R. R.; Murdzek, J. S.; Bazan, G. C.; Robbins, J.; DiMare, M.; O'Regan, M. *J. Am. Chem. Soc.* **1990**, *112*, 3875.

20. Torecki, R.; Schrock, R. R. *J. Am. Chem. Soc.* **1990**, *112*, 2448.

21. Krska, S. W.; Zuckerman, R. L.; Bergman, R. G. *J. Am. Chem. Soc.* **1998**, *120*, 11828.

22. Cantrell, G. K.; Meyer, T. Y. *J. Am. Chem. Soc.* **1998**, *120*, 8035.

23. Cantrell, G. K.; Meyer, T. Y. *J. Chem. Soc. Chem. Commun.* **1997**, 1551.

24. Cantrell, G. K.; Meyer, T. Y. *Organometallics* **1997**, *16*, 5381.

25. Feldman, J.; Schrock, R. R. *Prog. Inorg. Chem.* **1991**, *39*, 1.

26. Moore, J. S. In *Comprehensive Organometallic Chemistry II*; Pergamon: New York, 1995; Vol. 12, Chapter 12.2.

27. Schrock, R. R. *Acc. Chem. Res.* **1990**, *23*, 158.

28. Fox, H. H.; Lee, J. K.; Park, L. Y.; Schrock, R. R. *Organometallics* **1993**, *12*, 759.

29. Grubbs, R. H.; Tumas, W. *Science* **1989**, *243*, 907.

30. Schrock, R. R.; Weinstock, I. A.; Horton, A. D.; Liu, A. H.; Schoefield, M. H. *J. Am. Chem. Soc.* **1988**, *110*, 2686.

31. Schrock, R. R.; Luo, S.; Lee, J. C.; Zanetti, N. C.; Davis, W. M. *J. Am. Chem. Soc.* **1996**, *118*, 3883.

32. Schrock, R. R. *Polyhedron* **1995**, *14*, 3177.

33. Wagener, K. B.; Boncella, J. M.; Nel, J. G.; Duttweiler, R. P.; Hillmyer, M. A. *Makromol. Chem.* **1990**, *191*, 365.

34. Coates, G. W.; Waymouth, R. M. In *Comprehensive Organometallic Chemistry*, Ed. Wilkinson, G., Ed.; Pergamon: London, 1995, vol. 12, 1193.

35. Ciardelli, F.; Carlini, C. In *Comprehensive Polymer Science*, Allen, G., Ed.; Pergamon: London, 1992, First Supplement, 67.

36. Möhring, P. C.; Coville, N. J. *J. Organomet. Chem.* **1994**, *479*, 1.

37. Grubbs, R. H.; Coates, G. W. *Acc. Chem. Res.* **1996**, *29*, 85.

38. (a) Boor, J. *Ziegler-Natta Catalysts and Polymerizations*; Academic: New York, 1979. (b) Jordan, R. F.; Bajgur, C. S.; Willet, R.; Scott, B. *J. Am. Chem. Soc.* **1986**, *108*, 7410.

39. Schmidt, G. F.; Brookhart, M. J. *J. Am. Chem. Soc.* **1985**, *107*, 1443.

40. Brookhart, M.; Lincoln, D. M.; Volpe, A. F.; Schmidt, G. F. *Organometallics* **1989**, *8*, 1212.

41. Brookhart, M.; Volpe, A. F.; Lincoln, D. M.; Horvath, I. T.; Millar, J. M. *J. Am. Chem. Soc.* **1990**, *112*, 5634.

42. Brookhart, M.; Lincoln, D. M. *J. Am. Chem. Soc.* **1988**, *110*, 8719.

43. Johnson, L. K.; Killian, C. M.; Brookhart, M. J. *J. Am. Chem. Soc.* **1995**, *117*, 6414.

44. Small, B. L.; Brookhart, M. *J. Am. Chem. Soc.* **1998**, *120*, 7143.

45. Small, B. L.; Brookhart, M.; Bennett, A. M. A. **1998**, *120*, 4049.

46. Evans, W. J.; Clark, R. D.; Ansari, M. A.; Ziller, J. W. *J. Am. Chem. Soc.* **1998**, *120*, 9555.

47. Stern, D.; Sabat, M. Marks, T. J. *J. Am. Chem. Soc.* **1990**, *112*, 9558.

48. Jeske, G.; Schock, L. E.; Swpston, P. N.; Schummann, H.; Marks, T. J. *J. Am. Chem. Soc.* **1985**, *107*, 8103.

49. Pfaltz, A. *Acc. Chem. Res.* **1993**, *26*, 339.

50. a) Huber, S. R.; Baldwin, T. C.; Wigley, D. E. *Organometallics* **1993**, *12*, 91. b) Cloke, F. G. N.; Day, J. P.; Green, J. C.; Morley, C. P.; Swain, A. C. *J. Chem. Soc.*,

Dalton Trans. **1991**, 789. c) Bulls. A. R.; Schaefer, W. P.; Serfas, M.; Bercaw, J. E. *Organometallics* **1987**, *6*, 1219.

51. McKnight, A. L.; Waymouth, R. M. *Chem. Rev.* **1998**, *98*, 2587.

52. a) Zhen, H. S.; Wang, C. M.; Hu, Y. M.; Flood, T. C. *Organometallics* **1998**, *17*, 5397. b) Zhou, R. J.; Wang, C. M.; Hu, Y. H.; Flood, T. C. *Organometallics* **1997**, *16*, 434. c) Wang, L.; Wang, C. M.; Bau, R.; Flood, T. C. *Organometallics* **1996**, *15*, 491. d) Wang, C. M.; Ziller, J. W.; Flood, T. C. *J. Am. Chem. Soc.* **1995**, *117*, 1647.

53. a) Sperry, C. K.; Bazan, G. C.; Cotter, W. D. *J. Am. Chem. Soc.* **1999**, *121*, 1513. b) Rogers, J. S.; Lachicotte, R. J.; Bazan, G. C. *J. Am. Chem. Soc.* **1999**, *121*, 1288. c) Rodriguez, G.; Graham, J. P.; Cotter, W. D.; Sperry, C. K.; Bazan, G. C.; Bursten, B. E. *J. Am. Chem. Soc.* **1998**, *120*, 12512.

54. Brown, S. J.; Gao, X.; Harrison, D. G.; Koch, L.; Spence, R. E.v.H.; Yap, G. P. A. *Organometallics* **1998**, *17*, 5445.

55. Wolczanski, P. T. *Polyhedron* **1995**, *14*, 3335.

56. Allen, K. D.; Bruck, M. A.; Gray, S. D.; Kingsborough, R. P.; Smith, D. P.; Weller, K. J.; Wigley, D. E. *Polyhedron* **1995**, *14*, 3315.

57. Lockwood, M. A.; Potyen, M. C.; Steffey, B. D.; Fanwick, P. E.; Rothwell, I. P. *Polyehdron* **1995**, *14*, 3293.

58. Vilardo, J. S.; Lockwood, M. A.; Hanson, L. G.; Clark, J. R.; Parkin, B. C.; Fanwick, P. E.; Rothwell, I. P. *J. Chem. Soc. Dalton Trans.* **1997**, 3353.

59. Lefebvre, F.; Leconte, M.; Pagano, S.; Mutch, A.; Basset, J. M. *Polyhedron* **1995**, *14*, 3209.

60. Eilerts, N. W.; Heppert, J. A. *Polyhedron* **1995**, *14*, 3255.

61. Alexander, J. B; La, D. S.; Cefalo, D. R.; Hoveyda, A. H.; Schrock, R. R. *J. Am. Chem. Soc.* **1998**, *120*, 4041.

62. La, D. S.; Alexander, J. B.; Cefalo, D. R.; Graf, D. D.; Hoveyda, A. H.; Schrock, R. R. *J. Am. Chem. Soc.* **1998**, *120*, 9720.

63. Gibson, V. C. *J. Chem. Soc., Dalton Trans.* **1994**, 1607.

64. Gibson, V. C.; Redshaw, C.; Clegg, W.; Elsewood, M. R. J.; Siemeling, U.; Türk, T. *J. Chem. Soc., Dalton Trans.* **1996**, 4513.

65. Bryson, N.; Youinou, M. –T.; Osborn, J. A. *Organometallics* **1991**, *10*, 3389.

66. Gibson, V. C.; Marshall, E. L.; Redshaw, C.; Clegg, W.; Elsewood, M. R. J. *J. Chem. Soc., Dalton Trans.* **1996**, 4107.

67. Bell, A.; Clegg, W.; Dyer, P. W.; Elsewood, M. R. J.; Gibson, V. C.; Marshall, E. L. *J. Chem. Soc., Chem. Commun.* **1994**, 2247.

68. Dilworth, J. R.; Gibson, V. C.; Lu, C.; Miller, J. R.; Redshaw, C.; Zheng, Y. *J. Chem. Soc., Chem. Commun.* **1997**, 269.

69. Nugent, W. A.; Mayer, J. M. *Metal-Ligand Multiple Bonds*; Wiley: New York, 1988.

70. Wigley, D. E. *Prog. Inorg. Chem.* **1994**, *42*, 239.

71. Hurthouse, M. B.; Moteralli, M.; Sullivan, A. C.; Wilkinson, G. *J. Chem. Soc., Chem. Commun.* **1986**, 1398.

72. Alcalde, M. I.; Gomez-Sal, P.; Martin, A.; Royo, P. *Organometallics* **1998**, *17*, 1144.

73. Cotton, F. A.; Duraj, S. A.; Roth, W. J. *J. Am. Chem. Soc.* **1984**, *106*, 4749.

74. Chao, Y. W.; Rodgers, P. M.; Wigley, D. E.; Alexander,, S. J.; Rheingold, A. L. *J. Am. Chem. Soc.* **1991**, *113*, 6326.

75. Gibson, V. C. *Adv. Mater.* **1994**, *6*, 37.

76. Walsh, P.J.; Hollander, F. J.; Bergman, R. G. *J. Am. Chem. Soc.* **1988**, *110*, 8729.

77. Cummins, C. C.; Baxter, S. M.; Wolczanski, P. T. *J. Am. Chem. Soc.* **1988**, *110*, 8731.

78. de With, J.; Horton, A. D. *Angew. Chem., Int. Ed. Engl.* **1993**,*32*, 903.

79. Schaller, C. P.; Cummins, C. C.; Wolczanski, P. T. *J. Am. Chem. Soc.* **1996**, *118*, 591.

80. Schafer, D. F.; Wolczanski, P. T. *J. Am. Chem. Soc.*, **1998**, *120*, 4881.

81. Schaller, C. P.; Wolczanski, P. T. *Inorg. Chem.* **1993**, *32*, 131.

82. Blake, R. E.; Antonelli. D. M; Henling, L. M.; Schaefer, W. D.; Handcastle. K. I.; Bercaw, J. E. *Organometallics* **1998**, *17*, 718.

83. Polse, J. L.; Andersen, R. A.; Bergman, R. G. *J. Am. Chem. Soc.* **1998**, *120*, 13405.

84. de With, J.; Horton, A. D.; Orpen, A. G. *Organometallics* **1993**, *12*, 1493.

85. Gibson, V. C.; Redshaw, C.; Clegg, W. Elsewood, M. R. J. *J. Chem. Soc., Chem. Commun.* **1994**, 2635.

86. a) Lappert, M. F.; Power, P. P.; Sanger, A. R.; Srivastava, R. C. *Metal and Metalloid Amides*, John Wiley, New York, 1980. b) Bradley, D. C.; Chisholm, M. H. *Acc. Chem. Res.* **1976**, *9*, 273.

87. Bradley, D. C.; Thomas, I. M. *J. Chem. Soc.* **1960**, 3857.

88. Bradley, D. C.; Gitlitz, M. H. *J. Chem. Soc. (A)* **1969**, 980

89. Bradley, D. C.; Thomas, I. M. *Can. J. Chem.* **1962**, *40*, 1355.

90. Chisholm, M. H.; Huffman, J. C.; Tan, L. S. *Inorg. Chem.* **1981**, *20*, 1859.

91. Johnson, A. R.; Davis, W. M.; Cummins, C. C. *Organometalllics* **1996**, *15*, 3825.

92. Shah, S. A. A.; Dorn, H.; Voight, A.; Roesky, H. W.; Parisini, E.; Schmidt, H. G.; Noltemeyer, M. *Organometallics* **1996**, *15*, 3176.

93. Shah, S. A. A.; Dorn, H.; Roesky, H. W.; Parisini, E.; Schmidt, H. G.; Noltemeyer, M. *Organometallics* **1996**, *15*, 4142.

94. Vanderlende, D. D.; Abboud, K. A.; Boncella, J. M. *Polym. Prep.* **1994**, *35*, 691.

95. Vanderlende, D. D.; Abboud, K. A.; Boncella, J. M. *Organometallics* **1994**, *13*, 3378.

96. Boncella, J. M.; Wang, S. Y.; Vanderlende, D. D.; Huff, R. L.; Vaughan, W. M.; Abboud, K. A. *J. Organomet. Chem.* **1996**, *530*, 59.

97. Huff, R. L.; Wang, S. Y.; Abboud, K. A.; Boncella, J. M. Abboud, K. A. *Organometallics* **1997**, *16*, 1779.

98. Wang, S. Y. S.; Abboud, K. A.; Boncella, J. M. *J. Am. Chem. Soc.* **1997**, *119*, 11990.

99. Wang, S. Y. S.; Vanderlende, D. D.; Abboud, K. A.; Boncella, J. M. *Organometallics* **1998**, *17*, 2628.

100. Vaughan, W. M.; Abboud, K. A.; Boncella, J. M. *J. Am. Chem. Soc.* **1995**, *117*, 11015.

101. Aoyagi, K.; Gantzel, P. K.; Kalai, K.; Tilley, T. D. *Organometallics* **1996**, *15*, 4299.

102. Aoyagi, K.; Gantzel, P. K.; Kalai, K.; Tilley, T. D. *Polyhedron* **1996**, *15*, 4299.

103. Armistead, L. T.; White, P. S.; Gagné, M. R. *Organometallics* **1998**, *17*, 216.

104. Hermann, W. A.; Denk, M.; Albach, R. W.; Behm, J.; Herdtweck, E. *Chem. Ber.* **1991**, *124*, 683.

105. Hermann, W. A.; Denk, M.; Behm, J.; Scherer, W.; Klingan, F. R.; Bock, H.; Solouki, B.; Wagner, M. *Angew. Chem. Int. Ed. Engl.* **1992**, *31*, 1485.

106. Jeon, Y. M.; Park, S. J.; Heo, J.; Kim, K. *Organometallics* **1998**, *17*, 3161.

107. Lee, C. H.; La, Y. H.; Park, S. J.; Park, J. W. *Organometallics* **1998**, *17*, 3648.

108. Scollard, J. D.; McConville, D. H.; Rettig, S. J. *Organometallics* **1997**, *16*, 1810.

109. Guérin, F.; McConville, D. H.; Vittal, J. J. *Organometallics* **1995**, *14*, 3154.

110. Guérin, F.; McConville, D. H.; Vittal, J. J. *Organometallics* **1997**, *16*, 1491.

111. Cai, S.; Schrock, R. R. *Inorg. Chem.* **1991**, *30*, 4106.

112. Horton, A. D.; de With, J.; van der Linden, A.; van de Weg, H. *Organometallics* **1996**, *15*, 2672.

113. Guérin, F.; McConville, D. H.; Vittal, J. J.; Yap, G. A. P. *Organometallics* **1998**, *17*, 1290.

114. Aizenberg, M.; Turculet, L.; Davis, W. M.; Schattenmmann, F.; Schrock, R. R. *Organometallics* **1998**, *17*, 4795.

115. Gade, L. H.; Mahr, N. *J. Chem. Soc., Dalton Trans.* **1993**, 489.

116. Schrock, R. R. *Acc. Chem. Res.* **1997**, *30*, 9.

117. Schrock, R. R.; Seidel, S. W.; Mösch-Zanetti, N. C.; Dobbs, D. A.; Shih, K. Y.; Davis, W. M. *Organometallics* **1997**, *16*, 5195.

118. Cummins, C. C.; Lee, J.; Schrock. R. R.; Davis. W. M. *Angew. Chem. Int. Ed. Engl.* **1992**, *31*, 1501.

119. Freundlich, J. S.; Schrock, R. R.; Davis, W. M. *Organometallics* **1996**, *15*, 2777.

120. Seidel, S. W.; Schrock, R. R.; Davis, W. M. *Organometallics* **1998**, *17*, 1058.

121. Cummins, C. C.; Schrock, R. R.; Davis, W. M. *Organometallics* **1992**, *11*, 1452.

122. Bochmann, M.; Wilkinson, G. Young, G. B. *J. Chem. Soc., Dalton Trans.* **1980**, 1879.

123. Malatesta, V.; Ingold, K. U.; Schrock, R. R. *J. Organomet. Chem.* **1978**, *152*,C53.

124. Kruse, W. *J. Organomet. Chem.* **1972**, *42*, C39.

125. Bower, B. K.; Tennent, H. G. *J. Am. Chem. Soc.* **1972**, *94*, 2512.

126. Roberts, R. M. G. *J. Organomet. Chem.* **1973**, *63*, 159.

127. Cross, R. J. In *The Chemistry of the Metal-Carbon Bond*; Hartley, F. R.; Patai, S., Eds.; John Wiley & Sons: New York, 1982.

128. Cohen, S. A.; Auburn, P. R.; Bercaw, J. E. *J. Am. Chem. Soc.* **1983**, *105*, 1136.

129. Polse, J. L.; Kaplan, A. W.; Andersen, R. A.; Bergman, R. G. *J. Am. Chem. Soc.* **1998**, *120*, 6316.

130. Kaplan, A. W.; Polse, J. L.; Ball, G. E.; Andersen, R. A.; Bergman, R. G. *J. Am. Chem. Soc.* **1998**, *120*, 11649.

131. Alt, H. G.; Denner, C. E.; Thewalt, U.; Rausch, M. D. *J. Organomet. Chem.* **1988**, *356*, C83.

132. Schrock, R. R.; Sharp, P. R. *J. Organomet. Chem.* **1978**, *100*, 2389.

133. Prouxl, G.; Bergman, R. G. *J. Am. Chem. Soc.* **1994**, *116*, 7953.

134. Burger, B. J.; Santarsiero, B. D.; Trimmer, M. S.; Bercaw, J. E. *J. Am. Chem. Soc.* **1988**, *110*, 3134.

135. Buchwald, S. L.; Kreutzer, K. A.; Fisher, R. A. *J. Am. Chem. Soc.* **1990**, *112*, 4600.

136. Negishi, E.; Cederbaum, F. E.; Takahashi, T. *Tetrahedron Lett.* **1986**, *27*, 2829.

137. Negishi, E.; Swanson, P. R.; Takahashi, T. *Chem. Lett.* **1987**, 623.

138. Negishi, E.; Holmes, S. J.; Tour, J. M.; Miller, J. A.; Cederbaum, F. E.; Swanson, D. R.; Takahashi, T. *J. Am. Chem. Soc.* **1989**, *111*, 3336.

139. Swanson, D. R.; Rousset, C. J.; Negishi, E.; Takahashi, T.; Seki, T.; Saburi, M.; Uchida, Y. *J. Org. Chem.* **1989**, *54*, 3521.

140. Schultz, A. J.; Brown, R. K.; Williams, J. M.; Schrock, R. R. *J. Am. Chem. Soc.* **1980**, *103*, 169.

141. Green, M. L. H.; Konidaris, P. C.; Mountford, P. *J. Chem. Soc., Dalton Trans.* **1994**, 2851.

142. Green, M. L. H.; Konidaris, P. C.; Mountford, P.; Simpson, S. J. *J. Chem. Soc., Chem. Commun.* **1992**, 256.

143. LaPointe, R. E.; Wolczanski, P. T.; Mitchell, J. F. *J. Am. Chem. Soc.* **1986**, *108*, 6382.

144. Robbins, J.; Bazan, G. C.; Murdzek, J. S.; O'Regan, M. R.; Schrock, R. R. *Organometallics* **1991**, *10*, 2902.

145. Dyer, P. W.; Gibson, V. C.; Clegg, W. *J. Chem. Soc., Dalton Trans.* **1995**, 3313.

146. Dyer, P. W.; Gibson, V. C.; Howard, J. A. K.; Whittle, B.; Wilson, C. *J. Chem. Soc., Chem. Commun.* **1992**, 1666.

147. Dyer, P. W.; Gibson, V. C.; Howard, J. A. K.; Wilson, C. *J. Organomet. Chem.* **1993**, *462*, C15.

148. Dyer, P. W.; Gibson, V. C.; Howard, J. A. K.; Whittle, B.; Wilson, C. *Polyhedron* **1995**, *14*, 103.

149. Rocklage, S. M.; Schrock, R. R. *J. Am. Chem. Soc.* **1982**, *104*, 3077.

150. Williams, D. S.; Schoefield, M. H.; Anhaus, J. T.; Schrock, R. R. *J. Am. Chem. Soc.* **1990**, *112*, 6728.

151. Clark, G. R.; Nielson, A. J.; Rickard, C. E. F.; Ware, D. C. *J. Chem. Soc., Dalton Trans.* **1990**, 1173.

152. Clark, G. R.; Nielson, A. J.; Rickard, C. E. F. *J. Chem. Soc., Dalton Trans.* **1995**, 1907.

153. Su, F. M.; Cooper, C.; Geib, S. J.; Rheingold. A. L.; Mayer, J. M. *J. Am. Chem. Soc.* **1986**, *108*, 3545.

154. Calderazo, F.; Pampaloni, G. *J. Organomet. Chem.* **1992**, *423*, 307.

155. Fischer, E. O.; Hafner, W. *Z. Naturforschg.* **1955**, *10B*, 665.

156. Jolly, P. W. *Acc. Chem. Res.* **1996**, *29*, 544.

157. Marr, G.; Rockett, B. W. In *The Chemistry of the Metal-Carbon Bond*; Hartley, F. R.; Patai, S., Eds.; John Wiley & Sons: New York, 1982.

158. Maslowsky, E. *J. Chem. Ed.* **1992**, *70*, 980.

159. Green, M. L. H. *J. Organomet. Chem.* **1980**, *200*, 119.

160. Yoon, M.; Lin, J.; Young, V. G.; Miller, G. J. *J. Organomet. Chem.* **1996**, *507*, 31.

161. Lockwood, M. A.; Fanwick, P. E.; Eisenstein, O.; Rothwell, I. P. *J. Am. Chem. Soc.* **1996**, *118*, 2762.

162. Maseras, F.; Lockwood, M. A.; Eisenstein, O.; Rothwell, I. P. *J. Am. Chem. Soc.* **1998**, *120*, 6598.

163. Calderazo, F.; Pampaloni, G. *J. Organomet. Chem.* **1992**, *423*, 307.

164. Ashmore, J.; Green, J. C.; Green, M. L. H.; Smith, M. L.; Mehnert, C.; Wucherer, E. J. *J. Chem. Soc., Dalton Trans.* **1995**, 1873.

165. Mehnert, C. D.; Chenega, A. N.; Green, M. L. H. *J. Organomet. Chem.* **1996**, *513*, 247.

166. Lockwood, M. A.; Fanwick, P. E.; Rothwell, I. P. *Polyhedron* **1995**, *14*, 3363.

167. Wexler, P. A.; Wigley, D. E.; Koerner, J. B.; Albright, T. A. *Organometallics* **1991**, *10*, 2319.

168. Horton, A. D.; de With, J. *J. Organometallics* **1997**, *16*, 5424.

169. Thorn, M. G.; Etheridge, Z. C.; Fanwick, P. E.; Rothwell, I. P. *Organometallics* **1998**, *17*, 3636.

170. Muso, F.; Solari, E.; Floriani, C.; Schenk, K. *Organometallics* **1997**, *16*, 4889.

171. Calderazo, F.; Ferri, I.; Pampaloni, G.; Troyanov, S. *J. Organomet. Chem.* **1996**, *518*, 189.

172. Lancaster, S. J.; Robinson, G. B.; Bochmann, M.; Coles, S. J.; Hurthouse, M. B. *Organometallics* **1995**, *14*, 2456.

173. Pellechia, C.; Grassi, A; Immirzi, A. *J. Am. Chem. Soc.* **1993**, *115*, 1160.

174. Gillis, D. J.; Tudoret, M. J.; Baird, M. C. *J. Am. Chem. Soc.* **1993**, *115*, 2543.

175. Troyanov, S. *J. Organomet. Chem.* **1994**, *475*, 139.

176. Troyanov, S.; Pisarevsky, A.; Struchkov, Y. T. *J. Organomet. Chem.* **1995**, *494*, C4.

177. Cotton, F. A.; Kibala, P. A.; Wojtczak, W. A. *J. Am. Chem. Soc.* **1991**, *113*, 1462.

178. Cotton, F. A.; Wojtczak, W. A. *Inorg. Chim. Acta.* **1994**, *217*, 187.

179. Cotton, F. A.; Kibala, P. A.; Shang, M.; Wojtczak, W. A. *Organometallics* **1991**, *10*, 2626.

180. Diamond, G. M.; Green, M. L. H.; Walker, N. M.; Howard, J. A. K.; Mason, S. A. *J. Chem. Soc., Dalton Trans.* **1992**, 2641.

181. Green, M. L. H.; Morise, X.; Wojtczak, W. A. *J. Organomet. Chem.* **1993**, *462*, 209.

182. Bruck, M. A.; Copenhaver, A. S.; Wigley, D. E. *J. Am. Chem. Soc.* **1987**, *109*, 6525.

183. Ballard, K. R.; Gardiner, I. M.; Wigley, D. E. *J. Am. Chem. Soc.* **1989**, *111*, 2159.

184. Arney, D. J.; Wexler, P. A.; Wigley, D. E. *Organometallics* **1990**, *9*, 1282.

185. Arney, D. J.; Bruck, M. A.; Wigley, D. E. *Organometallics* **1991**, *10*, 3947.

186. Smith, D. P.; Strickler, J. R.; Gray, S. D.; Bruck, M. A.; Holmes, R. S.; Wigley, D. E. *Organometallics* **1992**, *11*, 1275.

187. Arney, D. S. J.; Fox, P. A.; Bruck, M. A.; Wigley, D. E. *Organometallics* **1997**, *16*, 3421.

188. Neithamer, D. R.; Dárkányi, L.; Mitchell, J. F.; Wolczanski, P. T. *J. Am. Chem. Soc.* **1988**, *110*, 4421.

189. Parker, D. In *The Chemistry of the Metal-Carbon Bond*; Hartley, F. R.; Patai, S., Eds.; John Wiley & Sons: New York. 1982.

190. James, B. R. In *Homogeneous Hydrogenation*; Wiley: New York, 1974.

191. Halpern, J.; Wong, C. S. *J. Chem. Soc., Chem. Commun.* **1973**, 629.

192. Chan, A. S. C.; Halpern, J. *J. Am. Chem. Soc.* **1980**, *102*, 838.

193. Halpern, J. *Science* **1982**, *217*, 401.

194. Sloan, M. F.; Matlack, A. S.: Breslow, D. S. *J. Am. Chem. Soc.* **1963**, *85*, 4014.

195. Halterman, R. L.; Vollhardt, P. C.; Welker, M. E.; Bläser, D.; Boese, R. *J. Am. Chem. Soc.* **1987**, *109*, 8105.

196. Halterman, R. L.; Vollhardt, P. C. *Organometallics* **1988**, *7*, 883.

197. Waymouth, R.; Pino, P. *J. Am. Chem. Soc.* **1990**, *112*, 4911.

198. Broene, R. D.; Buchwald, S. L. *J. Am. Chem. Soc.* **1993**, *115*, 12569.

199. Jeske, G.; Lauke, H.; Mauermann, H.; Schumann, H.; Marks, T. J. *J. Am. Chem. Soc.* **1985**, *107*, 8111.

200. Conticello, V. P.; Brard, L.; Giordello, M. A.; Tsuji, Y.; Sabat, M.; Stern, C. L.; Marks, T. J. *J. Am. Chem. Soc.* **1992**, *114*, 2761.

201. Willoughby, C. A.; Buchwald, S. L. *J. Am. Chem. Soc.* **1992**, *114*, 7562.

202. Pinad, G. J.; Thornton-Pett, M; Bochmann, M. *J. Chem. Soc., Dalton Trans.* **1998**, 393.

203. Fox, H. H.; Yap, K. B.; Robbins, J.; Cai, S.; Schrock, R. R. *Inorg. Chem.* **1992**, *31*, 2287.

204. Nugent, W. A. *Inorg. Chem.* **1983**, *22*, 965.

205. Amor, F.; Sal, P. G; de Jesus, E.; Martin, A.;Perez, A. I.; Royo, P.; Vazquez, A. *Organometallics* **1996**, *15*, 2103.

206. Nugent, W. A.; Harlow, R. L. *J. Am. Chem. Soc.* **1980**, *102*, 1759.

207. Leung, W. H.; Danopoulos, A. A.; Wilkinson, G.; Bates, B. H.; Hursthouse, M. B. *J. Chem. Soc., Dalton Trans.* **1991**, 2051.

208. Walsh, P. J.; Hollander, F, J.; Bergman, R. G. *J. Am. Chem. Soc.* **1988**, *110*, 8729.

209. Chisholm, M. H.; Folting, K.; Huffman, J. C.; Ratermann, A. L. *Inorg. Chem.* **1982**, *21*, 978.

210. Thorn, D. L.; Nugent, W. A.; Harlow, R. L. *J. Am. Chem. Soc.* **1981**, *103*, 357.

211. Danopoulos, A. A.; Wilkinson, G. *Polyhedron* **1990**, *9*, 1009.

212. Nugent, W. A.; Harlow, R. L. *Inorg. Chem.* **1979**, *18*, 2030.

213. Dyer, P. W.; Gibson, V. C.; Clegg, W. *J. Chem. Soc., Dalton Trans.* **1995**, 3313.

214. Sullivan, A. C.; Wilkinson, G.; Moteralli, M.; Hursthouse, M. B. *J. Chem. Soc., Dalton Trans.* **1988**, 53.

215. Danopoulos, A. A.; Leung, W. H.; Wilkinson, G.; Battes, B. H.; Hursthouse, M. B. *Polyhedron* **1990**, *9*, 2625.

216. Chan, D. M. T.; Fultz, W. C.; Nugent, W. A.; Roe, D. C.; Tulip, T. H. *J. Am. Chem. Soc.* **1985**, *107*, 251.

217. Morrison, D. L.; Wigley, D. E. *Inorg. Chem.* **1995**, *34*, 2610.

218. Galindo, A.; Gutierrez, E.; Monge, A.; Paneque, M; Pastor, A.; Perez, P. J.; Rogers, R. D.; Carmona, E. *J. Chem. Soc., Dalton Trans.* **1995**, 3801

219. Green, M. L. H.; Konidis, P. C.; Mountford, P. *J. Chem. Soc., Dalton Trans.* **1994**, 2851.

220. Goedheijt, M. S.; Akkerman, O. S.; Bickelhaupt, F.; can Leeuwen, P. W. N. M.; Veldman, N.; Spek, A. L. *Organometallics* **1994**, *13*, 2931.

221. Borgmann, C.; Limberg, C.; Driess, A. *J. Organomet. Chem.* **1997**, *541*, 367.

222. Dilworth, J. R.; Gibson, V. C.; Lu, C.; Miller, J. R.; Redshaw, C.; Zheng, Y. *J. Chem. Soc., Dalton Trans.* **1997**, 269.

223. Limberg, C.; Buchner, M.; Heinze, K.; Walter, O. *Inorg. Chem.* **1997**, *36*, 872.

224. Yooh, K.; Parkin, G.; Rheingold, A. L. *J. Am. Chem. Soc.* **1992**, *114*, 2210.

225. Allen, F. H.; Kennard, O. *Chemical Design Automation News* **1993**, *8*, 31.

226. Chou, C. Y.; Huffman, J. C.; Maatta, E. A. *J. Chem. Soc., Chem. Comm.* **1984**, 1184.

227. Vaughan, W. M.; Abboud, K. A.; Boncella, J. M. *Organometallics* **1995**, *14*, 1567.

228. Schrock, R. R.; Murdzek, J. S.; Bazan, G. C.; Robbins, J.; DiMare, M.; O'Regan, M. *J. Am. Chem. Soc.* **1990**, *112*, 3875.

229. Casty, G. L; Tilley, T. D.; Yap, G. P. A.; Rheingold, A. L. *Organometallics* **1997**, *16*, 4746.

230. Dyer, P. W.; Gibson, V. C.; Howard, J. A. K.; Whittle, B.; Wilson, C. *J. Chem Soc. Chem. Comm.* **1992**, 1666.

231. Dyer, P. W.; Gibson, V. C.; Howard, J. A. K.; Wilson, C. *J. Organomet. Chem.* **1993**, *462*, C15.

232. Brookhart, M.; Green, M. L. H.; Wang, L. *Prog. Inorg. Chem.* **1988**, *36*, 1.

233. Coles, M. P.; Gibson, V. C.; Clegg, W.; Elsewood, M. R. J. *Polyhedron*, **1998**, *17*, 2483.

234. Jaffart, J.; Mathier, R.; Etienne, M.; McGrady, J. E.; Eisenstein, O.; Maseras, F. *J. Chem. Soc., Chem. Comm.* **1998**, 2011.

235. Cole, J. M.; Gibson, V. C.; Howard, J. A. K.; McIntyre, G. J.; Walker, G. L. P. *J. Chem. Soc., Chem. Comm.* **1998**, 1829.

236. Rietveld, M. H. P.; Teunissen, W.; Hagen, H.; van de Water, L.; Grove, D. M.; van der Schaaf, P. A.; Mühlebach, A. L.; van Koten, G. *Organomentallics* **1997**, *16*, 1674.

237. Haaland, A.; Scherer, W.; Ruud, K.; McGarrady, G. C.; Downs, A. J.; Swang, O. *J. Am. Chem. Soc.* **1998**, *120*, 3762.

238. Jordan, R. F.; Bradley, P. K.; Baenziger, N. C.; LaPointe, R. E. *J. Am. Chem. Soc.* **1990**, *112*, 1289.

239. Sandström, J. *Dynamic NMR Spectroscopy*, Academic Press, New York, 1982.

240. Oskam, J. H.; Fox, H. H.; Yap, K. B.; Mcconville, D. H.; O'Dell, R.; Lichtenstein, B. J.; Schrock, R. R. *J. Organomet. Chem.* **1993**, *459*, 185.

241. Schoettel, G.; Kress, J.; Osborn, J. A. *J. Chem Soc., Chem. Comm.* **1989**, 1962.

242. Vanderlende, D. D. *PhD. Dissertation*, University of Florida, 1994.

243. Wang, S. Y. S. *PhD. Dissertation*, University of Florida, 1998.

244. Lain, S. J.; Schrock, R. R. *J. Am. Chem. Soc.* **1978**, *100*, 1315.

245. Lain, S. J.; Sancho, J.; Schrock, R. R. *J. Am. Chem. Soc.* **1980**, *102*, 5610.

246. Encrich, R.; Heinemann, O.; Jolly, P. W.; Krüger, C.; Verhounik, G. P. J. *Organometallics* **1997**, *16*, 1511.

247. Meijboom, N,; Schaverien, C. J.; Orpen, A. G. *Organometallics* **1990**, *9*, 774.

248. Knight, K. S.; Wang, D.; Waymouth, R. M.; Ziller, J. *J. Am. Chem. Soc.* **1994**, *116*, **1845**.

249. Cohen, S. A.; Auburn, P. R.; Bercaw, J. E. *J. Am. Chem. Soc.* **1983**, *105*, 1136.

250. Erker, G.; Dorf, U.; Rheingold, A. L. *Organometallics* **1988**, *7*, 138.

251. Dyer, P. W.; Gibson, V. C.; Howard, J. A. K.; Whittle, B.; Wilson, C. *Polyhedron* **1995**, *14*, 103.

252. Dyer, P. W.; Gibson, V. C.; Clegg, W. *J. Chem. Soc., Dalton Trans.* **1995**, 3313.

253. Dyer, D. W.; Gibson, V. C.; Howard, J. A. K.; Whittle, B.; Wilson, C. *J. Chem. Soc., Chem. Comm.* **1992**, 1666.

254. Bryson, N; Youinou, M. T.; Osborn, J. A. *Organometallics* **1991**, *10*, 3389.

255. Burger, B. J.; Santarsiero, B. D.; Trimmer, M. S.; Bercaw, J. E. *J. Am. Chem. Soc.* **1988**, *110*, 3134.

256. Clark, J. R.; Fanwick, I. P.; Rothwell, I. P. *J. Chem. Soc., Chem. Comm.* **1995**, 553.

257. Mitchell, A. D.; Cross, L. C. *Tables of Interatomic Distances and Configurations in Molecules and Ions.*

258. Allen, F. H.; Kenward, O. *Chemical Design and Automation News* **1993**, *8*, 31.

259. Clark, G. R.; Nielson, A. J.; Richard, C. E. F.; Ware, D. C. *J. Chem. Soc., Dalton Trans.* **1995**, 1907.

260. Clark, G. R.; Nielson, A. J.; Richard, C. E. F. *J. Chem. Soc., Dalton Trans.* **1990**, 1173.

261. Wick, D. D.; Jones, W. D. *Organometallics* **1999**, *18*, 495.

262. Alvarado, Y.; Boutry, O.; Gutierrez, E.; Marge, A.; Nicasio, M. C.; Poveda, M. L.; Perez, P. J.; Ruiz, C.; Bianchini, C.; Carmona, E. *Chemistry-Eur* **1997**, *3*, 860.

263. Busca, G.; Finocchio, E.; Lorenzelli, V.; Trombetta, M.; Rossini, S. A. *J. Chem. Soc., Faraday Trans.* **1996**, 4687.

264. Richardson, D. E.; Alameddin, N. G.; Ryan, M. F.; Hayes, T.; Eyler, J. R.; Siedle, A. R. *J. Am. Chem. Soc.* **1996**, *118*, 11244.

265. Baruah, J. B.; Samuelson, A. G. *J. Chem. Soc., Chem. Comm.* **1987**, 36.

266. He, Y. X.; Sutton, D. *J. Organomet. Chem.* **1999**, *572*, 213.

267. Sakaki, S.; Satoh, H.; Shono, H.; Ujino, Y. *Organometallics* **1996**, *15*, 1713.

268. Allen, F. H.; Kennard, O. *Chemical Design Automation News* **1993**, *8*, 31.

269. Mansel, S.; Thoma, D.; Lefeber, C.; Heller, D.; Kempe, R.; Baumann, W.; Rosenthal, U. *Organometallics* **1997**, *16*, 2886.

270. Negishi, E.; Holmes, S. J.; Taur, J. M.; Miller, J. A.; Cederbaum, F. E.; Swanson, D. R.; Takahashi, T. *J. Am. Chem. Soc.* **1989**, *111*, 333.

271. Manriquez, J. M.; McAlister, D. R.; Sanner, R. D.; Bercaw, J. E. *J. Am. Chem. Soc.* **1978**, *100*, 2716.

272. Rothwell, I. P. *J. Chem. Soc., Chem. Commun.* **1997**, 1331.

273. Millar, S. P.; Zubris, D. L.; Bercaw, J. E.; Eisenberg, R. *J. Am. Chem. Soc.* **1998**, *120*, 5329.

274. Pleune, B.; Poli, R.; Fettinger, J. C. *J. Am. Chem. Soc.* **1998**, *120*, 3257.

275. Lee, H.; Desrosiers, P. J.; Guzei, I.; Rheingold, A. L.; Parkin, G. *J. Am. Chem. Soc.* **1998**, *120*, 3255.

276. Bayse, C. A.; Hall, M. B. *Organometallics* **1998**, *17*, 4861.

277. Evans, W. J.; Bloom, I.; Hunter, W. E.; Atwood, J. L. *J. Am. Chem. Soc.* **1983**, *105*, 1401.

278. Sabo-Etienne, S.; Chaudret, B. *Chem. Rev.* **1998**, *98*, 2077.

279. Esteruelas, M. A.; Oro, L. A. *Chem. Rev.* **1998**, *98*, 577.

280. Traylor, T. G.; Stewart, K. J.; Goldberg, M. J. *J. Am. Chem. Soc.* **1984**, *106*, 4445.

281. Traylor, T. G.; Stewart, K. J. *Organometallics* **1984**, *3*, 325.

282. Harrison, J. J. *J. Am. Chem. Soc.* **1984**, *106*, 1487.

283. Trost, B. M.; Strege, P. E.; Weker, L.; Fullerton, T. J.; Dietsch, T. J. *J. Am. Chem. Soc.* **1978**, *100*, 3407.

284. Tulip, T. H.; Ibers, J. A. *J. Am. Chem. Soc.* **1979**, *101*, 4201.

285. Szymanska, B. T.; Jaroszewski, M.; Wilgocki, M.; Ziolkowski, J. J. *J. Mol. Cat. A* **1996**, *112*, 203.

286. Cavell, K. J.; Chan, K. Y.; Peacock, E. J.; Ridd, M. J.; Davies, N. W. *Aus. J. Chem.* **1991**, *44*, 171.

287. Sheldrick, G. M. (1997). *SHELXL-97*. Program for the refinement of crystal structures. University of Gottingen, Germany.

288. Sheldrick, G. M. (1998). *SHELXTL5*. Bruker-AXS, Madison, Wisconsin, USA.

289. Cook, K. S.; Piers, W. E.; Rettig, S. J. *Organometallics* **1999**, *18*, 1575.

290. Klazinga, A. H.; Teuben, J. H. *J. Organomet. Chem.* **1980**, *192*, 75.

BIOGRAPHICAL SKETCH

Carlos Gilberto Ortiz Vazquez was born on January 29th, 1973 in San Juan, Puerto Rico to loving parents Carlos G. Ortiz and Rosa Vazquez de Ortiz. Since an early age his parents instilled in him the values by which he would lead his life: work hard and have fun, respectively. With that in mind, the author went through grade school, middle school, and high school at the Colegio San Carlos in the small fishing town of Aguadilla, Puerto Rico, graduating with honors in May 1990. Through all of the years at San Carlos, he participated in school track and volleyball teams, and extracurricular activities like the Boy Scouts and Junior Achievement programs.

The author decided to leave Puerto Rico to pursue college studies in chemistry at Purdue University in the small midwestern town of West Lafayette, Indiana. While at Purdue, the author worked as an undergraduate assistant in the chemical research laboratories of Dr. Richard A. Walton for whom he holds great respect and appreciation. Among his projects he worked in the two-electron reduction of small molecules by multiply bonded di-rhenium centers. He then successfully completed his Bachelor of Science degree in May 1994.

The author then decided to move to warmer climates while completing his college career. In August 1994, he started working on his doctoral degree in chemistry at the University of Florida, under the supervision of Dr. James M. Boncella. His time at the University of Florida was well spent as he continued his formation as a scientist and a

person. His work with early-transition metal complexes in high oxidation states brought him great joy and intellectual motivation. Finally, he completed his doctorate in chemistry in the summer of 1999.

I certify that I have read this study and that in my opinion it conforms to acceptable standards of scholarly presentation and is fully adequate, in scope and quality, as a dissertation for the degree of Doctor of Philosophy.

James M. Boncella, Chairman
Associate Professor of Chemistry

I certify that I have read this study and that in my opinion it conforms to acceptable standards of scholarly presentation and is fully adequate, in scope and quality, as a dissertation for the degree of Doctor of Philosophy.

Lisa McElwee-White
Professor of Chemistry

I certify that I have read this study and that in my opinion it conforms to acceptable standards of scholarly presentation and is fully adequate, in scope and quality, as a dissertation for the degree of Doctor of Philosophy.

Kirk Schanze
Professor of Chemistry

I certify that I have read this study and that in my opinion it conforms to acceptable standards of scholarly presentation and is fully adequate, in scope and quality, as a dissertation for the degree of Doctor of Philosophy.

John F. Helling
Professor of Chemistry

I certify that I have read this study and that in my opinion it conforms to acceptable standards of scholarly presentation and is fully adequate, in scope and quality, as a dissertation for the degree of Doctor of Philosophy.

Gar Hoflund
Professor of Chemical Engineering

This dissertation was submitted to the Graduate Faculty of the Department of Chemistry in the College of Liberal Arts and Sciences and to the Graduate School and was accepted as partial fulfillment of the requirements for the degree of Doctor of Philosophy.

August, 1999

Dean, Graduate School